UNIVERSITÀ DI PADOVA

DIPARTIMENTO DI INGEGNERIA INDUSTRIALE

TESI MAGISTRALE IN CHEMICAL AND PROCESS ENGINEERING

Master's degree Thesis in

Chemical and Process Engineering

Design of dynamic experiments to optimize the high value compounds in *Coccomyxa onubensis* in a novel high cell density cultivation system

Supervisor: Prof. Sforza Eleonora

Graduating Student: Grendene Pietro

ACADEMIC YEAR 2023/2024

Riassunto

Le microalghe sono microrganismi fotosintetici che sono emersi come alternativa sostenibile per produrre composti di alto valore aggiunto. I bioprodotti derivati dalle microalghe stanno registrando un aumento significativo nelle applicazioni industriali, che vanno dai prodotti farmaceutici alla bioenergia, grazie alla loro elevata produttività e al loro basso impatto ambientale rispetto alle alternative sintetiche. Una sfida per il futuro è quella di migliorare e ottimizzare la crescita delle microalghe per aumentare la produttività, limitando al contempo la contaminazione da parte di altri microrganismi come i batteri. In questo studio è stata utilizzata un'alga acidofila *Coccomyxa onubensis*, selezionata principalmente per due motivi.

In primo luogo, per la sua abilità di resistere a pH molto acidi, intorno a 2.5, riducendo in questo modo il rischio di contaminazioni da parte di altri organismi, e inoltre per la sua abilità di produrre diversi composti ad alto valore aggiunto come carotenoidi, tra i quali la luteina, un carotenoide primario che agisce come agente protettivo nei confronti di patologie ossidative dell'occhio.

La coltura è stata coltivata in un fotobioreattore ad alta densità, ottimizzato per fornire l'apporto ideale di luce e di CO_2, ottenendo in tal modo tassi di crescita notevolmente superiori ai sistemi di coltivazione tradizionali.

La campagna sperimentale, suddivisa in 39 differenti condizioni sperimentali, è stata eseguita seguendo un design dinamico degli esperimenti nel quale le variabili operative erano in funzione del tempo.

Sono stati testati diversi profili dinamici d'intensità luminosa (da 80 a 800 $\mu mol/m^2/s$) e diversi profili d'alimentazione d'azoto (tra 60 e 600 mg/L), la pressione parziale di CO_2 invece era costante durante una singola condizione sperimentale e poteva assumere 3 diversi valori (0.04,1 e 10%).

Alla fine della campagna sperimentale è stato costruito un modello sui dati ottenuti e si sono andate a ottimizzare le varie variabili per trovare i profili ideali per massimizzare i diversi output d'interesse (produttività di biomassa, contenuto e produttività di carotenoidi totali).

I risultati si sono mostrati superiori rispetto a studi condotti su *Coccomyxa onubensis* presenti in letteratura per la crescita di biomassa e per quantità di carotenoidi totali, mentre la produzione di luteina si è attestata su valori comparabili con quelli presenti in letteratura.

Abstract

Microalgae are photosynthetic microorganisms that have emerged as a sustainable alternative to produce high-value bioactive molecules. Microalgae-derived bioproducts are experiencing a significant increase in industrial applications, ranging from pharmaceuticals to bioenergy, owing to their high productivity of the compounds of interest and their low environmental impact compared to synthetic alternatives. However, stringent European regulatory restrictions pose challenges to microalgae production for human applications. These challenges limit such endeavours to closed photobioreactors characterized by high levels of automation and significant sterilization costs. A challenge for the future is to enhance and optimize the growth of microalgae to increase productivity while limiting contamination from other microorganisms such as bacteria. In this study, the acidophilic microalgae *Coccomyxa onubensis* capitalizes on its ability to thrive in acidic conditions, yielding high amounts of carotenoids, especially lutein, and preventing bacterial contamination. The study applied a design of dynamic experiments (DoDE) to *Coccomyxa onubensis* to optimize the production of biomass and high-value compounds. Cultivation was conducted in a batch system with automated control and monitoring of environmental variables. The microalgae were grown in a high-density cell system equipped with a hydrophobic membrane, optimizing photoautotrophic growth through CO_2 provision by diffusion. This allowed for the establishment of different profiles of light intensity and CO_2 partial pressure.By employing DDoE, meticulous control over key variables, including dynamic light intensity profiles ranging from 80 to 800 $\mu mol/m^2/s$, the feeding strategy of nitrogen between 60 and 600 mg/L, and constant partial pressure of CO_2, systematically optimized growth conditions. The study explores three-tiered CO_2 partial pressure, with the highest concentration reaching 10%, establishing a correlation with the mitigation of CO_2 emissions from significant industrial sectors, including power plants.

Table of Contents

Chapter 1
State of art

1.1 Microalgae

Microalgae are photosynthetic, unicellular microorganisms that primarily live in aquatic environments and are able to exploit solar light and inorganic substances to produce chemical energy in the form of organic material.

They can be prokaryotic or eukaryotic, and their size varies depending on the species, ranging from a few micrometers to few hundred micrometers.

Microalgae are adaptable to a variety of environmental conditions, including salty or fresh water, arctic to tropical water, and a wide pH range (Barsanti et al., 2008).

They are essential to the equilibrium of ecosystems because with the photosynthesis they help to oxygenate aquatic environments, furthermore microalgae are primary producers that support the wide variety of life in aquatic ecosystems by acting as the base of the food chain.

In the last decades they are reaching higher relevance at commercial level thanks to their ability to produce high value bioproducts as polysaccharides, lipids, pigments, proteins, vitamins, bioactive compounds, and antioxidants.

The continuous production during the year, quick growth (for many species) and the large range of products synthetized are the significant features of microalgae (Rath, 2012).Due to these features, nowadays they find several applications in a wide range of sectors, mainly as food supplements and animal feeds, biofuels cosmetics and pharmaceuticals (Khan et al., 2018) as shown in figure 1.

The global microalgae market in 2022 was valued at USD 1002 million and is expected to increase by 5% annually in the years to come (https://www.polarismarketresearch.com, n.d.).
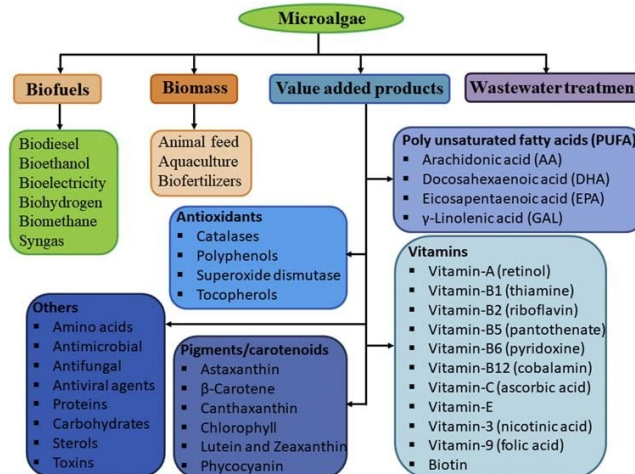
Figure 1 Applications of microalgae

Microalgae are very adaptable organism, they can be cultivated with different systems and by regulating the environmental variables, they can produce different compounds. Furthermore they can growth following different metabolism such as photoautotrophic, heterotrophic or mixotrophic metabolism.

In the first case the algae fix inorganic carbon through photosynthesis while in the second case the algal culture uses organic carbon to growth in a dark environment, the mixotrophic condition is a combination of the previous metabolisms.

In conclusion, the research is essential to make the most of their potential from an industrial-commercial perspective, but above all from an environmental point of view given their low impact.

1.2 Environmental variables

For optimal growth, microalgae necessitate cultivation within an environment characterized by the presence of essential environmental variables and nutrients in appropriate quantities. These variables primarily encompass nutrients, light, temperature, and pH.

Below, a comprehensive elucidation of these key growth parameters is provided.

1.2.1 Nutrients

Microalgae require several key nutrients for their growth and metabolism. These nutrients typically obtained from their surrounding environment and can vary depending on the species of microalgae and the environmental conditions. Optimizing nutrient supply strategies can lead to variations in the biochemical composition of microalgae. This discussion examines various approaches to nutrient availability and their effects on composition, focusing on their effectiveness in maintaining desired biochemical profiles in algae.

Looking at the general formula of the microalgae $CH_{1.7}O_{0.4}N_{0.15}P_{0.0094}$ (Khan et al., 2018) it can be noticed that the main nutrients are carbon, nitrogen and phosphorus, identified as macronutrients. Other elements, mainly metals, are needed from microalgae but in much smaller quantities, and they are called micronutrients.

The condition related to extracellular nutrients availability in an algal culture can vary between a replete condition, where the nutrients are abundant and don't influence the algal growth, and a deplete condition where the nutrient scarcity become a limiting factor for algal growth (Procházková et al., 2014).

Nutrients deprivation causes a reduction in cell division, photosynthesis, and respiration, while storage compounds like starch, lipids, and secondary metabolites as carotenoids increase (Davies and Grossman, 1998).

It is paramount to properly balance the nutrient limitation to avoid a sharp decrease in the growth rate of the culture: using a multi-stage cultivation system can be an optimal solution where in the first stage the aim is to concentrate the culture while in the second stage a stress condition is applied to increase the production of the compound of interest (Markou et al., 2014).

1.2.1.1 Carbon

Carbon dioxide (CO_2) is a fundamental substrate for microalgal growth, influencing biomass productivity and biochemical composition. Carbon, the most important element for microalgae, constitutes approximately 50% of their biomass on a mass basis (Sánchez Mirón et al., 2003). It is the element primarily involved in photosynthesis, the metabolic process through which microalgae convert CO_2 into organic compounds, driving their growth and providing the energy needed for cellular processes.

Carbon dioxide (CO_2) is essential for microalgal growth, serving as a primary source of inorganic carbon for photosynthesis. Alongside CO_2, some microalgae utilize different inorganic carbon sources such as bicarbonate (HCO_3^-), thanks to specialized biological mechanisms such as membrane transporters and dedicated enzymatic pathways for efficient assimilation of inorganic carbon. For instance, microalgal cells possess the carbonic anhydrase enzyme that plays a role in maintaining the equilibrium between CO_2 and bicarbonate in the cytoplasm. However, the availability of these inorganic carbon compounds in the aquatic environment is influenced by various environmental factors, including temperature, pH, and the concentration of dissolved ions, as shown in Figure 2.
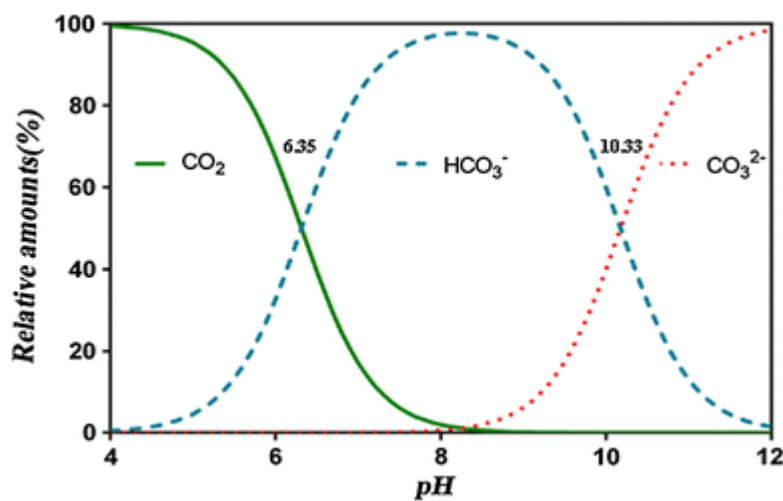
Figure 2 CO2-bicarbonate- carbonate equilibrium at different pH

Figure 3 displays the response of different microalgae strains in terms of biomass productivity, and CO_2 fixation rate to difference concentrations of CO_2 (Zhao and Su, 2014).It is evident that the relationship between CO_2 concentration and carbon fixation, as well as biomass production, varies among microalgal species, resulting in a diverse framework. Generally, most microalgae exhibit optimal growth at lower CO_2 concentrations, with growth inhibition observed beyond 5% (v/v). However, some microalgae strains experience growth inhibition when exposed to CO_2 concentrations above 1% (v/v). While most robust microalgae can microalgae can adapt to CO_2 concentrations up to 10–15%, commonly found in flue gas emissions, their carbon fixation and biomass production rates often decline compared to lower CO_2 levels. Nonetheless, utilizing flue gas as a CO_2 source poses challenges due to impurities such as sulfur dioxide (SO_2), nitrogen oxides (NO_x), and particulate matter, requiring careful management for effective and sustainable CO_2 utilization (Prasad et al., 2021).
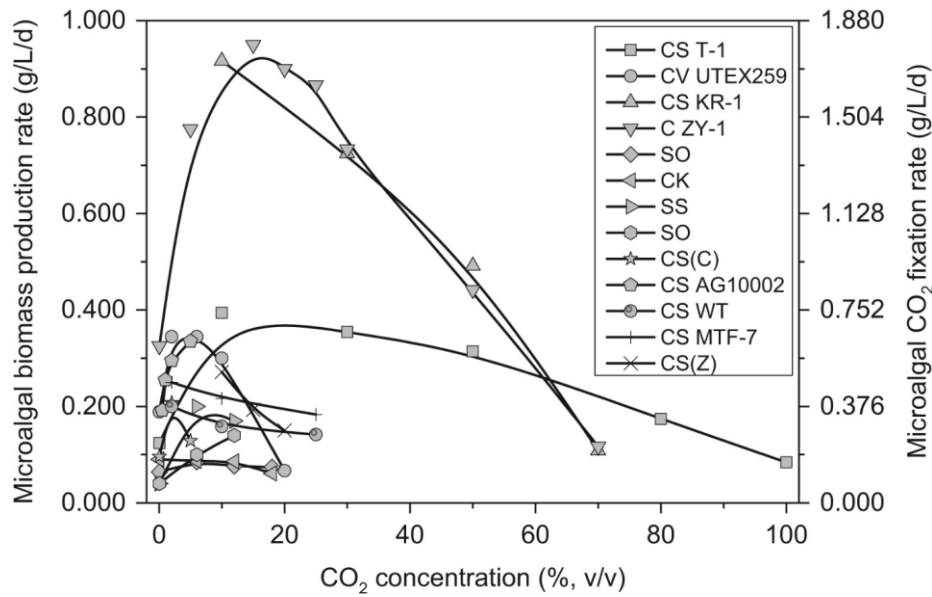
Figure 3 Effect of CO2 concentration on microalgal CO2 fixation and biomass production (Zhao et al., 2024).

Therefore, maintaining the optimal CO_2 concentration in the cultivation environment is crucial to maximize biomass yields and overall productivity. Efficient mass transfer of CO_2 from the gas phase to the liquid medium is the critical key factor ensuring an adequate substrate supply for microalgae. Mass transfer mechanisms, such as gas-liquid absorption and diffusion, govern CO_2 transport across the gas-liquid interface. Factors like aeration rates, mixing intensity, and bioreactor design significantly affect mass transfer rates and CO_2 utilization efficiency. Strategies to enhance CO_2 utilization efficiency include optimizing aeration strategies, increasing gas-liquid contact area, and improving bioreactor design to facilitate efficient mass transfer (Maghzian et al., 2024). On the other hand, challenges emerge, particularly when addressing the need to balance CO_2 availability with energy consumption, scaling up cultivation systems while maintaining efficient mass transfer, and integrating microalgal processes into industrial workflows.

1.2.1.2 Nitrogen

Nitrogen constitutes approximately 7–10% of cell dry weight in microalgae, making it the second most abundant component in the biomass (Richmond, 2004).

Furthermore, microalgae have a higher amount of protein in dry weight (30-60%) respect the terrestrial plants (Becker, 1994), so the nitrogen requirement is high.

Nitrogen is present in key biomass compounds, such as nucleic acids amino acids (proteins) and pigments such as chlorophylls, carotenoids and phycobiliprotein from microalgae and cyanobacteria (Markou et al., 2014).

Its availability significantly changes the growth rate and the chemical composition of the algal culture, its depletion cause an increase in compounds as lipid and carbohydrates while the protein productivity drastically decreases (Van Vooren et al., 2012; Yaakob et al., 2021).

Different studies highlighted the effect of nitrogen limitation on microalgae: (Han et al., 2013) showed that the strain of *Chlorella pyrenoidosa* accumulates the highest amount of lipids under nitrogen limitation, 3.64-fold higher respect the nutrient repletion condition.

A study on the marine green microalga *Tetraselmis subcordiformis* display an higher starch productivity under nitrogen limited condition (3mM) respect the condition where nitrogen was not a limiting factor (11mM) (Yao et al., 2012). Nitrogen is mainly assimilated in inorganic form such as nitrate, nitrite, and ammonium but also in organic matter like urea or amino acids. The nitrate is most used form for the cultivation of microalgae, as it doesn't affect the growth of the cells and concentrations up 100mM can be tolerated (Jeanfils et al. 1993).

On the other hand, ammonium is the preferred source of nitrogen since its absorption and assimilation require less energy in comparison to alternative nitrogen sources.

$$NH_4^+ + OH^- \leftrightarrow NH_3 + H_2O$$
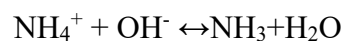
The problem with ammonium is when the pH of the solution is higher than 9.25, in this situation the equilibrium is shift to the right and the nitrogen is present as free ammonia. This, especially at low concentrations, could be harmful for the microalgal biomass (Azov and Goldman 1982), a proper pH control is fundamental to operate in safe conditions.

1.2.1.3 Phosphorus

Phosphorus stands out as a crucial nutrient crucial for the growth of microalgae, with biomass content ranging from 0.05% to 3.3% (Grobbelaar, 2004). It serves as a constituent in numerous organic compounds essential to metabolism, including nucleic acids (RNA and DNA), membrane phospholipids, and ATP.

Among the macronutrients, phosphorus is often the limiting nutrient for microalgae (Oliver and Ganf 2000) mainly due to formation of complexes with metal ions.

In nature, phosphorus is present in different forms such as orthophosphate, polyphosphate, pyrophosphate, metaphosphate, and their organic form (Cembella et al. 1982, Yeoman et al. 1988).

The preferred form of phosphorus supply is in form of orthophosphate, the other forms of inorganic phosphorus before the up take must be converted to orthophosphate, this process is performed by various phosphatase enzymes (Kuenzler and Perras 1965, Lin 1977).

pH, temperature, light and the presence of metals or other inhibitors affect the action of these enzymes (Kuenzler and Perras 1965, Lin 1977, Whitton et al. 2005)

1.2.1.4 <u>Trace Elements</u>

Other than carbon nitrogen and phosphorus algae require micronutrients Mo, K, Co, Fe, Mg, Mn, B, and Zn in trace amounts but have a strong impact on microalgae growth and enzymatic activities in algal cells.

1.2.2 Light

Light is a crucial factor influencing algal growth serving as it is primary energy source for the photosynthetic processes.

The effect of the light on the microalgae is not limited only at the intensity, but also the (Richmond, 2004) light cycle and spectrum used can change significantly the growth of the biomass and its biochemical composition (Khan et al., 2018). The absorption bands of pigments in microalgae vary, making certain wavelengths more effective for photosynthesis. Red light (600-700 nm) is often optimal due to efficient chlorophyll absorption, while blue light can cause photo-inhibition(McGee et al., 2020). Understanding how different wavelengths affect growth and metabolism is essential for optimizing light sources in microalgae cultivation. Variations in light intensity can lead to changes in microalgal physiology and metabolism, affecting photosynthetic efficiency and biomass production.

The effect of the light intensity can be explained by looking at the curve that relates light intensity(I) to the photosynthetic rate(P) (Figure 3)
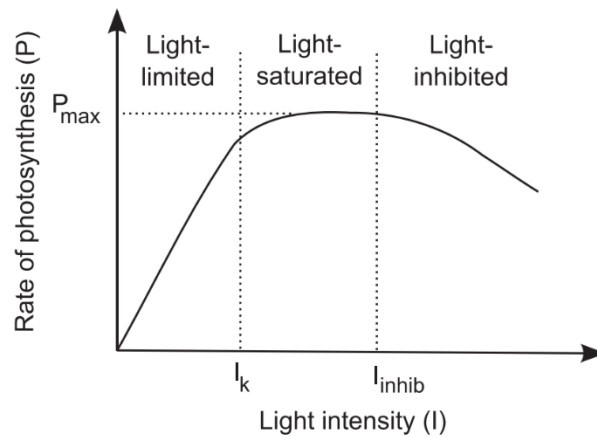
Figure 4 correlation between light intensity and photosynthetic rate.

The relationship between light intensity (I) and photosynthetic rate (P) follows a distinct pattern. At low light intensities, there's a linear correlation between light and photosynthetic rate, leading to increased biomass production. However, this trend levels off once the saturation threshold (I_k) is reached, as further increases in light intensity do not enhance photosynthetic efficiency. Surpassing the inhibitory threshold (I_{inhib}) results in a decline in photosynthetic rate due to the deactivation of crucial proteins within the photosynthetic units (Béchet et al., 2013). Consequently, deviations from the species-specific optimal light intensity, either excessive or insufficient, can lead to photoinhibition or light stress, respectively. These conditions can significantly impact overall productivity.

Adjusting the intensity of the light source based on species-specific requirements and growth phases can enhance biomass or metabolite yields while minimizing energy consumption and operational cost (Carvalho et al., 2010). To maximize biomass productivity, it is essential to determine the optimal light intensity tailored to each species' requirements, ensuring robust growth and metabolic activity while avoiding photo-inhibition or light stress. Strategies for improving light utilization include dynamic light profiles, altering light wavelengths, and modifying photobioreactor structures (Ramanna et al, 2017). Designing efficient photobioreactors to increase light efficiency poses challenges due to light attenuation within the culture medium, requiring optimization of light paths and distribution methods. In stirred photobioreactors (PBRs), microalgal cultures experience varying photosynthetic performance under sunlight, influenced by factors like light saturation and mutual shading. Additionally, considering the duration and pattern of the light/dark cycle, along with turbulent mixing in photobioreactors, plays a crucial role in microalgae growth and metabolism. Proper cycling

between light and dark periods, coupled with turbulent flow, enhances photosynthetic efficiency and metabolic processes.

Incremental light intensity strategies are essential for optimizing biomass growth in microalgae cultivation. By starting with lower light levels and gradually increasing them as biomass accumulates, these strategies effectively prevent issues like photoinhibition or light stress. This approach maximizes biomass productivity and the accumulation of desired products by fine-tuning photosynthetic efficiency and metabolic activity.

For instance, in the study by Yan et al. (2016) by gradually increasing light exposure over successive cultivation phases, the strategy optimized microalgae growth. Under this approach, microalgae achieved a dry weight of 446.98 ± 25.32 mg/L. These results underscore the effectiveness of the incremental light intensity strategy in contributing to energy savings compared to using a constant high light intensity, thereby reducing operational costs. In summary, incremental light intensity is a possible approach for enhancing productivity, ensuring energy efficiency, and facilitating product accumulation in microalgae cultivation systems, benefiting those who rely on this technology.

1.2.3 Temperature

Temperature represents another crucial element impacting the growth of microalgae, exerting a direct influence on biochemical processes such algal growth rate, cell size, biochemical composition, and nutrient requirements.

Each microalgae have its own optimal growth temperature but the cultivation of the majority of commercial and isolated microalgal species typically occurs within the temperature range of 20 to 28 °C (Daneshvar et al., 2021).

In figure below is proposed the model by Rosso et al. (1993) which correlates the effect on the temperature on the growth rate of microalgae.

It can be noticed that under minimum temperature (T_{min}) and above maximum temperature (T_{max}) the growth rate of the algae is equal to 0, while inside this interval the growth rate is positive and reach its maximum value at the optimal temperature as displayed in figure 5.

$$\mu_{\mathrm{max}} = \begin{cases} 0 \text{ for } T < T_{\mathrm{min}} \\ \mu_{\mathrm{opt}} \cdot \phi(T) \text{ for } T_{\mathrm{min}} < T < T_{\mathrm{max}}, \\ 0 \text{ for } T > T_{\mathrm{max}}, \end{cases}$$

where

$$\phi(T) = \frac{(T-T_{\mathrm{max}})(T-T_{\mathrm{min}})^2}{(T_{\mathrm{opt}}-T_{\mathrm{min}})[(T_{\mathrm{opt}}-T_{\mathrm{min}})(T-T_{\mathrm{opt}})-(T_{\mathrm{opt}}-T_{\mathrm{max}})(T_{\mathrm{opt}}+T_{\mathrm{min}}-2T)]}$$
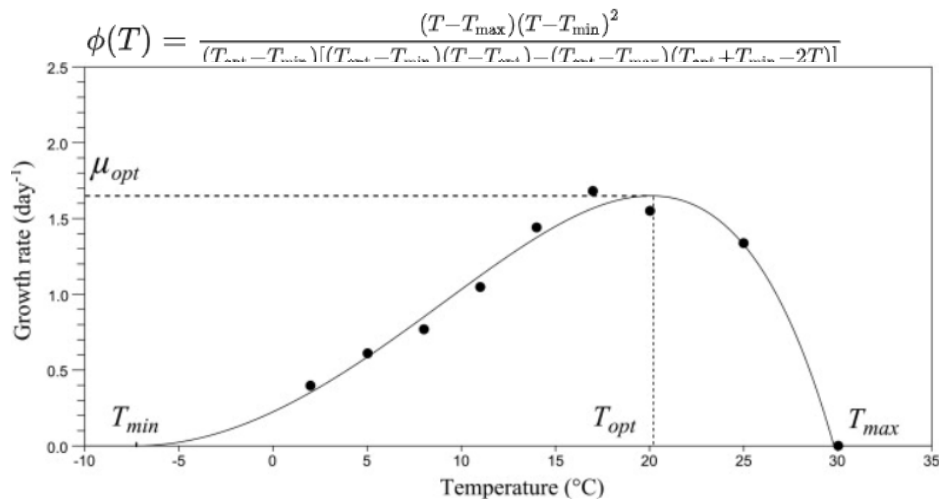

Figure 5 Dependence of temperature on growth rate.

The temperature can also has an impact on the production of biochemical, as reported by (Converti et al., 2009) the culture of *Chlorella vulgaris* produced more carbohydrates and lipids (2.5 time higher) if grown at 25 °C than at 30 °C without changing significantly its growth rate. In conclusion we can say that at low temperatures, photosynthesis is hindered as carbon assimilation activity decreases. Conversely, excessively high temperatures hinder photosynthesis by deactivating photosynthetic proteins (Khan et al., 2018).

1.2.4 Effect of pH

pH stands out as a critical factor in algal cultivation due to its role in determining the solubility and accessibility of CO_2 and essential nutrients, as well as the ammonium-ammonia equilibrium presented in paragraph 1.2.1.2. Additionally, pH can exert a substantial influence on algal metabolism. pH dynamics experience fluctuations during carbon dioxide fixation and microalgal proliferation, intricately influenced by the dissolution and uptake of carbon dioxide, underscoring the imperative for comprehensive pH control strategies (Sills, 2018). Figure 6 shows variation pH and partial pressure of CO_2 as influence by the availability of light: the pH decreases and pCO_2 increases during the dark period, while pH rises and pCO2 decreases during

the daytime (a). The magnitude of pH and pCO2 changes, as well as the light exposure per cell, vary with higher biomass density (b) (Gao, 2021).
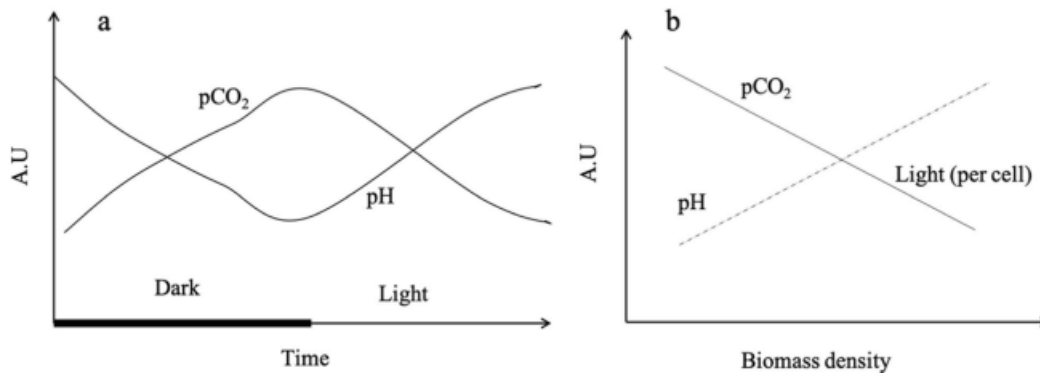
Figure 6 The changes in pH and pCO₂ during a diel cycle, with pH declining and pCO₂ rising during dark and pH rise with pCO₂ decrease during daytime (a). Amplitude of changes in pH and pCO₂ as well as light received per cell change with increased biomass density

Each microalga has its own optimal pH value for optimal growth, even though the majority grow in a pH range that typically from in sub alkaline conditions that spans from 6 to 8.76 (Khan, Shin, and Kim, 2018). However, some algal species are extremophilic and able to grow at extreme acidic and alkaline condition extreme pH conditions.

For instance, acidophilic microalgae and can resist very low pH values below 2.5 (Abiusi et al., 2022) Examples of acidophilic microalgae include *Coccomyxa onubensis, Galderia sulphuraria, Chlamydomonas acidophila*, and *Dunaliella acidophila.* The adoption of extreme growth conditions, particularly suitable for acidophilic microalgae, represents a significant advancement in industrial production, especially in tightly regulated sectors like food-grade and nutraceutical industries. Overall, incorporating these conditions brings several benefits, such as boosting productivity, enhancing quality, ensuring compliance with regulations, and improving resource efficiency.

However, maintaining optimal pH levels is crucial in microalgae cultures to ensure favorable conditions for growth and productivity. Several key pH control strategies are employed in the cultivation of microalgae.

Chemical buffers are commonly used to stabilize pH by resisting changes in acidity or alkalinity These buffers, such as bicarbonate, phosphate, and citrate buffers, help maintain pH within the desired range. Additionally, the addition of carbonates such as calcium carbonate or sodium

bicarbonate can help buffer pH fluctuations in the culture medium (Sills, 2018). These carbonates provide a source of carbonate ions that absorb excess protons or hydroxide ions, stabilizing pH.

Maintaining a steady CO_2 supply is crucial for optimal growth, with methods like pCO_2 electrodes or estimating CO_2 from pH values ensuring precise control.

Carbon dioxide (CO_2) injection is another effective strategy for pH control. pH levels are closely linked to CO_2 concentrations in the culture medium. Injecting CO_2 into the culture allows for the adjustment of pH by modulating the equilibrium between dissolved CO_2, carbonic acid, bicarbonate ions, and carbonate ions, thereby maintaining pH within the optimal range for microalgae growth (Gao, 2021).

pH stat systems are generally employed for pH adjustment in industrial microalgae cultivation. These systems constantly monitor pH levels and adjust the addition of acidic or alkaline solutions to maintain pH at the desired setpoint.

Nowadays research about optimized of control strategies is focusing on highly precise control of pH control and development of accurate sensor. Sophisticated control algorithms enhance CO_2 utilization efficiency, minimizing pH gradients and enhancing productivity.

pH is commonly measured using glass electrodes or ISFET probes, with CO_2 levels monitored using various methods like IR analyzers. Coupling CO_2 control with pH regulation enables accurate adjustment of dosage, crucial for optimizing microalgae growth pH in the culture (Bernard et al., 2016).

In conclusion, pH control is crucial in algal cultivation other environmental factor like CO_2 solubility but also metabolic processes. Microalgae have diverse pH requirements, with some species thriving in extreme conditions. Therefore, suitable, and effective strategies can be applied among chemical buffers, CO_2 injection, and pH stat systems to minimize pH fluctuations and maximizing microalgae growth and productivity.

1.3 Nutritional modes

Algae can exploit different sources energy and carbon and growth following different metabolism path.

The 3 different modes are: autotrophic, heterotrophic and mixotrophic.
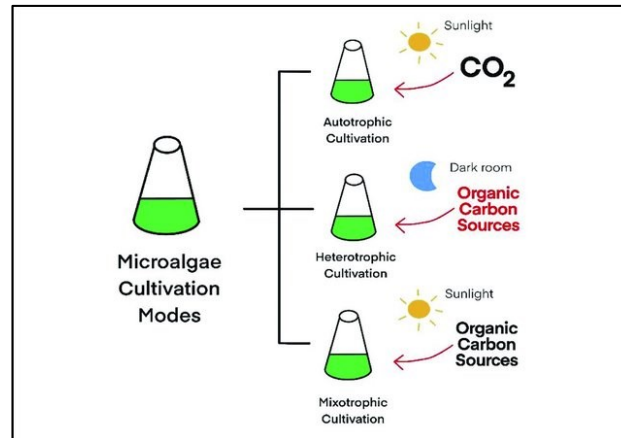
Figure 7 Trophic modes

1.3.1 AUTOTROPHIC

The autotrophic cultivation is by far the most used one:n this configuration microalgae use light as energy source and inorganic carbon as carbon source to produce organic matter through photosynthesis(Richmond, 2004).

The main advantage of this configuration is the fixation of the CO_2 which leads to two advantages: the reduction of greenhouse gases present in the atmosphere, one of the main causes of the global warming, and second the production of products with high added value(Venkata Subhash et al., 2017).

Another advantage of this type of cultivation is the low risk of contamination, in fact the absence of organic carbon reduces the competition with bacteria or other heterotrophic organism.

The drawback of this method is the light supply because it depends deeply on the location of the cultivation and using artificial light could be very expensive.

Furthermore, the productivity is lower compared to the other methods, one cause is the self-shading effect that prevents the penetration of light, limiting the growth of the cells far away from the surface (Daneshvar et al., 2021).

1.3.2 HETETROPHIC

In the heterotrophic cultivation the microalgae use as carbon source organic carbon and growth in absence of light.

The independence from the light avoids the self-shading effect which leads to 2 main benefits: higher productivity because the growth is disconnected from the light (both light-dark cycle or artificial illumination) and then because the design of the reactor is more simple reducing in this way the design costs.

On the other hand, this method has some drawbacks, the presence of organic carbon could be a source of strong contamination from other organisms as bacteria, fungi, and yeast, affecting the production and the quality of the compounds of interest(Daneshvar et al., 2021).

The bacteria can affect significantly the growth of the culture because their growth rate is higher and also their reproduction is faster (Dao et al., 2018).

So, in conclusion when a heterotrophic cultivation is performed it is paramount to sterilize properly all the equipment necessary for the growth of the culture.

1.3.3 MIXOTROPHY

In the mixotrophy regime the culture uses at the same time inorganic carbon and organic carbon as carbon source.

A clear transition from autotrophy to heterotrophy is not distinctly evident, as both processes coexist, except under complete darkness(Richmond, 2004).

The exploitation of both form of carbon and light maximize the supply of resources, it is requested less light respect the autotrophic modes and the organic carbon is less respect the heterotrophic one.

Furthermore, the high growth rate of the heterotrophic mode is maintained and also the production of pigments and carotenoids is present like in the autotrophic mode(Daneshvar et al., 2021).

The main drawbacks instead are similar to the two previous methos: like in the heterotrophic mode there is a high risk of contamination due to the presence of organic carbon, the sterilization of the equipment is fundamental.

The self-shading phenomena is also present in this configuration, it is necessary to design properly the reactor to distribute uniformly the light, increasing the cost of the equipment.

1.4 Cultivation Modes

Microalgae can be cultivated with different methods:

- Batch system
- Continuous system

1.4.1 Batch System

The batch system is the most common and simple method for cultivate microalgae.

It is a closed system, a bioreactor is filled at the beginning with the fresh medium and the algal inoculum at the right environmental condition for the growth, the CO_2 is supplied by an air stream that bubbles inside the reactor.

Ligh can be provided both from natural or artificial source, it is important to maintain the system mixed to improve the gas diffusion and to reduce the self-shading effect.

The trend of a batch run can be divided into different phases presented in figure.
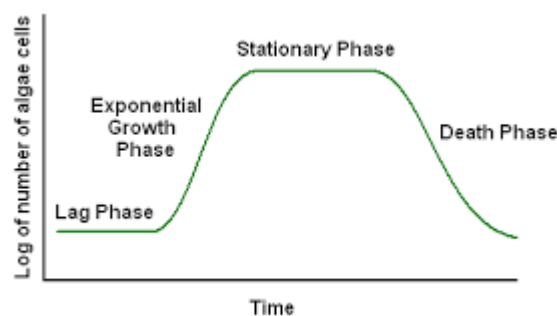
Figure 8 phases of a batch culture

The first one is the lag phase, here the growth rate of the culture is below its maximum value, this situation could happen if there are some non-viable cells in the inoculum or more frequently it happens because the cells have to acclimatize to the new environment.

This phase can be avoided if the cells used for the inoculum derived from the exponential phase.

Once acclimatize the exponential phase starts, here the cells can reproduce at maximum rate because the nutrients and the light are not limiting factors.

The growth phase can be evaluated according to the Monod model, presented in equation (2.1).

$$\frac{dC_x}{dt} = \mu_{max} \cdot \frac{S}{K_S + S} \cdot C_x \qquad\qquad (1.1)$$

Where:

- C_x is the biomass concentration [g/L]

- μ is the specific growth rate [h^{-1}]

- t is the time [h]

- μ_{max} is the maximum growth rate

- ks half saturation constant (the value of S when $\frac{\mu}{\mu_{max}} = 0.5$)

- S is the concentration of the limiting factor

This phase continues until a environmental variable becomes limiting and here we observe the stationary phase, the rate at which the cells multiply is comparable to rate of the death of the cells keeping constant the total number of cells in the system.

The last phase is the death phase where the nutrients are quite completely depleted, here the rate of death of the cells is higher respect the growth rate, the total number of cells decreases during this phase.

The main features of batch system are its simplicity and the possibility to obtain high concentration, on the other hand this system has several drawbacks.

The nutrient depletion and the accumulation of inhibitory metabolites affect the productivity, furthermore the need of manual intervention and the presence of several dead times between cultivation cycle have reduced the development of this system in the industrial sector.

1.4.2 Continuous System

The continuous system is defined as an open system where medium and product are continuously added and removed from the reaction environmental.

This approach allows to sustain the growth of the culture avoiding the nutrient depletion or accumulation of the biomass.

In this type of system, the fresh medium is constantly added to the reactor with a pump, CO_2 is supplied through bubbling and the light is provided by a natural or artificial source as in the batch system.

The biomass is removed from the reactor and collected, at the same flowrate.
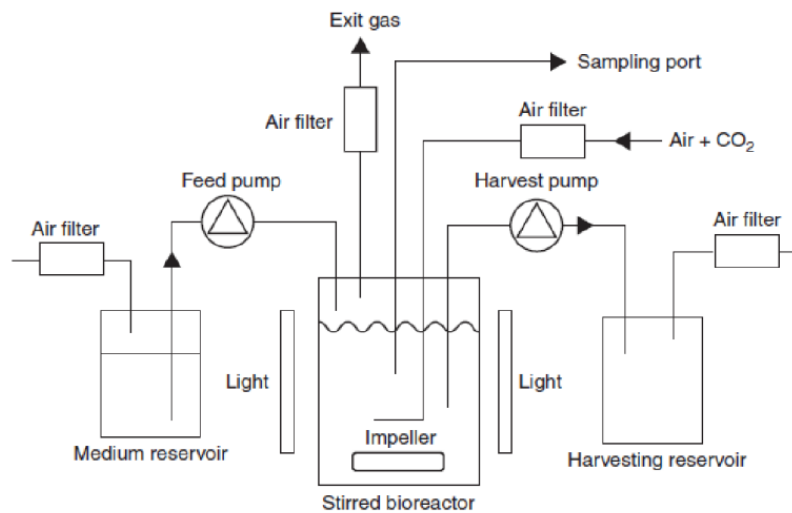
Figure 9 Schematic representation of a continuous system

The mass balance on biomass of this type of system is expressed as:

$$V_r \cdot \frac{dC_X}{dt} = \dot{V}_{in} \cdot C_{in} - \dot{V}_{out} \cdot C_{out} + \mu \cdot C_X \cdot V_r \qquad (1.2)$$

Where:

- V_r is the volume reactor
- $\frac{dC_X}{dt}$ is the accumulation term
- $\dot{V}_{in}$ is the inlet flowrate
- C_{in} is the inlet concentration
- $\dot{V}_{out}$ is the outlet flowrate
- C_{out} is the outlet concentration
- μ is the growth rate

Assuming constant the flowrate, the volume of reaction and steady state condition ($\frac{dC_X}{dt} = 0$) we can simplify the balance as:

$$0 = (C_{in} - C_X) \cdot V + \mu \cdot C_X \cdot V_r$$

Assuming also the system as a perfect CSTR (perfectly mixed) the concentration inside the reactor is equal to the one in the outlet flowrate, furthermore the inlet concentration is equal to 0 because only fresh medium is added in the system.

The equation can be rearranged as follows:

$$D = \frac{1}{\theta} = \frac{\dot{V}}{V_r} = \mu$$

θ is the residence time and can be defined as the time required to process a volume of culture equal to the volume of the reactor, the opposite of this parameter D is called dilution rate.

The dilution rate regulates the growth rate inside the reactor, decreasing its value the biomass concentration increases but the productivity of the system decreases, on the other hand increasing the dilution rate allows for greater productivity.

However, the value of the dilution rate cannot grow infinitely, but rather up to a maximum value beyond which a wash out phenomena occurred, in this situation the dilution is too high, and it doesn't give the culture the time required to growth and replicates: setting the optimal value of dilution rate is paramount to avoid the wash out and optimize the productivity.

The continuous cultivation can be performed following different cultivation methods, the most common are the turbidostat, luminostat and chemostat(Fernandes et al., 2015).

In the turbidostat system thanks to an automated control loop composed by a turbidity sensor, a pump and a controller the turbidity, so the concentration, is maintained constant inside the reactor adjusting the flowrate of fresh medium(Tang et al., 2012).

A different approach is used in the luminostat, here a light sensor is present in the rear of the reactor to measure the back irradiance.

This system aims to optimize the absorption of the light, maximizing the photosynthetic efficiency of microalgae in the PBR(Cuaresma et al., 2011).

Lastly, the chemostat is a system where fresh medium and culture inside the reactor are respectively added and removed at the same rate, keeping in this way the specific growth rate constant(Richmond, 2004).

The continuous system offers several advantages over batch systems in terms of productivity, resource utilization, and process stability, nowadays are the predominant systems at industrial level.(Fernandes et al., 2015)

1.5 Cultivation system

Various factors must be considered when selecting a culture system. These factors encompass the biology of the alga as well as the associated costs such as land, labor, energy, water, nutrients, and prevailing climate conditions.

The primary technologies utilized for microalgae cultivation encompass open system as open pons, lake or raceway ponds and closed systems, photobioreactors.

These systems can work in continuous or discontinuous mode, both are used in industry and have different advantages and drawbacks.

1.5.1 Open ponds

Open ponds technology was the first one for algae culturing, nowadays is still widely used due to its simplicity and because its well established.

Open ponds are very flexible systems, they can vary in size from lab scale to large industrial operations.

The size of this ponds may assume different shapes, usually circular or oval (Figure 6),
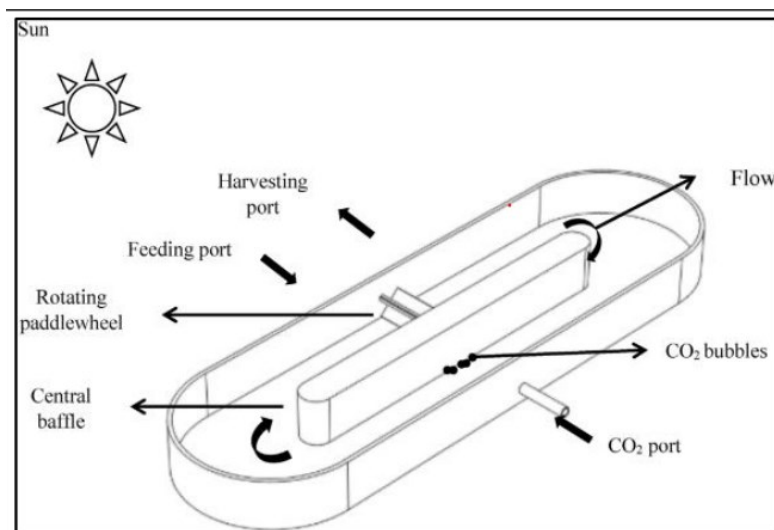
Figure 10 Open Pond system for algae cultivation

The depth varies from centimeters to few meters while the construction material is usually concrete but also plastic or brick.

Optimizing the dimensions of the pond, the mixing is fundamental to avoid deposition and to maximize the light penetration to avoid the self-shading phenomena.

The advantages of these ponds is regarded to their simple and economical construction and high production capacities (Ahmad et al., 2021).

The main drawbacks of these system are the poor light distribution, evaporation due to the impossibility of controlling environmental parameters.

Another drawback is the high risk of contamination that can reduce drastically the productivity of the system, only a small number of algal species can grow successfully in open air pons (Borowitzka, 1999)

1.5.2 Closed system

To overcome the problem of the open ponds different type of photobioreactor were developed. Closed photobioreactors are enclosed systems designed to provide optimal conditions for microalgae growth and productivity. They come in various configurations, including tubular, flat-panel, bubble column PBRs.

PBRs allow control over environmental factors, minimize contamination risks, and can be operated year-round.

The main advantages of closed systems are a better control on growth conditions, higher productivity, and the possibility to work in axenic condition limiting in this way the risk of contamination.

The closed PBRs due to the high surface over volume ratio are much more efficient than the open system, on the other hand, all these features make the system more expensive, limiting its large-scale development.

Tubular PBR

Tubular PBR are the most widely spread photobioreactors, in this type of configuration several straight transparent tubes are connected in series by U-bends to form a serpentine that can be arranged either vertically or horizontally(Richmond, 2007).

The diameter of the pipes is usually less than 10 centimeters in order to have a large illuminated surface inside the system, the culture flows inside the pipes by the aim of a pump.

In this type of configuration are present 3 different areas: the solar array exposed to the light to the cell growth, the harvesting unit, and the degassing column.

In this last section fresh medium and air (or air enriched with CO_2) are added, and it is present also a temperature control system(Wang et al., 2012).

In figure a tubular PBR is schematized.
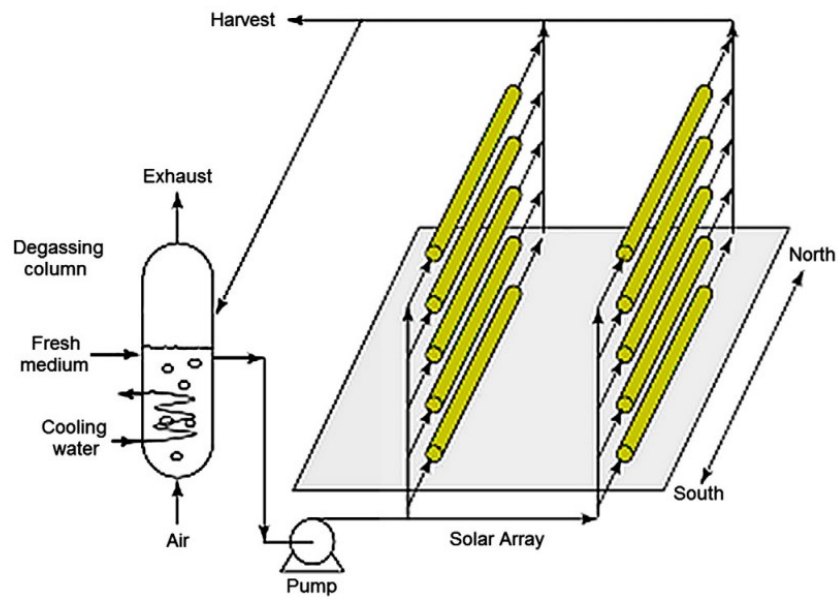
Figure 11 Tubular PBR for microalgae cultivation

Flat Panel PBR

Flat panel photobioreactors are rectangular shaped reactors composed by transparent boxes of plexiglass, polycarbonate, or glass.

The high surface over volume ratio enables a homogeneous distribution of the light enhancing the growth and biomass productivity(Takenaka and Yamaguchi, 2014).

The aeration is provided by tubes or sparger at the bottom of the flat panel, a stirrer could be present to increase the mixing, illumination can be both natural and artificial.

Figure 12 Flat panel PBR for microalgae cultivation

In the figure above is presented an imagine of a flat panel.

This configuration however has some drawbacks, mainly the difficulty to scale-up and the adhesion on the surface that decrease the light penetration.

Column PBR

Vertical tubular reactors are simple systems in which mixing is achieved by injecting compressed air.

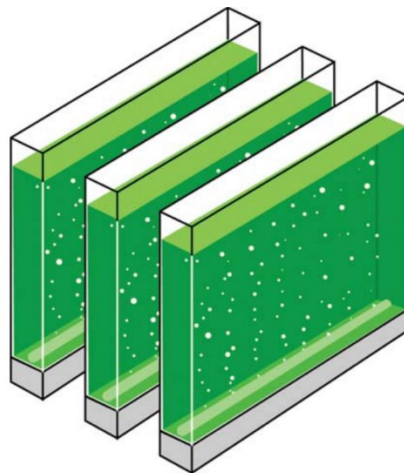They are usually cylinders with radius of up to 0.2 m and heights of up to 4 m, these proportions are required to increase the surface–volume ratio.

The schematic diagram of a conventional internal loop airlift PBR is shown in Fig.9B, typically comprised a transparent column, an internal column, and an air sparger.

In the internal column the gas is released in pressure by the sparger which moves upward also the culture medium, in the outer tube the culture moves downward back to the bottom of the column.

Figure 13 Bubble column PBR
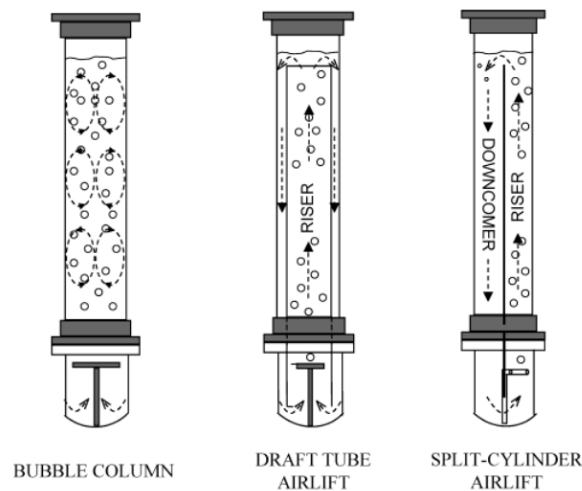

The main advantages of this type of system are: high surface area to volume ratio, satisfactory heat and mass transfer, relatively homogeneous culture density and no moving parts(Ahmad et al., 2021)

The main disadvantage of this type of configuration is the formation of algal deposition in the surface of the reactor, however the replacement is easy and cheap(Takenaka and Yamaguchi, 2014).

1.6 CellDEG

CellDEG system is a new patented technology for the microalgae cultivation in autotrophic mode, it allows an excellent use of the light and a controlled and adjustable supply of carbon dioxide.

It belongs to the category of porous membrane PBRs, in this type of reactors the gas dispersion is maximized thanks to the great interfacial area provided by the membrane (Chanquia et al., 2022)

CellDEG allows a rapid growth up to extremely high biomass concentrations. Biomass yields are about 10 times higher than those reached with classic bubble-stream techniques.

The system is divided in two sections separated by a thin hydrophobic and highly gas-permeable membrane: the lower chamber is a channel where a rich CO_2 atmosphere is present, the CO_2 concentration is controlled by a CO_2 injection.

The upper chamber contains 9 algal cultivators with a variable working volume between 100 and 150 milliliters.

Oxygen is released by the upper membrane by diffusion preventing its accumulation in the system.

Turbulent liquid flow close to the membrane surface causes an extremely fast bubble-free mass transfer of CO_2 into the bulk culture, avoiding CO_2 deficiency in the cultivators. Another benefit of the turbulent mixing is the formation of an optimized layer thickness of the culture, this allows an excellent and homogeneous transfer of the light inside the cultivators, ensuring a high quantum yield of photosynthesis in the cultivators and avoiding the self-shading effect.
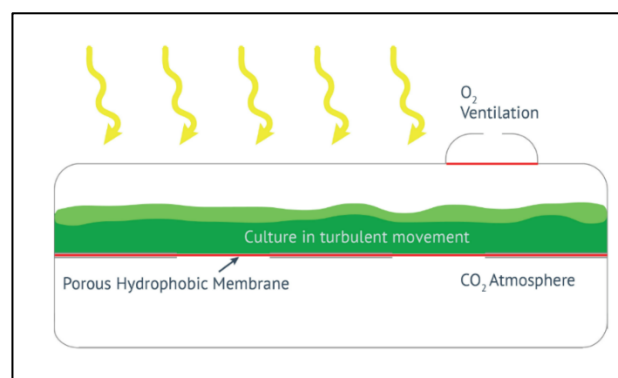

Figure 14 CellDEG technolgy(Lippi et al., 2018)

This system is regulated by a growth control unit (GCU), it is designed to enable precise adjustment of CO_2 partial pressure and LED light intensity, two crucial factors influencing microalgae growth. This unit features advanced functionalities, including the ability to set constant, linear, or exponential progressions and combination of these for light intensity and CO_2 partial pressure, allowing for customized growth conditions tailored to specific microalgae strains and cultivation objectives.

Furthermore, the presence of multiple cultivators enables the testing of several condition at the same time, several comparative analyses can be performed in a single run in order to find the optimal growth condition
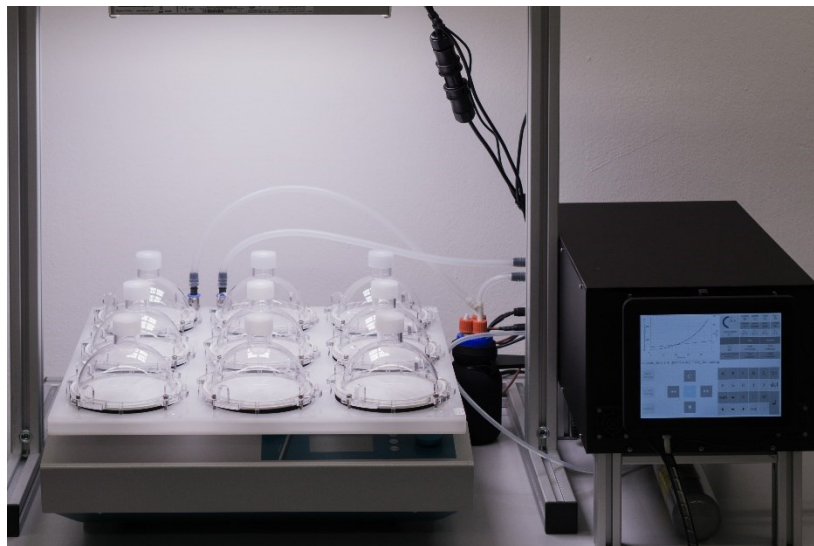
Figure 15 CELLDeg system with HD100 cultivators

The CellDEG system has found applicability in various studies, yielding excellent results,

a research from Lippi et al., 2018 investigate the production of cyanophicin from BW86, an engineered strain of the cyanobacteria *Synechocystis,* in a high cell density cultivation.

This study displayed that the strain BW86 reach a maximum of 1 gram of cyanophicin after 4 days, whereas conventional cultivation yields a maximum value of 0.28 g CP per L culture, attained after 12 days of cultivation.

Freudenberg et al., 2021 studied the production of cadaverine between 3 different systems, a 6-well microtiter plates, the HD100(CellDEG) and a 2L Erlenmeyer flasks.

The results displayed that in the HD100 system, the volumetric yield and productivity of cadaverine were twofold higher compared to cultivation in 6-well microtiter plates, reaching 248 mg/L and 100 mg/L/d, respectively, representing the highest yields among the three systems analyzed.

This highlight the importance of sufficient CO_2 supply facilitated by a high surface area for effective cadaverine production, while also suggesting that a steep light gradient may not have as adverse an effect if adequate mixing is ensured.

1.7 Coccomyxa onubensis

Coccomyxa onubensis is a species of green microalga belonging to the genus *Coccomyxa*. This unicellular organism is characterized by its small size, about 3 μm in length and 2 μm wide, its shape is approximately ellipsoidal.

It shows a distinct cell wall and it possess a very large chloroplast that partially surrounds the nucleus and seems to occupy about half of the total cell volume.

It was observed that it contains lipid droplets, an increased number of starch bodies as well as electron-dense deposits and plastoglobules (Garbayo et al., 2012).

The nucleus and nucleolus are about 1 μm in length, 1 μm wide, and 0.25–0.15 μm in diameter, respectively, and are located in the central portion of the microalga(Garbayo et al., 2012).

It belongs to the extremophile algae, a category of microalgae that are able to grow under high or low temperature, under high or low pH, in the presence of metal ions, under high irradiance, and also in the presence of a number of other extremophile microorganisms in the same habitats(Varshney et al., 2015)

This category of microalgae is experiencing particular interest thanks to its adaptability, it can be cultivated in harsh environmental conditions where the growth of most species is inhibited.

Another feature is the possibility of cultivating them in open systems for large production, the risk of contamination from bacteria, fungi and other microorganism is drastically reduced.

The particularity of *Coccomyxa onubensis* is its ability to growth in very acid environment and with a high rate of salinity, *Coccomyxa onubensis* was firstly isolated from Tinto River area

near Huelva (Spain), an acidic river that exhibits very low value of pH, between 1.5 and 3, furthermore heavy metals such as Fe, Cu, Mn, Ni, and Al are present in high concentrations.
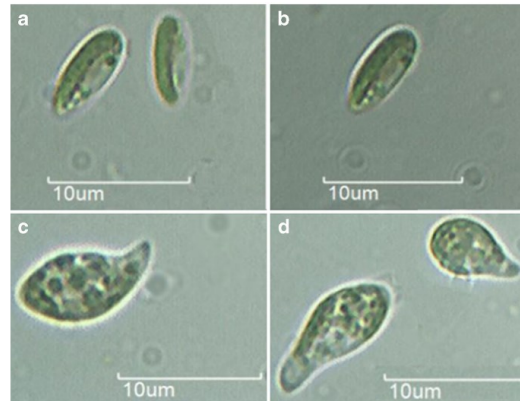
Figure 16 Light microscope image of Coccomyxa onubensis

This novel microalga is reaching interest for its interesting features, it has a high growth rate when cultivated photoautotrophycally (up to 0.6 d^{-1}) respect other acidophilic microalgae and the compounds produced are of particular interest. The pigment composition of the algae is notably abundant in carotenoids, with a particular emphasis on lutein. This observation implies that the microalgae could hold promise to produce antioxidants, specifically xanthophylls.

(Ruiz-Domínguez et al., 2015) it has been reported that when *Coccomyxa onubensis* is cultivated under nutrient deprivation fatty acids were accumulated, resembling those found in non-extremophile microalgae, with linolenic acid (C18:3) being the most prevalent fatty acid.

1.8 Lutein

Lutein((3R,6R,3′R)-β,ε-Carotene-3,3′-diol) is a primary carotenoid belonging to the xanthopyll class, appears as a yellowish-orange solid.

The structure of lutein is very similar to the beta-carotene with the difference that it has two terminal hydroxyl groups(Figure 13)

From a biological point of view lutein participates in light harvesting and serves as a structural component in the photosynthetic apparatus.

It is also important in preserving the photosynthetic apparatus from oxidative damage under high light intensities through a mechanism termed non-photochemical quenching. (Zheng et al., 2022)
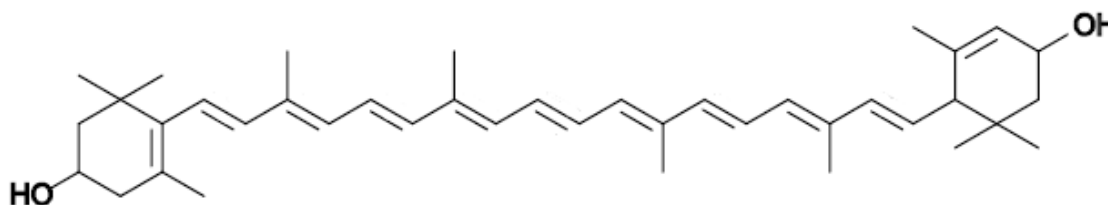
Figure 17 Chemical structure of lutein

Lutein finds wide-ranging applications across various industries, mainly in feed, food, health care and pharmaceuticals. Lutein is the only carotenoid that can be absorbed in the bloodstream after ingestion (John et al. 2002) and accumulated in the human retina and is assumed to have a protective effect due to its ability to filter out blue light and age-related macular degeneration (AMD) (Roberts et al., 2009), furthermore multiple research shown that lutein has other benefits against retinal nerve disease (Ozawa et al., 2012; Sasaki et al., 2009), Alzheimer's disease (Kiko et al., 2012; Min and Min, 2014), and diabetic retinopathy (Arnal et al., 2009). Lutein market size was valued 381 million dollars in 2023 with a growth rate of 6% from 2024 to 2032 ("Lutein Market Size & Share, Growth Analysis Report 2024-2032,")

Figure 18 Lutein market trend between 2024 and 2032

Lutein is synthesized only by plants and it is found in high quantities in green leafy vegetables like spinach or yellow carrots, at industrial level the marigold flowers are the major fount of

lutein production(Breithaupt et al., 2002),however the content of lutein in dry weight is extremely low(around 0.03%)(Sánchez et al., 2008a), moreover there are other problems related to the availability of the land and seasonality.

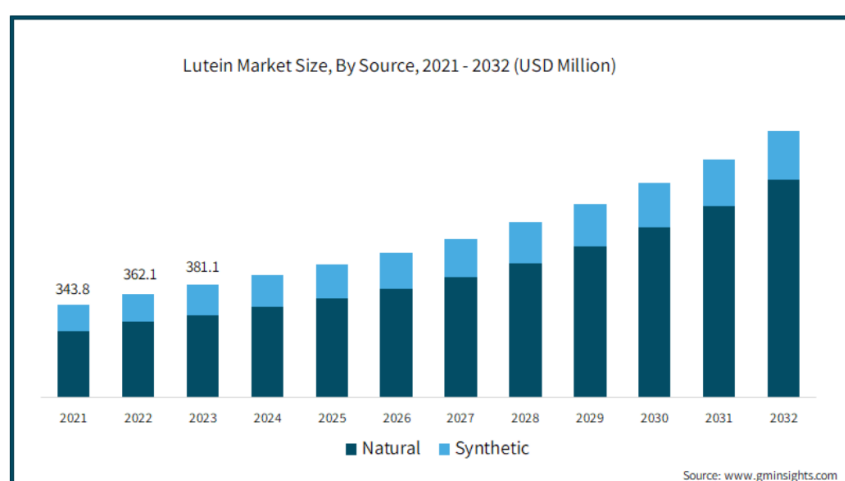Lutein can also be produced synthetically but the low yields of the this process makes this way totally off the market.(Fernández-Sevilla et al., 2010)

Due to these problems microalgae are receiving attention as alternative source of lutein production. Microalgae have several benefits when used as a lutein source, first there is no seasonal harvesting restrictions and the growth rate is higher than marigold (Lin et al., 2015); furthermore, the lutein content (up to 0.5–1.2% dry weight) in the microalgal biomass and the lutein productivity are high.

On the other hand, the production of lutein from microalgae has not taken off yet because the high costs of cultivation technology and extraction treatments do not make it economically advantageous.

As reported by Xie et al. 2021 and(Fernández-Sevilla et al., 2010) several studies reported that the species where the lutein was present in higher concentration were *Scenedesmus, Chlorella, Parachlorella and Tetraselmis* the amount of lutein present in these species was between 5-7.7 mg/g.

Recently some studies were conducted to evaluate the amount of lutein present in the *Coccomyxa onubensis* to exploit its ability to grown in very harsh conditions reducing the risk of contamination.

A study conducted by (Bermejo et al., 2018) evaluated the production of lutein in a two steps process, the first one with 100 mM of NaCl for 72 hr to increase the biomass and then the salinity was increased to 500 mM of NaCl to stress the culture and increase the amount of carotenoids.

The study reported that the amount of lutein present in the culture was 7.8 mg/g, an excellent result when compared with other microalgae of interest.

In another study of (Fuentes et al., 2020) *C. onubensis* was cultivated using an 800 L vertical tubular PBR placed outdoors, the system was controlled and kept at pH equal to 2.5 while the temperature was bounded between 5 and 26 °C.

They found a maximum lutein concentration of 10 mg/g and a productivity of 1.42 mg/(L d)

In light of this, *C.onubensis* would appear to be an excellent candidate for large-scale lutein production.

1.9 Design of Dynamic Experiment

Design of Experiment (DoE) is a systematic and structured approach used by researchers and scientists to plan, conduct, and analyze experiments in various fields, including engineering, chemistry, biology, and social sciences. The primary goal of DoE is to investigate the relationship efficiently and effectively between input variables (factors) and output variables (responses).

The main advantage of this method is the possibility to minimizing sources of variability and maximizing the information gained from the experiment.

Unfortunately, in a batch process, the time evolution of an operating condition, such as temperature, can have a substantial impact on the result.

 In such cases, the classical DoE methodology does not offer an efficient and systematic way to explore the impact that a multitude of time dependencies of one or several operating conditions have in the process performance.

Using a dynamic approach the limitation of time independent variable is removed, proposing an important generalization that will be referred to as Design of Dynamic Experiments (DoDE).(Georgakis, 2013).

At this moment this approach is not still used extensively, in particular for microalgae biotechnology but some studies had reported some interesting results, a research proposed by (Trentin et al., 2023) aimed to maximize the production of cyanophicin from *Synechocystis sp.* showed that information derived from the initial model required a strict interval in order to find out the optimum for temperature, phosphorus feeding strategy and light intensity. After the application of the updated dynamic design, the updated model was employed to pinpoint the optimum at the condition of the cyanophicin production increased by 20% equal to 228.2 ± 20.0 mg/L respect the maximum value reported before the optimization (184.3 ± 0.8 mg/L).

Further application of DoDe methodology have been applied in few studies for the pharmaceutical industry for instance to optimize a crucial asymmetric catalytic hydrogenation reaction (Makrydaki et al., 2010),for process improvement in the manufacture of monoclonal antibodies (Luo et al., 2023), to effectively optimize batch crystallization processes (Fiordalis and Georgakis, 2013), to study the reaction kinetics of penicillin fermentation process (Klebanov and Georgakis, 2016). However, despite its design to maximize information while minimizing the number of experimental runs, the increasing complexity and variability of inputs over time in this field lead to a high number of experiments, often lasting weeks, and significant cost constraints, limiting its widespread application.

In summary, the DoDE involves carefully planning and executing experiments to investigate how a system evolves over time in response to dynamic conditions of the input variables.

By manipulating variables over time and observing their effects on the system, a complete insight into complex systems can be assessed.

1.10 Aim of the thesis

In this thesis, the acidophilic microalgae *Coccomyxa onubensis* was investigated as an excellent candidate for the production of high added values compounds such as lutein, given its ability to withstand very low pH environments significantly reducing the risk of bacterial contamination.

A design of dynamic experiments (DoDE) was applied to maximize the information while minimizing the number of experimental runs. The objective of applying investigate and optimize the production of biomass and high-value compounds such as carbohydrates, chlorophyll, and carotenoids.

The experimental campaign of 13 weeks was conducted in the CellDEG system, a high cell density cultivator which allows to perform several experiments at the same time with an accurate control on the input variables.

In particular, 39 different condition varying light intensity, carbon dioxide partial pressure and nitrogen amount will be set to evaluate the influence of these variables on the algal growth and on its composition.Surface plot will be produced to find the optimal conditions for the different compounds of interest.

Chapter 2
Material and Methods

In this chapter, detailed accounts of the microalgae species, the culture medium, and cultivation system employed are reported. Subsequently, the experimental campaign is outlined, accompanied by comprehensive descriptions of all analytical procedures utilized to monitor microalgal growth and the biochemical composition, specifically focusing on the content of hydrophobic pigments, carbohydrates in the algal biomass, and the nitrogen quota. The primary research focus centres on carotenoids, particularly the accessory pigment lutein. Finally, the procedure for extraction and quantification of carotenoids, with a specific emphasis on lutein content, is presented.

2.1 Algal strain and culture media

The strain *Coccomyxa onubensis* SAG 2510 (Figure 1) was purchased from SAG-Göttingen (Germany) and identified as polyextremophilic microalgae, demonstrating remarkable resilience and adaptability to extreme environmental conditions, including variations in pH, salinity, and heavy metal tolerance.

Figure 19 Optical microscope image of Coccomyxa onubensis SAG 3510

In this study, the microorganism has been initially maintained in a 100 ml shake flask at room temperature in a 100 ml flask K9 medium, with orbital shaking. In this study, the microorganisms were initially cultured in 100 mL shake flasks using K9 medium at room temperature with orbital shaking. Subsequently, a two-step scale-up process was implemented to enhance the inoculum size. The pre-culture system of *C. onubensis* was established using bubble column photobioreactors, transitioning first from flasks to 250 mL bubble columns (BC), and then advancing to a working volume of 1000 mL in a borosilicate bottle (DURAN) as shown in Figure 21. The culture underwent bi-weekly refreshment, where half of the algal culture volume was removed and replenished with freshly prepared growing media. This process aimed to supply nutrients necessary for sustaining growth and maintaining the culture in the exponential phase.

Figure 20 Bubble column photobioreactor

Continuous light exposure was provided by an LED panel set at $100 \frac{\mu mol}{m^2/s}$ and inorganic carbon was supplied through a constant flux of air enriched with CO_2 (5% v/v). Mixing was ensured using a magnetic stirrer positioned at the bottom of the reactor. The system was housed in an incubator with a consistent temperature maintained at 24°C. The described culture conditions were held constant throughout all the experiments.

According to the chemical composition of the natural environment, cultures were grown at pH 2.5 in a culture medium based on the K9 medium. The modified K9 medium composition is

reported in Table 2.1, the pH was brought to the specified value with a 5M HCl solution. The concentrations of macronutrients in the culture medium utilized for the experiments conducted in the high cell density cultivation system were doubled compared to the original recipe to prevent nutrient limitation. Meanwhile, the nitrate concentration in the medium was adjusted according to the design of dynamic experiments.

Table 1 composition of the K9 medium

Components	*K9*	*K9(2X)*
K_2SO_4 (g/L)	3.95	7.90
KCl (g/L)	0.1	0.2
K_2HPO_4 (g/L)	0.5	1
$MgCl_2$ (g/L)	0.41	0.82
KNO_3 (g/L)	2.29	0
$CaCL_2$ (g/L)	0.01	0.02
Hutner trace elements(ml/L)	5	10

Table 2 Composition of Hutner trace elements solution

Components	*Concentrations*
$Na_2EDTA \cdot 2H_2O$ (g/L)	50
$ZnSO_4 \cdot 7H2O$ (g/L)	22
H_3BO_3 (g/L)	11.4
$MnCl_2 \cdot 4H2O$ (g/L)	5.06
$FeSO_4 \cdot 7H2O$ (g/L)	4.99
$CoCl_2 \cdot 6H2O$ (g/L)	1.61
$CuSO_4 \cdot 5H2O$ (g/L)	1.57
$(NH_4)_6Mo_7O_{24} \cdot 4H2O$ (g/L)	1.10

2.2 Cultivation system

In the experimental setup, *C. onubensis* has been grown using the CellDEG photobioreactor (CellDEG, Germany), a novel high-density cultivation system. It comprised nine detachable HD100 cultivators, integrated with the CellDEG Growth-Control-Unit (GCU) as represented in Figure 3.

This configuration enables robust and parallel growth, is useful for achieving heightened cell densities, beneficial for comparative analyses aimed at optimizing culture conditions or media formulations. The cultivators are securely mounted on EPDM gaskets with a bayonet locking mechanism. Equipped with a bottom-mounted gas supply membrane, the HD100 Cultivator ensures efficient gas exchange while minimizing shear stress. Before each experiment, the cultivators undergo sterilization, requiring treatment with 10% v/v H_2O_2 followed by two washes with autoclaved deionized water to render them deployable. The Growth Control Unit (GCU) serves as a sophisticated gas mixing unit, providing precise control over CO_2 partial pressure and LED light intensity. Sensor-driven gas dosing enables seamless adjustments in light intensity and CO_2 partial pressure, whether linear or exponential. The CO_2 was provided on each cultivator by the chamber below the cultivators through the hydrophobic membrane mounted at the bottom of the HD100, the oxygen accumulation in the cultivators was avoided thanks to a gas-outlet membrane attached in the cap of the cultivators. The CO_2 partial pressure in the bottom chamber was controlled by the Growth control unit of the CellDEG directly connected to a CO_2 cylinder.

The light source utilized in the experiment consisted of an LED lamp (Valoya RX500) featuring an optimized light spectrum. Positioned above the culture, the lamp's height was adjustable to ensure different ranges of light intensities. The cultivators were kept in agitation by an orbital oscillator (GFL 3017) at 150 rpm to increase the turbulent mixing and avoid the deposition of microalgae on the cultivators' surface.

To maintain constant growth conditions, the cultivation system was placed inside a growth chamber where ambient temperature was controlled. A sensor placed inside one of the cultivators ensured that the algal culture remained at the set point. Temperature control was achieved using an on/off controller connected to an infrared ultra-thin heating panel positioned behind the cultivation platform.

In this study, the system can be assumed as a fed-batch because it was open only in the inlet, CO_2 and nitric nitrogen in form were supplied during the experimental runs while in the outlet nothing was taken until the end of the experiment.

The system was composed by 9 parallel HD100 cultivators with a working volume of 150 ml, the light was provided by a led lamp with an adjustable intensity between 80 and 1000 $\frac{\mu mol}{m^2 \cdot s}$. The system was maintained at a constant temperature of 27 °C and 24 hours illumination.

Figure 21 CellDEG system equipped with HD100 cultivator, GCU and LED lamp

2.3 Experimental Setup

The factors considered for the experiment campaign were:

- The light intensity profile with a variable time for reaching the final peak
- The nitrogen-fed profile with a variable time to stop the feeding
- The partial pressure of CO_2

Since dynamic factors are considered, a Design of Dynamic experiments (DoDE) was used to plan the experimental campaign. Specifically, 1 factor described the variable time for reaching the light intensity peak, 2 subfactors described the light intensity profile, 1 factor described the

variable time to end the feeding, and 2 subfactors described the profile of feed nitrogen. Accordingly, 7 dynamic factors are considered.

The total number of experiments required to build the model was 36 plus 3 additional runs to assess the lack of fit, to perform the 39 experiments planned by the design 13 weeks were required.

The experimental runs were set according to DoDE specifications to evaluate the combined effect of light intensity, nitrogen amount, and CO_2 partial pressure. After 96 hours, the pre-cultures were used to inoculate HD cultivators. All cultures were diluted to an optical density (OD) at the wavelength of 750nm equal to 0.5, and each experimental condition was performed in 3 biological replicates. For each experimental batch, 3 different experimental runs were performed in parallel.

The experimental runs lasted for 7 days, and the cultivators were sampled daily. One milliliter of culture was taken daily to monitor growth through measurements of OD. Additionally, every 2 to 3 days, 8 milliliters of culture were taken for analysis of dry weight, carbohydrates, pigments, and nitrogen quota. The final volume of each cultivator after 1 week was around 130 milliliters.

2.3.1 CO_2 partial pressure

The value of CO_2 partial pressure was kept constant during the experimental runs, 3 different values were studied to evaluate the growth at different conditions.

The first one was in the air (0.04%) to evaluate the growth of *Coccomyxa onubensis* in atmospheric conditions, the second was at 1% while the third was at 10% a value like the CO_2 percentage in the flue gas.

2.3.2 Light Intensity

The light was the same for all the runs of the experimental batch, in figure 4 the different light profiles are presented.
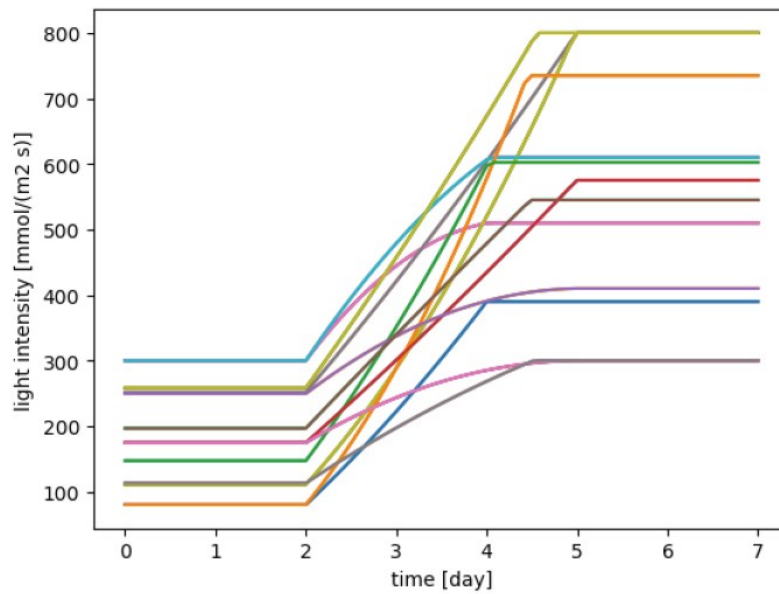
Figure 22 Planned light intensity profiles for all 13 batches through DoDE

As shown in figure 4 the light profiles alternate constant and linear trends.

The initial values of the light were between 80 and 300 $\frac{\mu mol}{m^2 \cdot s}$ and were kept constant for 2 days to photo-acclimatize the growth culture. After 2 days a ramp profile started, the duration of this profile lasted between 48 and 72 hours until reaching the peak value that remained constant until the end of the experimental batch. The peak value was bounded between 300 and 800 $\frac{\mu mol}{m^2 \cdot s}$

2.3.3 Nitrogen feeding

Another factor analyzed was the nitrogen fed to the cultures; nitrogen was supplied in the form of nitrate using concentrate stocks of potassium nitrate (KNO_3).

The amount of nitrogen fed along the entire culture was bounded between 6 and 60 mg and it was added with different profiles that are presented in figure 3. As shown in figure 5 each run started with the initial nitrogen concentration required by the design and then, in the following days nitrogen was added at discrete time intervals, once a day at the same hour every day.

The feeding duration of the runs was variable, and it was bounded between 2 and 5 days.
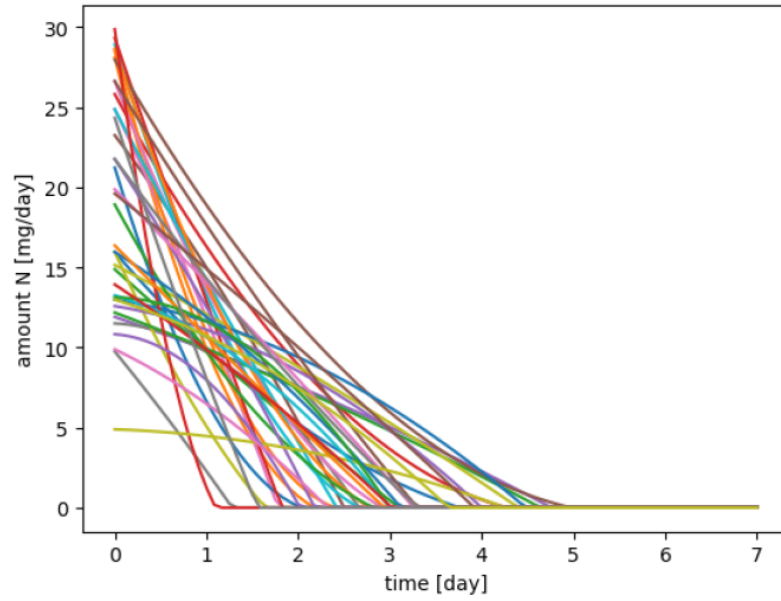
Figure 23 Planned fed nitrogen profiles for all 39 experimental runs through DoDE

2.4 DoDE problem statement

2.4.1 Light profiles DoDE

DoDE determines factors profiles for light intensity according to a normalized time τ_1 calculated as:

$$\tau_1 = \frac{t - t_i}{t_f}$$

(2.1)

where $t_i = 2\ days$ is the absolute time at which profiles starts to variate, and t_f is the time at which profiles end their variation. It is determined to be $t_f \in [4, 5]$ days as:

$$t_f = (4.5 - t_i) + 0.5\ x_1$$

(2.2)

Where x_1 is the first factor controlling the end of the light profile. The constraints on x_1 are $-1 \leq x_1 \leq 1$. During the variation the light profile is constrained to start [80, 300] $\mu mol/m^2\ s$ and end [300, 800] $\mu mol/m^2\ s$, resulting bounded within the profiles:

$$r_L = 80 + 220\ \tau_1$$

(2. 3)

$$r_U = 300 + 500\ \tau_1$$

(2. 4)

From this it is possible to calculate the light profiles:

$$I_0 = (r_U + r_L)/2 = 190 + 360\ \tau_1$$

(2. 5)

$$\Delta I = (r_U - r_L)/2 = 110 + 140\ \tau_1$$

(2. 6)

$$I(\tau_1) = I_0(\tau_1) + \Delta I(\tau_1)\ (x_2 - x_3 + 2\ \tau_1\ x_3)$$

(2. 7)

Considering the light profiles as controlled by to dynamic subfactors (x_2 and x_3). The constraints on the dynamic subfactors are $-1 \leq x_2 \pm x_3 \leq 1$. To ensure to obtain a monotone increasing profile of light a constraint on first derivative is:

$$\frac{dI}{d\tau_1} \geq 0$$

(2. 8)

$$360 + 140\ x_2 + 80\ x_3 + 560\ \tau_1\ x_3 \geq 0$$

(2. 9)

This can be considered as an increasing line in function of τ_1; hance it must have the point at $\tau_1 = 1$ greater than zero.

$$360 + 140\ x_2 + 80\ x_3 + 560\ x_3 \geq 0$$

(2. 10)

2.4.2 Nutrient profiles DoDE

DoDE determines factors profiles for the fed nitrogen according to a normalized time τ_2 calculated as:

$$\tau_2 = \frac{t}{t_{f2}}$$

(2. 11)

Where t_{f2} is the time at which the nitrogen feeding is stopped. It is determined to be $t_{f2} \in [1,5]$ days (no feeding action is performed at and after day 5) as:

$$t_f = 3 + 2\,x_4$$

(2. 12)

Where x_4 is the factor controlling the end of the nitrogen fed profile. The constraint on x_4 is $-1 \le x_4 \le 1$. To determine the ranges for the fed nitrogen it is supposed that at maximum half of the total nitrogen can be provided within the first day of culture. Accordingly, the initial ranges for the nitrogen fed is [3, 30] mg/day. Accordingly, the fed nitrogen profiles are bounded within the profiles:

$$u_L = 3 - 3\,\tau_2$$

(2. 13)

$$u_U = 30 - 30\,\tau_2$$

(2. 14)

From this it is possible to calculate the fed nitrogen profiles

$$u_0 = (u_U + u_L)/2 = 16.5 - 16.5\,\tau_2$$

(2. 15)

$$\Delta u = (r_U - r_L)/2 = 13.5 - 13.5\,\tau_2$$

(2. 16)

$$u(\tau_2) = u_0(\tau_2) + \Delta u(\tau_2)\,(x_5 - x_6 + 2\,\tau_2\,x_6)$$

(2. 17)

Considering the fed nitrogen profiles as controlled by to dynamic subfactors (x_5 and x_6). The constraints on the dynamic subfactors are $-1 \le x_5 \pm x_6 \le 1$. To ensure to obtain a monotone decreasing profile of fed nitrogen a constraint on first derivative is imposed:

$$\frac{du}{d\tau_2} \geq 0$$

(2. 18)

$$-16.5 - 13.5\, x_5 + 40.5\, x_6 - 54\, \tau_2\, x_6 \leq 0$$

(2. 19)

This can be considered as a decreasing line in function of τ_2; hance it must have the points at $\tau_2 = 0$ and $\tau_2 = 1$ smaller than zero.

$$-16.5 - 13.5\, x_5 + 40.5\, x_6 \leq 0$$

(2. 20)

$$-16.5 - 13.5\, x_5 + 40.5\, x_6 - 54\, x_6 \leq 0$$

(2. 21)

To ensure that the total amount of nitrogen fed along the entire culture is between 6 and 60 mg another constraint is given by:

$$6 \leq \int_0^{t_{f2}} [(16.5 - 16.5\, \tau 2) + (13.5 - 13.5\, \tau 2)(x5 - x6 + 2\, \tau 2\, x6)]dt \leq 60$$

(2. 22)

$$6 \leq (8.25 + 6.75\, x_5 - 2.25\, x_6)(3 + 2\, x_4) \leq 60$$

(2. 23)

2.4.3 Carbon dioxide

Partial pressure of CO_2 is constrained to assume the value of 0.04%,1% and 10%. From these constraints it is possible to calculate the boundaries for the factors:

$$u_0 = 5.02\%$$
$$\Delta u = 4.98\%$$

Accordingly, the constraints results:

Tabella 3 Partial pressure of CO_2 constraints in term of value and factors

pCO$_2$	x$_7$
0.04%	-1
1%	-0.8072
10%	1

2.5 Microalge growth monitoring

2.5.1 Optical density

Microalgae growth was monitored every day by verifying the OD.

OD measurements were performed using a double-beam spectrophotometer (Shimadzu – UV 1900) and plastic cuvettes with 1 cm light path (*l*). The instrument was set at 750 nm. Absorbance was measured daily by using 1 mL of culture sample and using as reference the K9 medium.

For absorbance values greater than 1 the growth medium was used as diluting agent so as not to lose the linear correlation between biomass concentration and absorbance given by the Lambert-Beer equation

2.5.2 Dry weight

The measurement of dry weight (DW) stands as a precise method for determining biomass concentration, typically denoted as the concentration of biomass per unit of culture volume (g/L). Establishing a correlation between daily OD measurements and periodic DW measurements enables the creation of a linear relationship for each experimental batch. This correlation facilitates quantitative measurement of biomass densities, enhancing the precision and reliability of experimental assessments.

The protocol for the measurement of DW can be summarized as:

1. A filter of 47 mm with a pore diameter of 0.45 μm (Whatsmann) was dried at 110 °C for at least 10 minutes in order to remove the moisture content.
2. Dried filter was weighted using a high precision balance (Biosan Microspin 12) with a sensitivity of 10^{-4} g for the tare evaluation.
3. A sample of 3 mL was filtrated using a vacuum pump.
4. The filter with the retained biomass was dried for at least 2 hours at 110 °C
5. Dried filter was weighed to evaluate the gross weight.

    The dry weight (W) was calculated using Equation 2.1, where W and V represent the dry weight and volume, respectively.

$$DW \left(\frac{g}{L}\right) = \frac{W_{filter+biomass} - W_{filter}}{V_{sample}}$$

(2. 24)

2.6 Analytical measurements

2.6.1 Hydrophobic pigments analysis

The measurement of hydrophilic pigment based on spectrophotometry involves quantifying pigment concentration in a liquid sample based on its absorption characteristics. This method allows for the precise determination of chlorophyll and carotenoids, providing insights into photosynthetic pigmentation in biological samples. In this study, the pigments during the experimental campaign were periodically analyzed over the 7 days of cultivation.

The protocol for the spectrophotometric measurement of pigment extraction can be summarized as:

1. Centrifugation (Microspin 12) of 1 ml of the sample for 10 minutes at 13500 rpm.
2. The supernatant was removed.
3. The pellet was suspended with 1 ml of N, N-dimethylformamide (DMF), an organic solvent able to extract hydrophobic pigments from the biomass.
4. The sample was subsequently stored at -18 °C for at least 24 hours for the extraction.
5. After the extraction phase the sample was brought to room temperature and then centrifuged for 10 minutes at 13500 rpm.
6. The quantification was performed with a spectrophotometer (Shimadzu UV-1900 UV-VIS Spectrophotometer) analyzing the absorbance of the sample in the light range between 350-750 nm, the DMF was used as reference.

If the absorbance was greater than 1 a dilution was necessary, the DMF was used as a diluting agent.

Pigment analytical quantification was obtained by applying correlations reported in equations 2.25 and 2.26 (Wellburn, 1994).

$$Chlo\ (\mu g/mL) \ = \ (OD_{664} - OD_{750}) * 11.92 * D$$

<div align="right">(2. 25)</div>

$$Carot\ (\mu g/mL) \ = \ ((OD_{461} - OD_{750}) - (OD_{664} - OD_{750}) * 0.04) * 4 * D$$

<div align="right">(2. 26)</div>

2.6.2 Carbohydrates analysis

The content of carbohydrates in the biomass were periodically analysed over the 7 days of cultivation. The measurement of carbohydrates in biomass involves employing a colorimetric method with an initial reaction sulfuric acid and Anthrone, followed by spectrophotometric analysis, facilitating the quantification of carbohydrate content.

The protocol for the spectrophotometric measurement of can be Carbohydrates summarized as:

1. A reactant composed by 2 g/L of Anthrone, 71% v/v of sulphuric acid and 29% v/v of distilled water was prepared.

2. 100 µL of sample was collected in an Eppendorf and then reacted with 900 µL of the reactant in a thermostated bath set at 100 °C for 10 minutes.

3. 100 µL volume of distilled water was used as a reference using the same procedure of the samples.

4. The samples were analysed using the spectrophotometer set at 625 nm and the reacted distilled water as reference.

5. The concentration of the carbohydrates was evaluated from a calibration curve, derived from a solution of pure glucose.
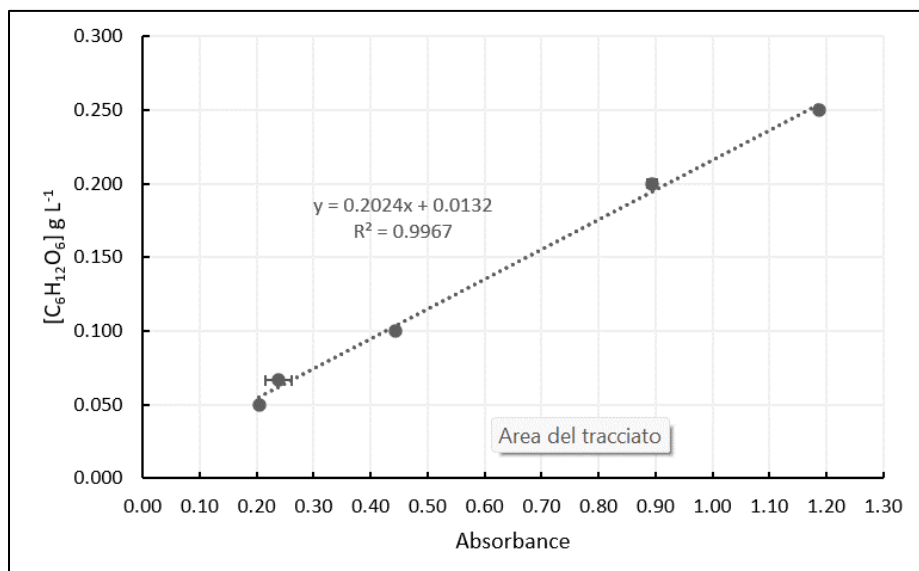

$$y = 0.2024x + 0.0132$$
$$R^2 = 0.9967$$

Figure 24 carbohydrates correlation curve

From the linear correlation between the concentration of pure glucose and the relative absorbance was identified the equation 2.4 for the quantification of the carbohydrates.

$$[C_6H_{12}O_6] = 0.2024*OD_{625} + 0.0132$$

(2. 27)

2.6.3 Total nitrogen

The evaluation of the concentration of nitrogen present in the culture was analysed with the Toc analyser (Shimadzu Corporation, Kyoto, Japan)

During the experimental campaign were analysed both the nitrogen concentration in the culture and the one present in the medium, to analyse the total nitrogen content inside the biomass and to understand the nitrogen uptake dynamics.

Before the analysis the samples were appropriately diluted to be within the calibration curve (5 µg L-1 - 100 mg L-1) using milli-Q water.

The formula for the evaluation of the total nitrogen amount is given by the ratio of the concentration inside the biomass (the difference between the total nitrogen in the culture and the nitrogen present in the medium) and the total biomass concentration.

$$C_{N,Biomass} = C_{N,cuture} - C_{N,supernatant}$$

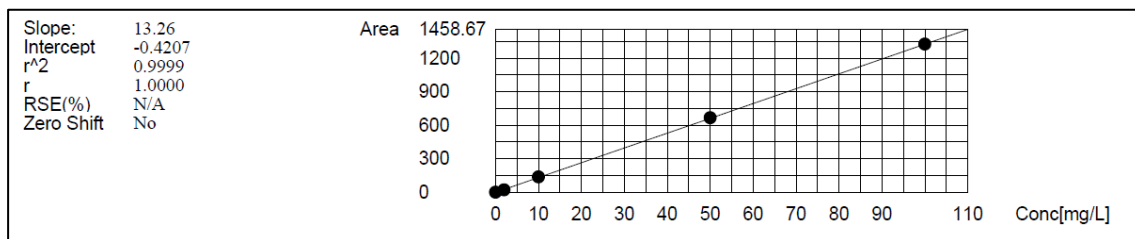(2. 28)

$$q_{N=\frac{C_N}{C_X}}$$

(2. 29)

Figure 25 Total Nitrogen calibration curve

2.6.4 Lutein extraction analysis

Lutein, accessory hydrophobic pigment, is commonly quantified in biological samples using high-performance liquid chromatography (HPLC), enabling precise analysis of its concentration and distribution. The protocol is divided in two steps, the extraction of the carotenoid and the quantification.

- Carotenoid extraction and saponification

  1. Carotenoid compounds, including lutein, were exhaustively extracted from 50 mg freeze-dried samples with 7 mL acetone and methanol (70:30 v/v) using Lysing Matrix E, 2 mL Tubes (MP Biomedicals).

  2. The tubes were placed in a horizontal holder and vortexed for 5 minutes (vortex-2 genie, Scientific Industries), followed by centrifugation (miniSpin plus, Eppendorf) at 9,000 g, at room temperature for 10 minutes until the supernatant turned colorless (Mandelli et al., 2012). All procedures were performed in dim light to prevent the oxidation and photodamage of the carotenoids.

  3. For the microalga *Coccomyxa onubensis*, the biomass turned colourless after 5 cycles of extraction with 1.4 ml of acetone and methanol (70:30 v/v).

  4. The extract was filtered through a 0.22 μm polyethylene membrane and concentrated under a nitrogen stream.

  5. The concentrated extract was further suspended in a 5 mL mixture of petroleum ether/diethyl ether (1:1 v/v) and saponified with 5 mL methanolic KOH 10% (w/v) at room temperature for 16 hours.

  6. Alkali in the sample was removed by washing with 5 mL sodium chloride 10% (w/v) (Fig. 1).

    [1]
- Lutein Standards preparations

  1. Stock solutions of 1 mg/mL of lutein (Sigma Aldrich) are prepared, separately, by dissolving with MeOH.

  2. 100 μL of each standard stock solution (step 1) reached 1mL by diluting with HPLC grade methanol and stock solutions of 100 mg/L of lutein will be achieved.

  3. Standard stock solutions are filtered through a 0.22 μm PTFE membrane before the HPLC determination.

4. Standard solutions used in the calibration procedure are obtained by diluting the stock solutions with methanol yielding final concentrations of 10, 25, 50, 70, and 100 mg/L for lutein. The above solutions are stored at -20 °C until HPLC analysis.

[2]

- Analysis of lutein content by HPLC

The analysis of lutein content was performed by Ultra-high-performance liquid chromatography, UHPLC with a UV-VIS detector (Ultimate 3000, Thermo Scientific, Denmark) and a C18 column 5 μm, 150 × 4.6 mm (Phenomenex). The mobile phase was composed of methanol and acetonitrile (96:4 v/v) (HPLC grade). The mobile phase needs to be filtered and sonicated prior to the experiments. The sample injection is 20 μL at room temperature, with a 0.7 mL/min flow rate of the mobile phase. The detection was performed at a wavelength of 450 nm. The retention time is 3.16 min for lutein. The chromatogram data was processed using the Chromeleon version 7.2.9 software (Thermo Scientific, Denmark).

Chapter 3
Experimental results and discussion

In this chapter the experimental results are presented.

The results of 39 experimental runs will be presented in the following order: biomass productivity, carotenoid concentrations, carotenoid productivity.

For each topic, the results will be first shown, highlighting the main effect of the parameters and their interaction on the proper response.

Subsequently, an optimization of the model will be presented to find the optimal value of each factor that leads to the maximization of the response, a suggested profile for each result will be suggested.

A comparison between the profiles of light, nutrient supply and carbon dioxide concentration will be assess with studies present in scientific literature. In the end preliminary results of lutein content will be presented and discussed.

3.1 Experimental condition

The initial experimental design was aimed at estimating a Response Surface Methodology (RSM) model to optimize the value of carotenoid concentration and productivity in the culture at the end of the batch (day 7). It was made of 36 independent experiments plus 3 additional replicates carried out at the central point of the domain. Specifically, the experimental campaign is composed of 39 experiments that were carried out in 13 weeks.

Every week, 3 conditions were performed in triplicate to reduce the experimental error.

The input variables considered in this study was the incremental incident light intensity, the nitrogen amount and the partial pressure of CO_2, and their effects were assessed on carotenoid production by *Coccomyxa onubensis* cultivated in batch experiments, of 7 days duration each. A total of seven factors were considered in the design: 3 sub-factors for the incident light intensity (dynamic factor), three sub-factors related to the nitrogen inlet profile (also a dynamic factor) and one for the pCO_2 (fixed factor). The details related to the factor can be summarized as follows:

1. The light intensity varied from an initial value between *80* and *300* $\frac{\mu mol}{m^2 \cdot s}$ and reached, between the fourth and fifth day, the luminous peak enclosed in a range between *300* and *800* $\frac{\mu mol}{m^2 \cdot s}$.

2. The amount of total nitrogen supplied to each photobioreactor was bounded between *6* and *60 mg/day* and was added in different time intervals, between 1 and 5 days, according to the requirements of the experimental design.

3. The partial pressure of CO_2 was divided into 3 levels *0.04* (air), *1* and *10 % (v/v)* and remained constant throughout the week.

Table 1 describes the details related to each factor for the 39 experiments.

Table 1 detailed description of DoDE variables

ID	pCO$_2$ $\left[\% \frac{v}{v}\right]$	Initial light intensity $\left[\frac{\mu mol}{m^2 \cdot s}\right]$	Time to reach the light peak [day]	Final light intensity $\left[\frac{\mu mol}{m^2 \cdot s}\right]$	Total nitrogen fed $[mg_N]$	Duration of the feeding [day]
B01_01	10	300	4.02	510	24.42462531	4
B01_02	10	300	4.02	510	26.28428519	2
B01_03	10	300	4.02	510	33.13165896	4
B02_01	0.04	251.6	4.995	800	22.90273635	3
B02_02	0.04	251.6	4.995	800	31.10742188	4
B02_03	0.04	251.6	4.995	800	33.69064566	4
B03_01	1	110.8	4.98	800	22.5088753	4
B03_02	1	110.8	4.98	800	51.73558879	5
B03_03	1	110.8	4.98	800	13.29087086	5
B04_01	1	300	4.035	610	41.38334199	5
B04_02	1	300	4.035	610	30.60147454	3
B04_03	1	300	4.035	610	23.936875	3
B05_01	0.04	80	4	390	30.48826983	5

B05_02	0.04	80	4	390	6.418670654	2
B05_03	0.04	80	4	390	27.42870773	4
B06_01	0.04	80	4.45	735	30.8605	3
B06_02	0.04	80	4.45	735	34.91561639	5
B06_03	0.04	80	4.45	735	23.79592991	3
B07_01	10	147.1	4.02	602.5	23.26612596	2
B07_02	10	147.1	4.02	602.5	29.44135484	3
B07_03	10	147.1	4.02	602.5	26.1625	3
B08_01	1	174.6	4.995	575	20.08708457	3
B08_02	1	174.6	4.995	575	35.75119002	5
B08_03	1	174.6	4.995	575	22.2674531	4
B09_01	0.04	249.4	4.995	410	11.76735735	2
B09_02	0.04	249.4	4.995	410	31.07715924	3
B09_03	0.04	249.4	4.995	410	14.30242611	3
B10_01	0.04	196.6	4.485	545	29.49576111	3
B10_02	0.04	196.6	4.485	545	21.62108999	3
B10_03	0.04	196.6	4.485	545	39.48444398	4
B11_01	10	174.6	4.99	300	15.96929907	3
B11_02	10	174.6	4.99	300	13.18344697	2
B11_03	10	174.6	4.99	300	12.82473757	3
B12_01	1	113	4.52	300	24.83452908	3
B12_02	1	113	4.52	300	24.80667363	3
B12_03	1	113	4.52	300	18.21699858	2
B13_01	10	258.2	4.555	800	29.92979551	5
B13_02	10	258.2	4.555	800	41.56239956	4
B13_03	10	258.2	4.555	800	27.57497726	4

As reported in chapter 2 to evaluate all these variables, 7 factors were required. The equations describing the different profile are reported in section 2.4:

1. 3 for the light, one represents the time to reach the peak and 2 to describe the light profiles.
2. 3 for the nutrient, one to describe the time to stop the feeding and 2 for the profiles.
3. 1 for the carbon dioxide partial pressure

In table 2 below the factors of the dynamic design are reported.

Table 2 factors of the DoDE

Name	Code	Factors
tf_light	X_1	Time at which light profile reaches the peak
light_1	X_2	First dynamic subfactor for light profile
light_2	X_3	Second dynamic factor for light profile
pCO$_2$	X_4	CO_2 partial pressure
tf_nutrient	X_5	Time at which nutrient feeding is stopped
nutrient_1	X_6	First dynamic subfactor for nutrient profile
nutrient_2	X_7	Second dynamic subfactor for nutrient profile

In the table below a detailed description of all factors in all different conditions is presented.

Table 3 value of the factors in different experimental condition

CONDITION	X_1	X_2	X_3	X_4	X_5	X_6	X_7
B01_01	-0.96	0.42	-0.58	1	0.38	-0.37	-0.33
B01_02	-0.96	0.42	-0.58	1	-0.59	0.9	-0.05
B01_03	-0.96	0.42	-0.58	1	0.13	0.3	0.05
B02_01	0.99	0.78	0.22	-1	-0.41	0.07	-0.79
B02_02	0.99	0.78	0.22	-1	0.5	0.04	0.33
B02_03	0.99	0.78	0.22	-1	0.15	0.24	-0.15
B03_01	0.96	0.14	0.86	-0.8072	0.05	-0.16	-0.04
B03_02	0.96	0.14	0.86	-0.8072	0.99	0.05	-0.8
B03_03	0.96	0.14	0.86	-0.8072	0.63	-0.71	0.15
B04_01	-0.93	0.62	-0.38	-0.8072	0.64	-0.03	-0.72
B04_02	-0.93	0.62	-0.38	-0.8072	-0.04	0.12	-0.63
B04_03	-0.93	0.62	-0.38	-0.8072	0	0.06	0.3
B05_01	-1	-0.82	0.18	-1	0.88	-0.24	0.1
B05_02	-1	-0.82	0.18	-1	-0.86	-0.47	0.03
B05_03	-1	-0.82	0.18	-1	0.06	0.14	0.18
B06_01	-0.1	-0.13	0.87	-1	-0.25	0.66	0.16
B06_02	-0.1	-0.13	0.87	-1	0.7	-0.02	0.08
B06_03	-0.1	-0.13	0.87	-1	-0.03	-0.03	-0.02
B07_01	-0.96	-0.09	0.3	1	-0.61	0.76	0.14
B07_02	-0.96	-0.09	0.3	1	-0.29	0.56	-0.06
B07_03	-0.96	-0.09	0.3	1	0	0.23	0.48
B08_01	0.99	-0.02	0.12	-0.8072	-0.17	0.03	0.4

B08_02	0.99	-0.02	0.12	-0.8072	0.74	0.07	0.33
B08_03	0.99	-0.02	0.12	-0.8072	0.01	-0.1	0.09
B09_01	0.99	-0.01	-0.55	-1	-0.68	-0.22	-0.18
B09_02	0.99	-0.01	-0.55	-1	-0.11	0.2	-0.7
B09_03	0.99	-0.01	-0.55	-1	-0.49	-0.05	0.37
B10_01	-0.03	0.02	-0.04	-1	-0.17	0.17	-0.75
B10_02	-0.03	0.02	-0.04	-1	-0.09	-0.22	-0.4
B10_03	-0.03	0.02	-0.04	-1	0.46	0.29	0.06
B11_01	0.98	-0.57	-0.43	1	-0.48	-0.27	-0.62
B11_02	0.98	-0.57	-0.43	1	-0.95	0.33	-0.66
B11_03	0.98	-0.57	-0.43	1	-0.34	-0.36	0.13
B12_01	0.04	-0.85	-0.15	-0.8072	-0.3	0.02	-0.87
B12_02	0.04	-0.85	-0.15	-0.8072	-0.41	0.5	0.11
B12_03	0.04	-0.85	-0.15	-0.8072	-0.72	0.47	-0.11
B13_01	0.11	0.81	0.19	1	0.82	-0.24	0.08
B13_02	0.11	0.81	0.19	1	0.15	0.59	-0.16
B13_03	0.11	0.81	0.19	1	0.32	-0.02	0.24

3.2 Biomass productivity

In this section, the experimental results of the biomass productivity of the experimental campaign will be presented. In the figure are displayed the productivity of 39 conditions obtained from experimental campaign.
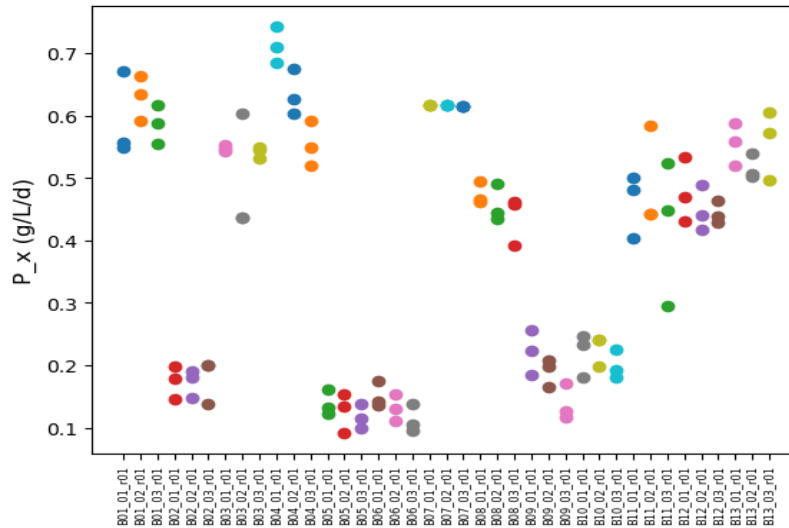

Figure 26 scatter plot of the biomass productivity of the 39 experimental results

Small differences among replicate measurements were detected for biomass productivity.

In some cases, measurements are very repeatable and very close to each other (see B03_01, B07_01, B07_02, B07_03). In other cases, larger differences among replicates have been observed in biomass productivity (B01_01, B03_02, B11_02, B11_03).

The values of productivity are very different among the different conditions tested: they vary between a minimum value of 0.1 g/L/d and a maximum productivity of 0.75 g/L/d for B_04_01. From the plot it is evident that B_02, B_05, B_06,B_09,B_10 grow less respect the others conditions, the biomass productivity in these condition is lower than 0.3 g/L/d.

 All these batches were all set at the minimum level of CO_2, it can be concluded that the carbon dioxide is a limiting factor when the algal cultures grow in air(0.04%).

3.2.1 PCA analysis

Principal Component Analysis (PCA) is a statistical technique used to analyse high-dimensional data by transforming it into a new coordinate system, it is commonly used for dimensionality reduction, visualization, and exploratory data analysis. PCA identifies patterns and relationships within the data, facilitating the interpretation of complex datasets and highlighting the most significant factors influencing the variability observed.

In this study, a principal components analysis was performed to evaluate the impact of the PBRs position and the similarity on the replicates.

In figure 27, a scatter plot with the position of the bioreactors in the different configurations is presented.
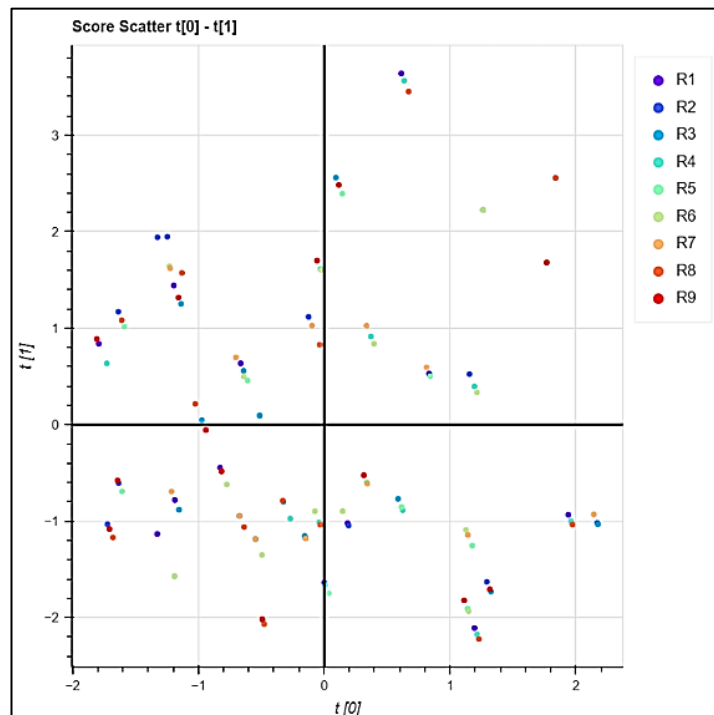
Figure 27 Scatter plot of the position of the PBRs

The absence of clustering associated with the position in the bioreactor suggests that there are no detectable effects attributable to bioreactor positioning. Furthermore, observations taken in the same bioreactor position exhibit a normal spread in the score space. This implies that the variability observed in the dataset is not primarily driven by differences in bioreactor positioning. Instead, it suggests that other factors, not related to bioreactor placement, are the main sources of variability in the dataset.

3.2.2 DoDE analysis for biomass productivity

3.2.2.1 Analysis of the main effects and interactions

In this section, it is presented the analysis of the main effect of interaction on biomass productivity. The analysis of main effects and interactions represents a fundamental aspect of experimental design, particularly where variables are time-varying. This concept refers to the systematic examination of how independent variables individually influence the dependent variable (main effects) and how they may interact with each other, leading to non-additive effects on the outcome of the experiment. Main effects refer to the independent influence of each variable on the dependent variable, averaged across all levels of other variables. In the context of dynamic experiments, main effects analysis allows researchers to understand the direct impact of each variable on the outcome over time, regardless of other factors. Interactions occur when the effect of one variable on the dependent variable depends on the level of another variable. In dynamic experiments, interactions may manifest as changes in the relationship between variables over time. Analysing interactions is crucial as they can reveal complex relationships that may not be apparent when considering variables in isolation.

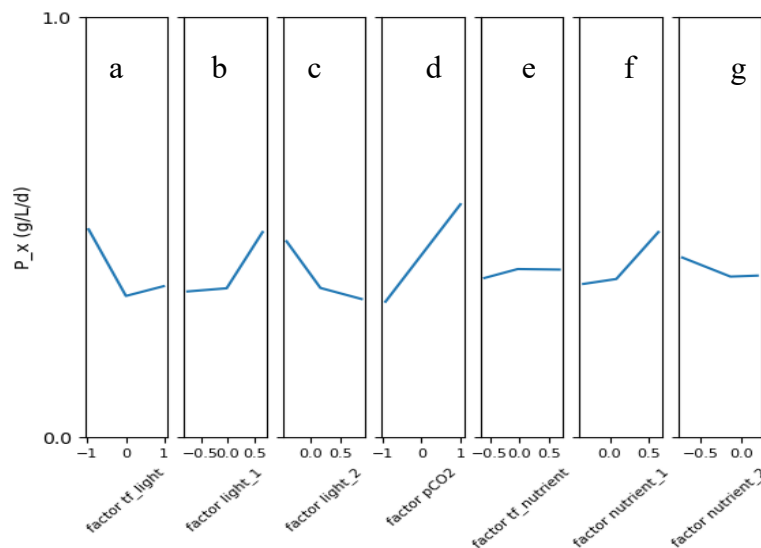In the figure below the main effect of the factors on the biomass productivity is presented.

Figure 28 Main factors effect on the response

From the plot some considerations can be done. The time at which the light peak (*tf_light*) is reached has a large negative effect, this means that to increase biomass productivity, the

maximum light intensity must be reached in the shortest possible time so that the algal culture can grow in high light for extended duration.

The profile of the light intensity profile controlled by the subfactors *light_1, light_2* show different effects: *light_1* having a positive effect on the response while light_2 exhibit a negative effect.

In the light of these results to increased biomass productivity the light profile should start from a high initial value and reach a final peak medium of light intensity.

The partial pressure of CO_2 (*pCO₂*) has a large positive effect, indicating that for maximize the productivity of the biomass the concentration of the CO_2 in the PBR must be approaching the upper limit.

The time to stop feeding (*tf_nutrient)* exert minimal influence: graph 28.e shows that the trend is almost a flat line, indicating it does not play a large role in determining the biomass productivity.

The factors associated to nutrient profile show different effects. *Nutrient_1* has a small positive effect with non-linearities, while *nutrient_2* has a small negative effect. Accordingly, to increase biomass productivity, the provided nutrient should be high at the beginning and decrease to zero with a small upward concavity.

In figure 29, a first suggested profile of light and nitrogen is presented.

The optimal light profile starts from the maximum value of the lower bound for light ($300 \frac{\mu mol}{m^2 \cdot s}$) and reach rapidly the peak value of $600 \frac{\mu mol}{m^2 \cdot s}$ that lasts for the remaining 3 days.

Regarding nitrogen, the optimized profile starts with a high initial nitrogen concentration, subsequently feeding continuously for three days before stopping for the rest of the week.

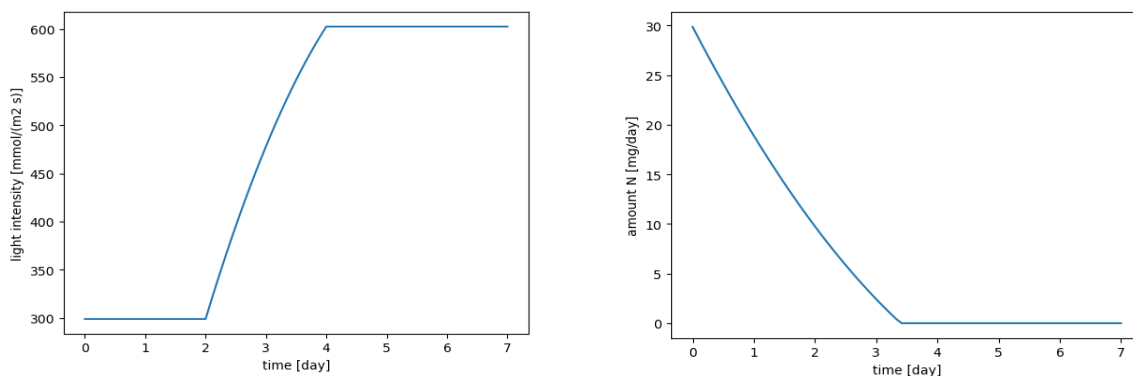The concentration of the CO_2 is set at its maximum value (10%).

Figure 29 suggested light and feeding profile for maximize biomass productivity

3.2.3 Modelling and analysis of the model

To model the relationship between factors and response (biomass productivity) a quadratic model with interactions was selected because it allows to further perform the optimization of the biomass productivity. The formulation of the quadratic model with interactions is:

$$y = \beta_0 + \sum_{i=1}^{F} \beta_i \cdot x_i + \sum_{i=1}^{F} \beta_{i,j} \cdot x_i \cdot x_j$$

where β_0 is the intercept, β_i are the coefficients of the linear terms, $\beta_{i,j}$ are the coefficients of the interaction and quadratic terms, x_i are the factors, and F is the total number of factors.

An iterative validation over 250 iterations was performed to assess the quality of the model to describe unseen experimental spaces. The validation of the model was performed by iteratively excluding 3 randomly selected observations while building the model on the remaining 36 observations.

Coefficient of determination was calculated for the validation observations and averaged over the 250 validation iterations.

Initial model

A complete quadratic model with interactions built over all 39 observations achieved a coefficient of determination $R^2 = 97.0$ % ($R^2_{adj} = 95.8\%$) indicating a very good representation of the calibration data. In validation, the model achieved a coefficient of determination $Q^2 = 90.8\%$ indicating good performance in representing unseen data. The validation performance can be considered satisfactory for a biological application characterized by large variability and affected by many factors.

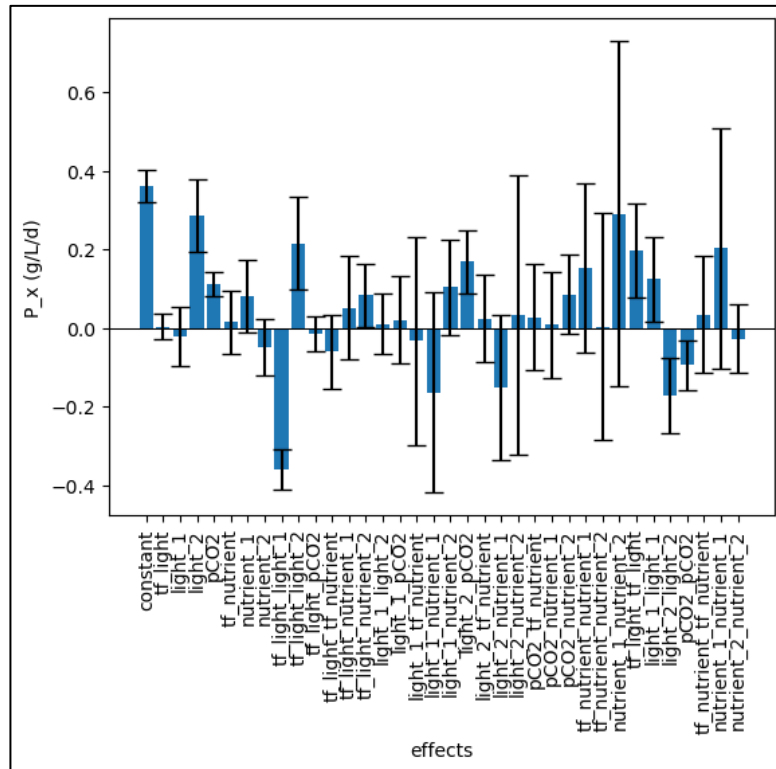The model parameters with their 95% confidence limits are reported.

Figure 30 Parameters of the complete quadratic model

At this point, the model is characterized by large confidence limits of the parameters; hence, improvements were required.

3.2.4 Model improvement

To improve the model a stepwise regression was performed. In stepwise regression, non-significant model terms, characterized by non-significant model parameters, were iteratively excluded according to the p-value (calculated during least square regression). The term with the highest p-value was excluded at each iteration until all model terms were significant (p-value < 0.05). The improved model built on all observations achieved a coefficient of determination $R^2 = 96.3\%$ ($R^2_{adj} = 95.8\%$) indicating a good representation the calibration data. However, results of the refined model were slightly inferior to the initial model, indicating that the exclusion of non-significant factor had no effect on the model performance. In validation, the model achieved a coefficient of determination $Q^2 = 89.9\%$ indicating good performance on validation data, especially for a biological application characterized by large

variability of the response. The refined model showed slightly lower performance on unseen data than the initial model. This can be due to the exclusion of effects that can have an influence on biomass productivity but cannot be estimated properly from the available experimental data.
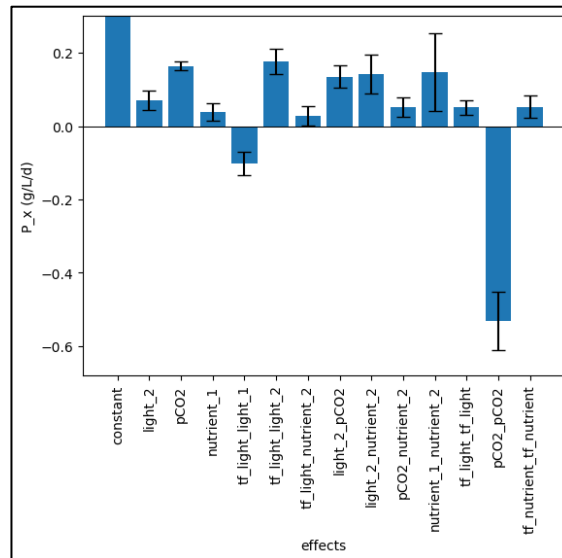

Figure 31 improved model parameters

From this plot the main effect of the model parameters after the improvement are presented. It is evident that the quadratic effect of CO_2 partial pressure is the parameters that influence more the response.

3.2.5 Analysis on the response

The effect of factors on biomass productivity was analysed through the Response Surface that can be obtained from the model improved. In the response surface, the value of the response was depicted as function of 2 factors, while the remaining ones are fixed or varied across multiple levels.

In the figure below a surface plot parametric at different *tf_light* as function of the 2 light subfactors is shown. The other factors are fixed as follows: *pCO₂=1, tf_nutrient=0, nutrient_1=*-0.59, nutrient_2=-0.4.
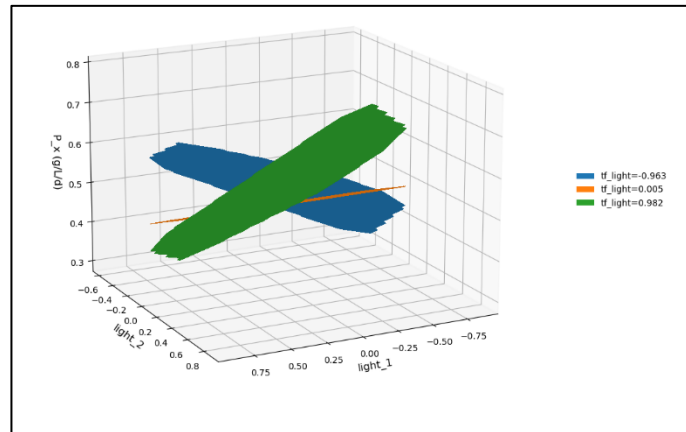
Figure 32 surface plot parametric in tf_light

The highest productivity is reached at a *tf_light* equal to -0.963 and for a high negative value of light_1 and a value close to 0 for factor light_1.

The total productivity is around 0.65 g/L/d.

In figure 33 a surface plot parametric in *tf_nutrient* as a function of the 2 factors that controls the nutrient profile is presented.
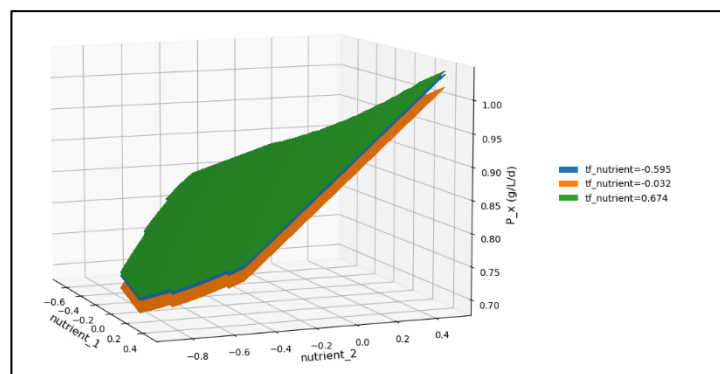

Figure 33 surface plot parametric in tf_nutrient

It can be noticed that the factor *tf_light* plays a marginal role because the shapes of the response curves are similar and close to each other.

The maximum of productivity is reached when factors *nutrient_1* has a value of 0.1 while the value of factor *nutrient_2* is set at 0.6.

In this configuration the productivity predict from the model is slightly higher than 1 g/L/d.

3.2.6 Optimization

The model developed was used for the optimization of biomass productivity. All DoDE constraints were considered during the optimization to satisfy the limitations imposed by the experimental campaign.

Optimization was initialized 100 times with different initial guesses selected randomly.

Starting the optimization from point identified through the response surfaces led to the predicted optimal biomass productivity of 1.42 g/L/day using the factor values [**1,0,1,0.3059,1,0.444,0.5555**].

The optimal light and nutrient profiles associated with these factors are reported in Figure 34, while the experiment pCO2 selected for the optimal experiment is equal to 6.54%. According to these results, the light should start at maximum value 300 $\frac{\mu mol}{m^2 \cdot s}$ increases for 3 days until reaches the maximum intensity set equal to 800 $\frac{\mu mol}{m^2 \cdot s}$ while staying to the peak values for the remaining 2 days.

Nutrient amount should be fed in large quantity and the feeding continuous for 5 days.

The total nitrogen fed in this configuration is 499.9 mg/L, a high value respect the nitrogen presents in the standard medium (330 mg/L).
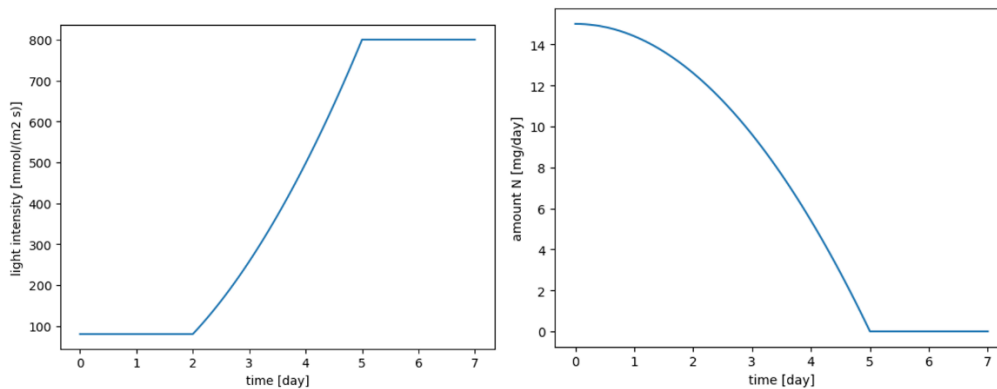

Figure 34 Optimal light and feeding profile for biomass productivity

3.2.7 Discussion

Maximizing biomass production is fundamental to any biotechnological application because biomass serves as the primary source of raw material for numerous industrial processes. Additionally, higher biomass yields directly correlate with increased production efficiency and scalability, thereby enhancing the economic viability of biotechnological ventures. Moreover, abundant biomass facilitates the extraction and isolation of valuable compounds.

The optimization profiles suggest that a productivity of 1.42 g/L/d could be achieved, which is a remarkable result, and it must be experimentally validated.

If we compare this value with other studies in literature large differences can be noticed.

An example is the work of Robles et al. (2023), in this study, the authors analysed the growth of *Coccomyxa onubensis* in a batch system with air enriched in CO_2 (2.5 %), at 25°C, and under continuous illumination at an intensity of 150 $\frac{\mu mol}{m^2 \cdot s}$. The results show that the maximum productivity was equal to 0.35 g/L/d on the 4th day of cultivation.

Another study by Bermejo et al. (2018) tested the effect of NaCl on *C. onubensis* at different concentrations ranging from 0 to 500 mM.

The experimental setup comprised a 2-litre flask with air enriched with CO_2 at 5%, illumination provided by fluorescent lamps set at 140 $\frac{\mu mol}{m^2 \cdot s}$, at 26°C.

The highest biomass productivity was observed with a sodium chloride concentration of 100 mM, where the culture reached a value of 0.244 g/L/d.

These large differences can be explained by the setup of the experiment and to the increment of CO_2.

Firstly, the exploitation of a high-cell density cultivation system allowed to achieve high productivity that cannot be matched by traditional cultivation systems.

CellDEG enables rapid growth of the culture due to its high mass transfer facilitated by the high exchange surface membrane. This allows for efficient gas transport within the algal culture, alongside guaranteed turbulent mixing and an optimal light path that addresses the self-shading problem.

Freudenberg et al. (2021) compared the cultivation of *Chlamydomonas reinhardtii* in a bubble column and the CellDEG system. After 5 days of cultivation, the productivity of the CellDEG was 2.5 higher than the bubble column. This trend in biomass productivity observed in our study aligns with findings from the literature, indicating that a high cell density cultivation system allows for higher productivity compared to classical systems like bubble columns.

Secondly, regarding CO_2, the results show that maximum productivity is achieved when CO2 is at 6.54%, thus suggesting that CO_2 is a limiting factor for algae growth. This condition is a common feature of acidophilic microalgae: different studies conducted on these microalgae have shown that high concentrations of CO_2 increase algae growth, not only because the carbon supply is higher, but also due to the corresponding decrease in pH resulting from CO_2 dissolution.

For example, *Chlamydomonas acidophila* in the study by Neves et al. (2019) was cultivated under different conditions of CO_2 partial pressure. The results showed that microalgae grown under 5% and 10% of CO_2 achieved productivity 25% higher compared to the case of air culturing.

The high demand for carbon dioxide by *Coccomyxa onubensis* was also evaluated by Piiparinen et al. (2018). The researchers studied the CO_2 uptake of six different microalgae, three acidophilic and three alkaliphilic. The results show that the acidophilic microalgae used more CO_2 compared to the alkaliphilic ones, with *Coccomyxa onubensis* consuming the highest quantity among the six species, at 4.6 gCO_2/gDW.

The importance of cultivating *C. onubensis* under high concentrations of CO_2 was also demonstrated by Vaquero et al. (2014). In this work, they initially cultivated *Coccomyxa onubensis* in a low-carbon regime (cultivated in air) for 36 hours and subsequently shifted to a high-carbon regime (5% CO_2) for 24 hours.

The results display an increase in biomass productivity, with a peak in the last 12 hours equal to 1.8 g/L/d. These studies reflect the trends of the present work: high concentrations of CO_2 enable higher growth of algal culture.

In literature, there is a knowledge gap related to the cultivation of this strain of acidophilic microalgae at CO_2 concentrations higher than 5% (v/v). It would be interesting to investigate the effect of higher concentrations to assess whether growth can be further increased or whether there is a growth-inhibiting effect at partial pressures higher than 10%.

Regarding the light, the optimal profile starts from a value of $100 \frac{\mu mol}{m^2 \cdot s}$ and after 3 days of ramp reaches the ultimate value of $800 \frac{\mu mol}{m^2 \cdot s}$. Unfortunately, in the literature, there are no studies available for *Coccomyxa onubensis* that evaluate the optimal light intensity profile as in the present work. However, some research studies the effect of different light intensities to find the optimal value for maximizing productivity. Vaquero et al. (2014) studied the effect of light on *Coccomyxa onubensis*, testing three different light intensities: 50, 140, and 400 μmol/(m^2·s)

in a 1-litre batch system incubated at 27°C with a constant bubbling of air and CO_2 (95:5). The initial results displayed that the maximum growth rate was achieved under 400 $\frac{\mu mol}{m^2 \cdot s}$, where the growth rate was equal to 0.4 d^{-1}, 37% higher compared to the case of 140 $\frac{\mu mol}{m^2 \cdot s}$ and 2.5 times higher compared to the case of a light intensity of 50 $\frac{\mu mol}{m^2 \cdot s}$. The concentration of the microalgae in all the experiments was 0.5 g/L.

In the same study, the authors also evaluated the effect of shifting the light from 140 to 400 $\frac{\mu mol}{m^2 \cdot s}$ with two different concentrations of the microalga, 0.5g/L and 1.5 g/L. The results showed that after the light shift, the low-concentrated culture increased the growth rate by 70% compared to the one grown under constant light at 140 $\frac{\mu mol}{m^2 \cdot s}$. A different situation occurred in the dense culture, where the growth rate was slightly higher compared to the case of constant light. This result is in accordance with the optimal light profile of the present work. The profile should increase over time to encourage the growth of the algal culture. However, it is not possible to make comparisons between the values of the light intensity due to the different configurations of the light systems of the two setups (bubble column and CellDEG).

3.3 Carotenoid content

In this section, the experimental results of the carotenoid content of the experimental campaign will be presented. In figure 35, the amount of total carotenoids of each condition on the last day of cultivation is reported. The batches that run in parallel have the same colour.
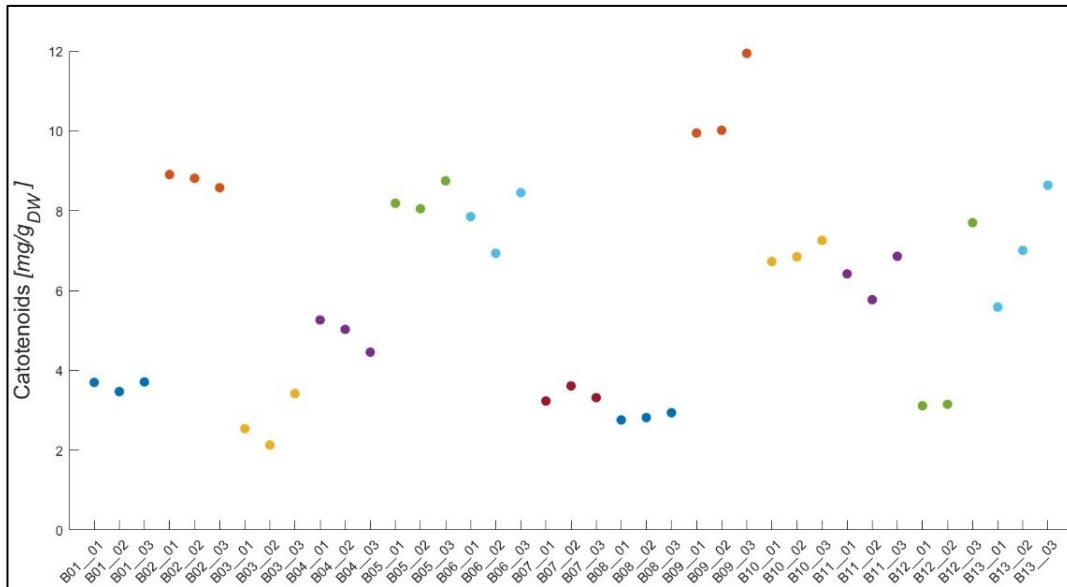

Figure 35 Scatter plot of the carotenoid content

It can be readily observed that the data across replicates exhibit a high degree of replicability, showing large consistency in the data of the study.

The amount of carotenoids was bounded between 2 and 12 mg/g$_{DW}$. Specifically, it is evident that the carotenoid content is mainly bounded into areas in the range 0 - 6 mg/g$_{DW}$ and 6-12 mg/g$_{DW}$

The higher content of carotenoids (mean value equal to 8.85 mg/gDW) where achieved in batch **B_02, B_05, B_06, B_09** where the content is bounded between 8 and 12 mg/gDW, in all these batch the partial pressure of CO_2 was set at its lower value (0.04%).

3.3.1 PCA analysis

Also here, a principal components analysis was performed to evaluate the impact of the PBRs position and the similarity on the replicates.

In the figure below a scatter plot with the position of the bioreactors in the different configurations is presented.
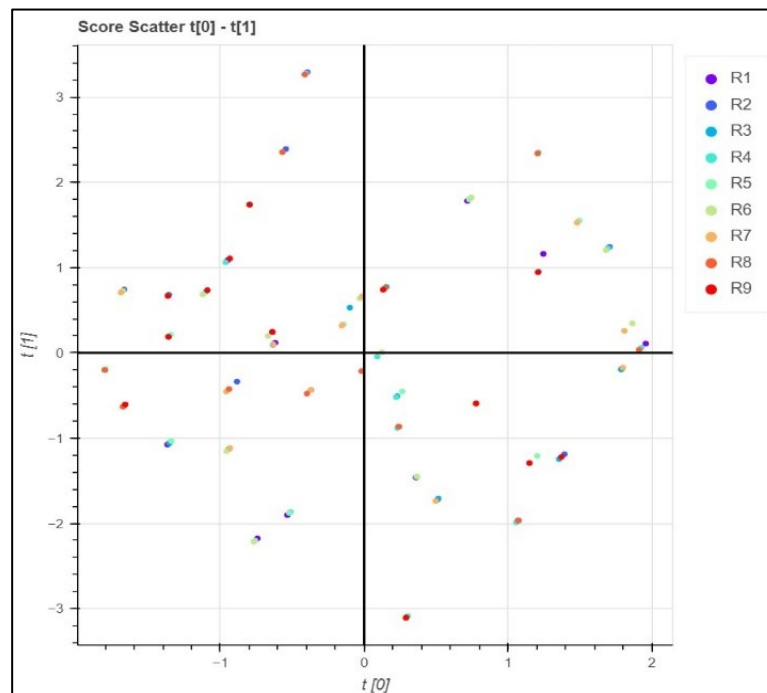

Figure 36 scatter plot of the position of the reactors

The absence of clustering associated with the position in the bioreactor suggests that there are no detectable effects attributable to bioreactor positioning. Furthermore, observations taken in the same bioreactor position exhibit a normal spread in the score space.

This implies that the variability observed in the dataset is not primarily driven by differences in bioreactor positioning. Instead, it suggests that other factors, not related to bioreactor placement, are the main sources of variability in the dataset.

3.3.2 DODE analysis for carotenoid content

In this section is presented the effect on the response, the carotenoid content, of the factors. The single effect of each factor on the carotenoid content is analysed, this analysis does not include the combined effect of more factors, but it may provide a preliminary insight on the impact of the individual factors on the response.

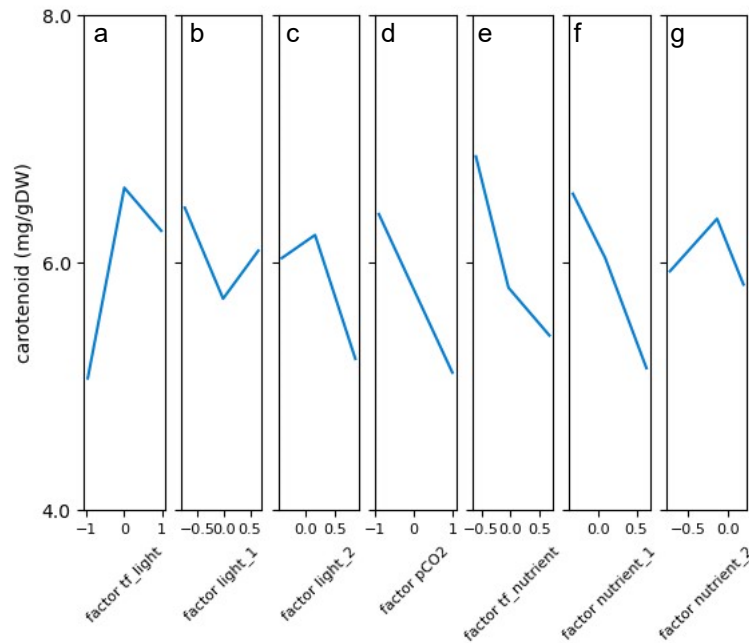In the figure below the main effect of the factors on the carotenoid content is presented.

Figure 37 effect of the factors on the carotenoid content

From figure 3 different considerations can be done.

The time at which the light peak (*tf_light*) is reached has a large positive effect, this condition indicates that reaching the light peak in a short time has a negative effect thereby reducing the carotenoid content of the algal culture.

Regarding light profiles (controlled by *light_1, light_2*) has low negative effect with some non-linearities, the effect of factor *light_2* has a major impact on the response respect the factor *light_1*.

Regarding the dynamics of the light intensity to maximize the carotenoid content, it can be initially suggested that lower light intensity is preferred in the first step when light is constant for two days, followed by long incremental, linear light phase, reaching the peak and consequent final constant phase with an average light intensity value.

From the figure 37d is also possible to evaluate the effect of the partial pressure of CO_2 on the response, it is clear that the factor pCO_2 has a big negative effect: the higher is the pCO_2, the

lower is the content of carotenoids. It can be concluded that to optimize the concentration of carotenoid in the algal culture the optimal value of CO_2 is 0.04% (air) while increasing its concentrations has a has a pronounced adverse effect.

The figures 37e, 37f, and 37g display the effect of the factors related to the nitrogen feeding strategy to the response.

The time at which the nutrient feeding is stopped (*tf_nutrient*) exhibits a strong negative effect. Therefore, it can be assumed that stopping the nutrient feeding in an early stage of microalgal growth increases consistently the content of the target compound.

The two dynamic subfactors related to nutrient feeding (*nutrient_1, nutrient_2*) have different trends, the first one has a large negative impact on the response while the second one has only a limited effect showing some non-linearities.

According to these results obtained from the analysis of the main effects, the optimal trend of feeding should start with a moderate mass of nitrogen in the tested boundaries, and the feeding should be stopped rapidly. However, it should be considered the limits of this preliminary approach that only considers each variable on dependent variable, averaged across all levels of others. From the previous conclusions, it can be suggested an optimal trends for the light profile and nitrogen feeding strategy presented in figure 37a and 37b, setting the partial pressure of CO_2 to the lower boundary (air).

The light profile initially assumes a constant value of 150 $\frac{\mu mol}{m^2 \cdot s}$ for the first 2 days.

Subsequently, the profile begins to rise with a concavity pointing downward, the profile increases for two days until it reaches a peak at 280 $\frac{\mu mol}{m^2 \cdot s}$, where it then remains constant until the end of the experiment.

Regarding the profile of nitrogen feeding, the curve has slight concavity pointing upward and the feeding stops at day 2, without adding any nitrogen for the consequent five days of cultivation.
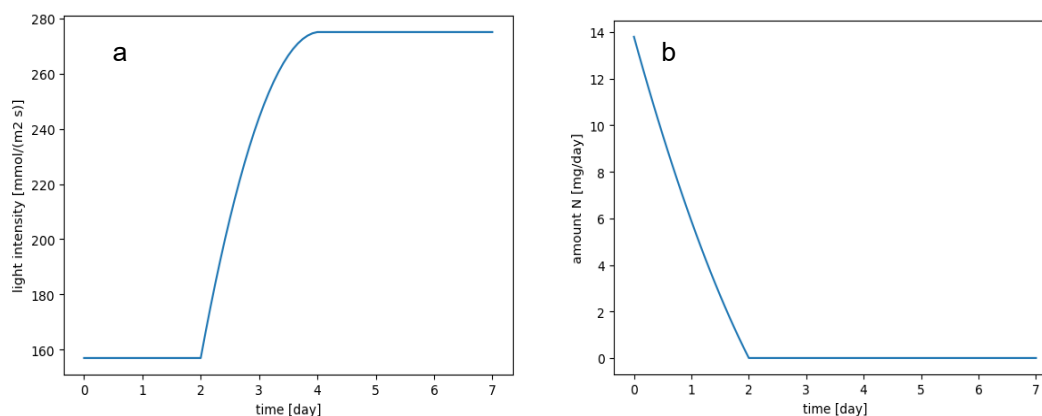
In figure 38 the suggested profiles are shown.

Figure 38 Suggested trends for light and nitrogen for carotenoid content

3.3.3 Modelling and analysis of the model

To model the relationship between factors and response (carotenoid content) a quadratic model with interactions was selected because it allowed to further perform the optimization of the carotenoid content.

The formulation of the quadratic model with interactions is:

$$y = \beta_0 + \sum_{i=1}^{F} \beta_i \cdot x_i + \sum_{i=1}^{F} \beta_{i,j} \cdot x_i \cdot x_j$$

where β_0 is the intercept, β_i are the coefficients of the linear terms, $\beta_{i,j}$ are the coefficients of the interaction and quadratic terms, x_i are the factors, and F is the total number of factors.

An iterative validation over 250 iterations was performed to assess the quality of the model to describe unseen experimental spaces. The validation of the model was performed by iteratively excluding 3 randomly selected observations while building the model on the remaining 36 observations.

The determination coefficient was calculated for the validation observations and averaged over the 250 validation iterations.

Initial model

A complete quadratic model with interactions built over all 39 observations achieved a coefficient of determination $R^2 = 78.5\%$ $(R^2_{adj} = 70.0\%)$ indicating a sufficiently good representation of the calibration data. In validation, the model achieved a coefficient of determination $Q^2 = 55.6\%$ indicating average performance in representing unseen data. However, this validation performance may be deemed satisfactory for a biological application marked by significant variability and influenced by numerous factors. The model parameters with their 95% confidence limits are shown down below.
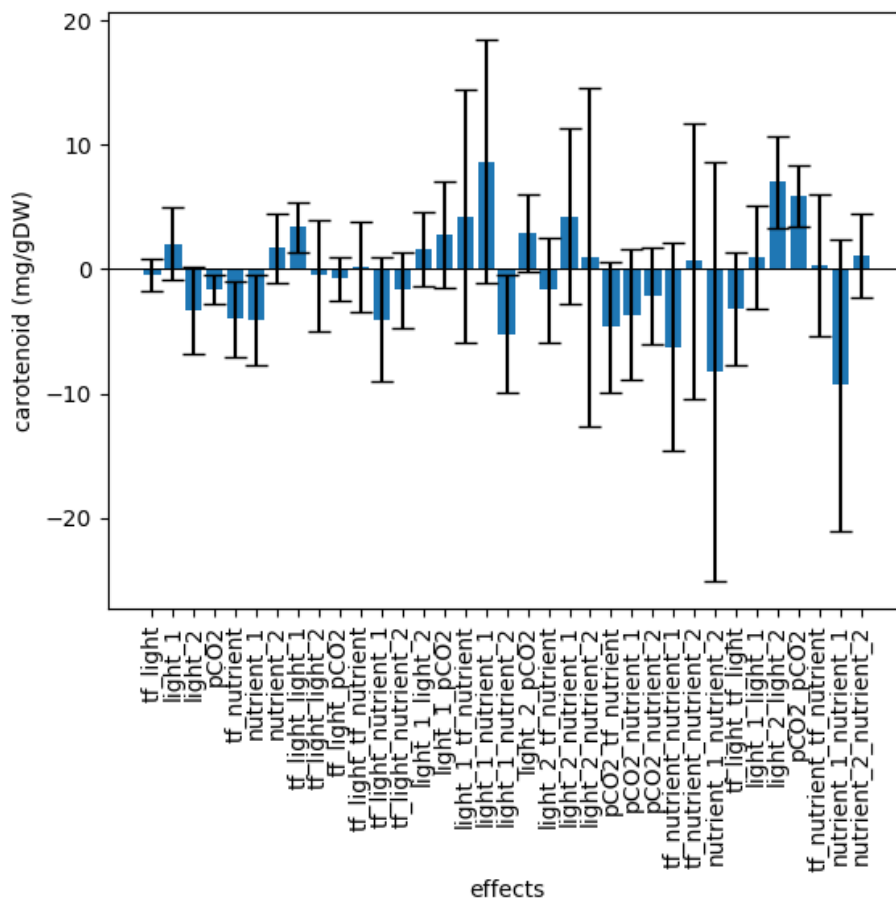

Figure 39 model parameters of carotenoid content

The model was characterized by large confidence limits of the parameters; hence, improvements are required.

To improve the model a stepwise regression was performed. In stepwise regression, non-significant model terms, characterized by non-significant model parameters, were iteratively excluded according to the p-value (calculated during least square regression). The term with the highest p-value was excluded at each iteration until all model terms were significant (p-value < 0.05).

The improved model built on all observations achieved a coefficient of determination $R^2 = 95.5\%$ ($R^2_{adj} = 94.7\%$) indicating a very good representation of the calibration data. In validation, the model achieved a coefficient of determination $Q^2 = 55.6\%$ indicating satisfactory performance on validation data, especially for a biological application characterized by large variability of the response.

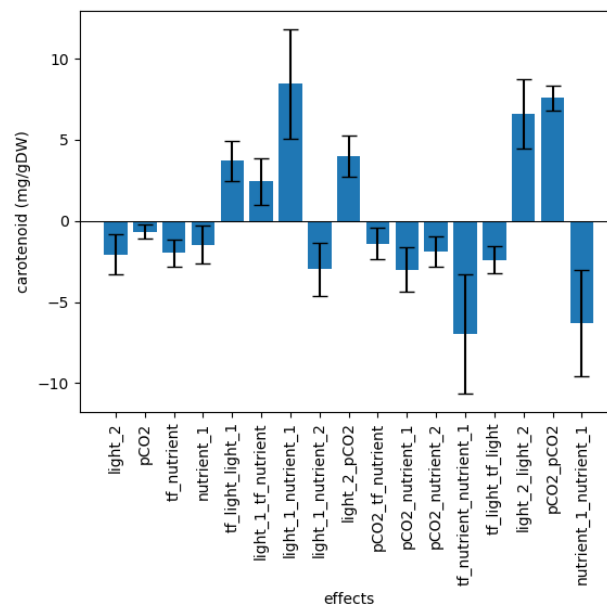The model parameters with their confidence limits are reported in Figure 39.

Figure 40 optimized model parameters of the carotenoid content

From this plot the main effect of factors on the response can be assess.

The linear effects are only marginal on the response.

The quadratic effects of factors *light_2, pCO₂*, have a great positive impact on the response while *nutrient_1* have a large negative impact.

Regarding the combined effects, there is a great positive impact on the response with the factors *light_1-nutrient _1, pCO2* and *nutrient_2*.

The interaction parameters *tf_nutrient/nutrient_1, light_1/nutrient_2, pCO2/nutrient_1* instead show a negative effect on the response.

3.3.4 Analysis of the response

The effect of factors on the response (carotenoid content) was analysed through the Response Surface that can be obtained from the model built.

In the response surface, the value of the response is shown as function of two factors, while the remaining ones are fixed or varied across multiple levels.

In the figure below the are visualized three parametric curve of factor *tf_light* while *light_1* and *light_2* are the variable on the axis.

The other parameters are set as follow*: pCO$_2$=-1, tf_nutrient=-1, nutrient_1=0.69, nutrient_2=0.199.*
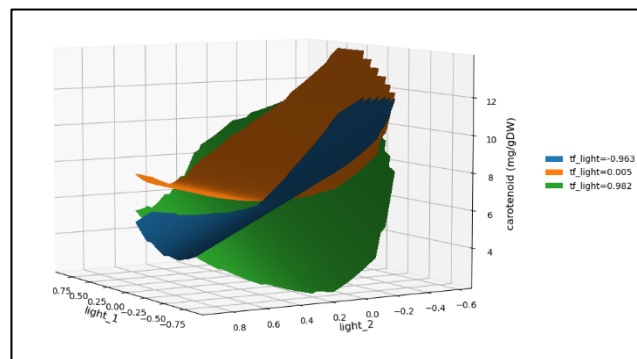

Figure 41 surface plot on carotenoid content (1)

From the plot we can see that the maximum content of carotenoid, slightly less than 14 mg/gDW, was reached for *tf_light*=0.005, a low value of *light_2* and a medium- high value of *light_1*.

In figure 42 a surface plot parametric in *tf_nutrient* as a function of the 2 nutrient factors.

The fixed parameters are: *tf_light*=0.005, *pCO$_2$*=-1, *light_1*=0.38, *light_2*=0.62.

The maximum content of carotenoids is found when both *nutrient_1* is around 0 while the effect of nutrient 2 is less impactful, the level of *tf_nutrient* is equal to 0.674.
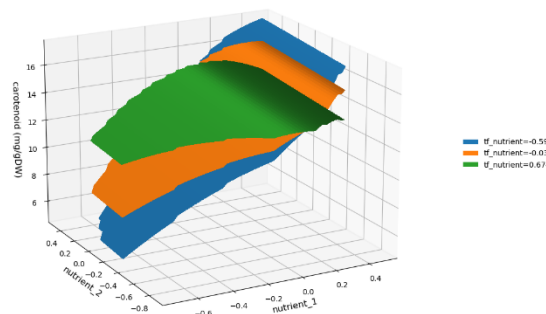

Figure 42 surface plot on carotenoid content(2)

3.3.5 Optimization

The model developed was used for the optimization of carotenoid content.

All DoDE constraints are considered during the optimization to satisfy the limitations imposed by the experimental campaign.

Starting the optimization from an experimental point with high carotenoid content leads to the predicted optimal carotenoid content of 20.1 mg/gDW using the factor values set in order (**0.2777,0.3601, -0.6398,-1,-1,0.8523**).

The light and nutrient profiles associated with these factors are reported in Figure 43, while the experiment pCO_2 selected for the optimal experiment is at the lower bound, 0.04%.
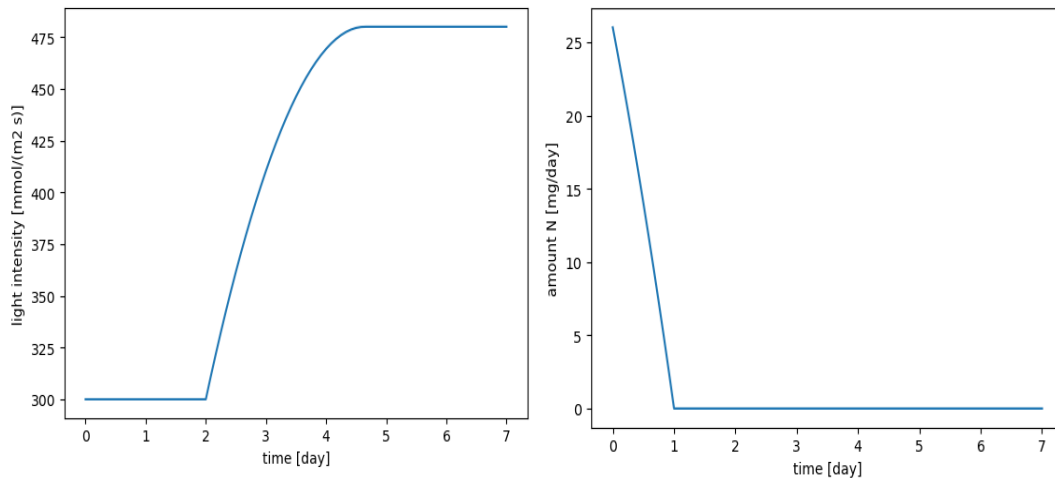
Figure 43 optimal light and nitrogen profile for maximize the carotenoid content

3.4 Carotenoid productivity

In this section, the experimental results of the carotenoid productivity of the experimental campaign will be presented. In the plot below a scatter plot of carotenoids productivity of each condition is presented, the three points for each conditions indicate the 3 biological replicates.
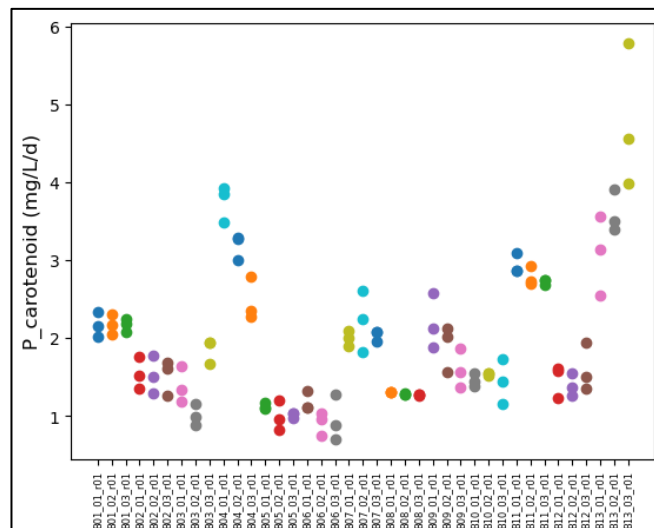

Figure 44 scatterplot of carotenoids productivity in the 39 experimental conditions

Data across replicates exhibit a high degree of replicability, showing large consistency in the data of the study.

However, some large differences (B04_01, B04_03, B09_02, B13_01, B13_03) are visible respect to the other replicates.

The carotenoids productivity in different experimental conditions reaches very different values, varying from a value slower than 1 mg/L/d until a maximum values of 5.8 mg/L/d.

The lower carotenoids productivity was achieved in batch **B_05, B_06** grown in air and under low light intensities, the carotenoid productivity stabilizes around 1 mg/L/d.

Batches **B_04** (1% CO_2),**B_13**(10% CO_2) grown under high light intensities, exhibited the highest carotenoid productivity, with a mean value of 3.5 mg/L/d.

3.4.1 PCA analysis

Also here, a principal components analysis was performed to evaluate the impact of the PBRs position.
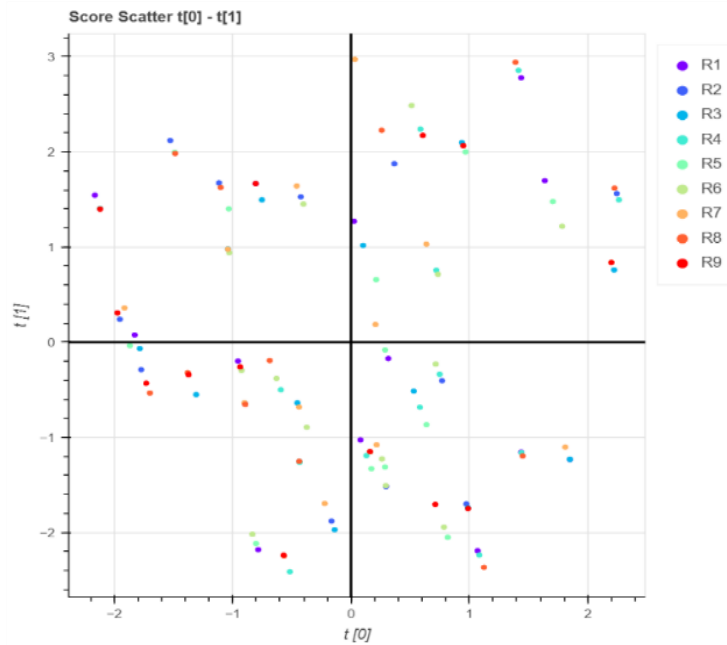

Figure 45 PBRs positioning scatter plot

As in the previous cases, the absence of clustering associated with the position in the bioreactor suggests that there are no detectable effects attributable to bioreactor positioning. Furthermore, observations taken in the same bioreactor position exhibit a normal spread in the score space. This implies that the variability observed in the dataset is not primarily driven by differences in bioreactor positioning. Instead, it suggests that other factors, not related to bioreactor placement, are the main sources of variability in the dataset.

3.4.2 DODE analysis for carotenoid productivity

In this section is presented the effect on the response, the carotenoid productivity, of the factors.
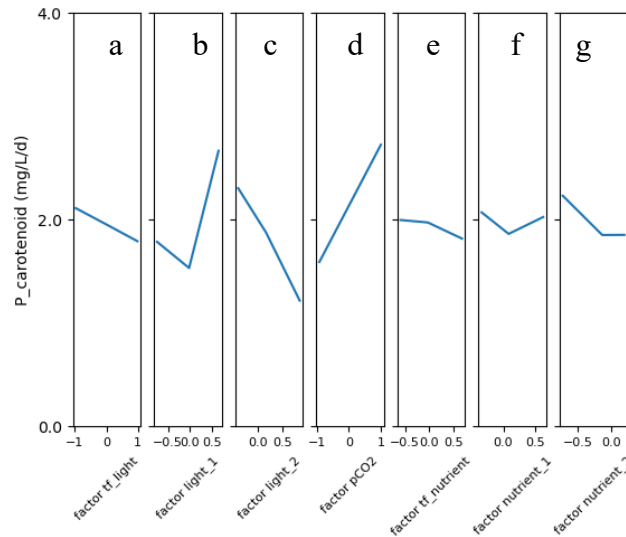

Figure 46 main effect of the factors on the carotenoid productivity

In figure 46 the main effect of the factors on the carotenoid content is presented.

The point at which light reaches the maximum values (*tf_light*) has a small negative effect, indicating small times to reach the peak light intensity are required to improve the carotenoid productivity.

The shape of the light intensity profile (*light_1, light_2*) show different main effects, with *light_1* having a positive effect with non-linearities and *light_2* showing a larger negative effect. Accordingly, the optimal light profile starts at high intensity and reach the peak intensity rapidly till a medium-high peak light intensity that lasts for 3 days.

The partial pressure of CO_2 (*pCO2*) has a large positive effect, indicating that setting the value of *pCO2* at its higher bound results in higher carotenoid productivity.

The time to stop feeding (*tf_nutrient*) has very small effect, indicating it does not play a large role in determining the carotenoid productivity.

The factors associated to nutrient profile show different effects. In particular, *nutrient_1* has a small effect with non-linearities, while *nutrient_2* has a small negative effect. Accordingly, the

feeding profile should be medium-high at the beginning and decrease to zero after 3 days with a visible upward concavity.

In figure 47, optimal light and feeding profiles are suggested based on experimental results.
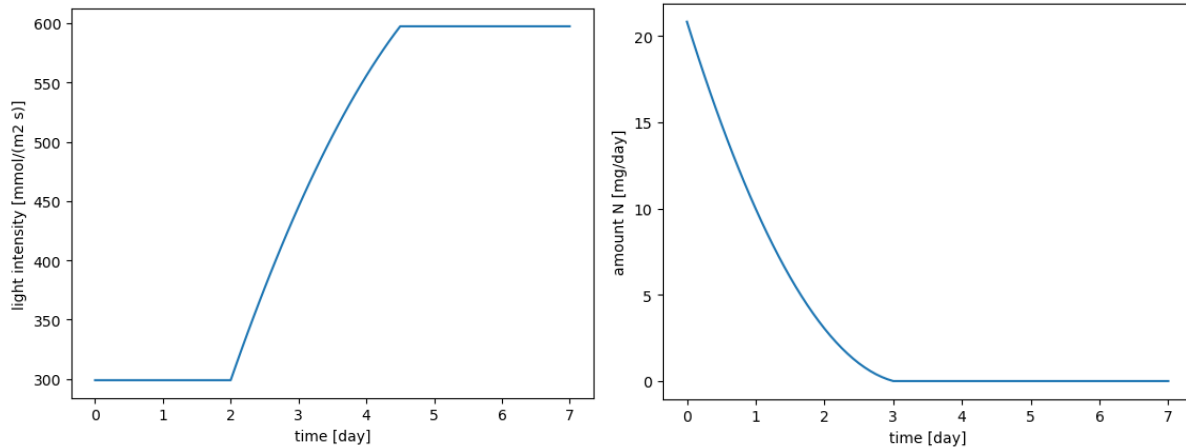

Figure 47 suggested profiles for carotenoid productivity

The light profile should start from the higher initial value $300 \frac{\mu mol}{m^2 \cdot s}$ and after 2 days of ramp reach the peak set at $600 \frac{\mu mol}{m^2 \cdot s}$ for the remaining 3 days.

The nitrogen is fed at the beginning at high quantity and continues for 3 days, then feeding is stopped until the end of the batch.

3.4.3 Modeling and analysis of the model

To model the relationship between factors and response (carotenoid productivity) a quadratic model with interactions was selected because it allowed to further perform the optimization of the carotenoid productivity. The formulation of the quadratic model with interactions is:

$$y = \beta_0 + \sum_{i=1}^{F} \beta_i \cdot x_i + \sum_{i=1}^{F} \beta_{i,j} \cdot x_i \cdot x_j$$

where $\beta 0$ is the intercept, βi are the coefficients of the linear terms, $\beta i,j$ are the coefficients of the interaction and quadratic terms, $x i$ are the factors, and F is the total number of factors.

An iterative validation over 250 iterations was performed to assess the quality of the model to describe unseen experimental spaces. The validation of the model was performed by iteratively excluding 3 randomly selected observations while building the model on the remaining 36 observations. Coefficient of determination is calculated for the validation observations and averaged over the 250 validation iterations.

A complete quadratic model with interactions built over all 39 observations achieved a coefficient of determination R^2=91.9% (R^2_{adj}=88.7%) indicating a good representation of the calibration data. In validation, the model achieved a coefficient of determination $Q2$=71.3% indicating good performance in representing unseen data. The validation performance can be considered satisfactory for a biological application characterized by large variability and affected by many factors. The model parameters with their 95% confidence limits are reported in figure 48.
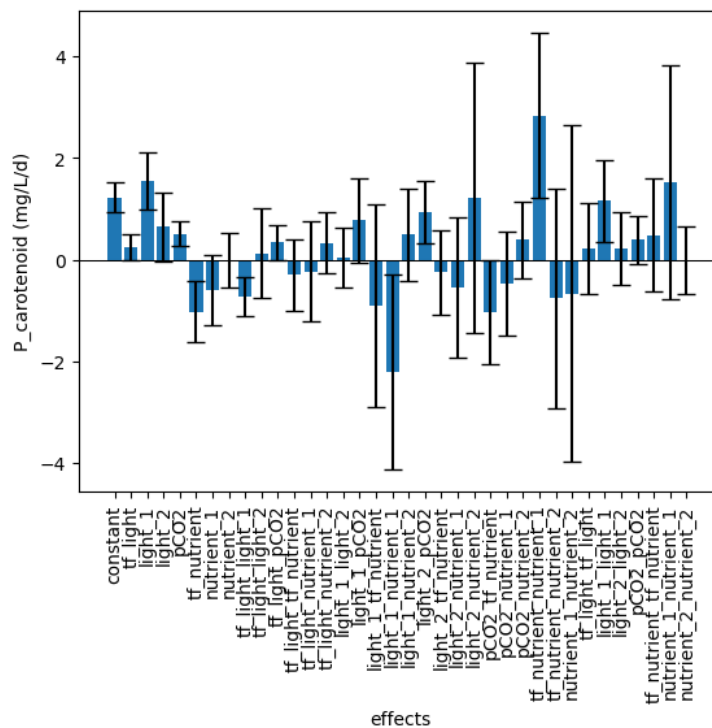

Figure 48 Model parameters of carotenoids productivity

The model is characterized by large confidence limits of the parameters; hence, improvements are required.

3.4.4 Model improvement

To improve the model a stepwise regression was performed. In stepwise regression, non-significant model terms, characterized by non-significant model parameters, were iteratively excluded according to the p-value (calculated during least square regression). The term with the highest p-value is excluded at each iteration until all model terms are significant (p-value < 0.05).

The improved model built on all observations achieved a coefficient of determination $R^2=91.4$ % ($R^2_{adj}=89.6\%$) indicating a good representation the calibration data. However, results of the refined model were slightly inferior to the initial model, indicating that the exclusion of non-significant factor has no effect on the model. In validation, the model achieved a coefficient of determination $Q^2=70.4\%$ indicating good performance on validation data, especially for a biological application characterized by large variability of the response. Despite the absence of improvement in the representation of calibration data, the refined model improved the prediction of unseen data. The model parameters with their confidence limits are reported in Figure 49.
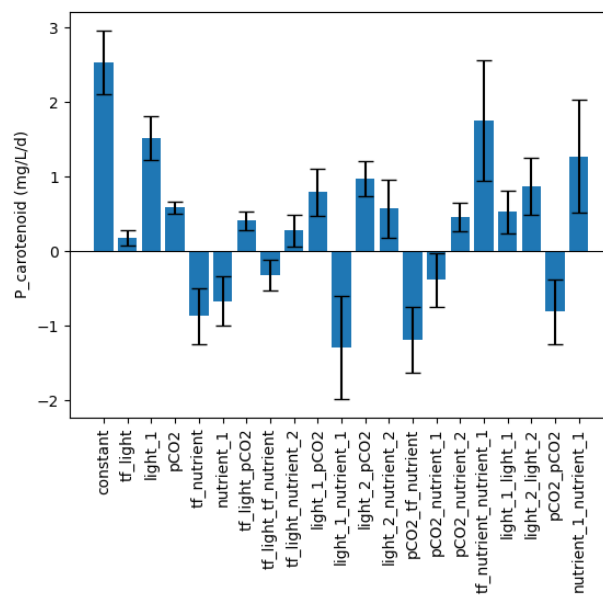

Figure 49 optimized model parameter for carotenoid productivity

From figure 49 is evident that *nutrient_1* have a large quadratic effect while *pCO₂* display a large negative effect on the response.

Regarding the interaction effects it can be notice that *light_1/pCO₂*, *light_2/pCO₂*, *tf_nutrient/nutrient_1* have great positive impact on the response while *light_1/nutrient_1, pCO₂/tf_nutrient*, have a large negative effect on the response.

The most significative linear effects are: *light_1,pCO₂* which has a positive effect on the response while *tf_nutrient, nutrient_1* have a negative impact on the carotenoid productivity.

3.4.5 Analysis of the response

The effect of factors on the response (carotenoid productivity) was analysed through the Response Surface Methodology, obtained from the model previously built. In the response surface, the value of the response is depicted as function of 2 factors, while the remaining ones are fixed or varied across multiple levels. Only the part of the response surface that satisfies the DoDE constraints is shown.

Figure 50 surface plot of carotenoid productivity
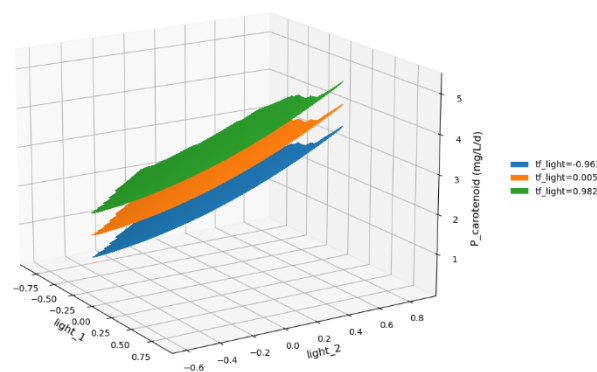
In figure 50 surface plots parametric in *tf_light* and as a function of the 2 light subfactors are presented.

The other factors are set as follow: *pCO₂=1, tf_nutrient=0, nutrient_1=0, nutrient_2=0*.

The higher value of the carotenoid productivity is close to 8 mg/L/d and it is reached when tf_light is equal to 0.982, light_1 is around 0 while light_2 is close to 1

In the figure 51 is presented a plot parametric in *tf_nutrient* and as a function of *nutrient_1* and *nutrient_2*

The other factors are set as follow*: tf_light=0.982, pCO₂=1, light1=0.79, light_2=-0.086.*
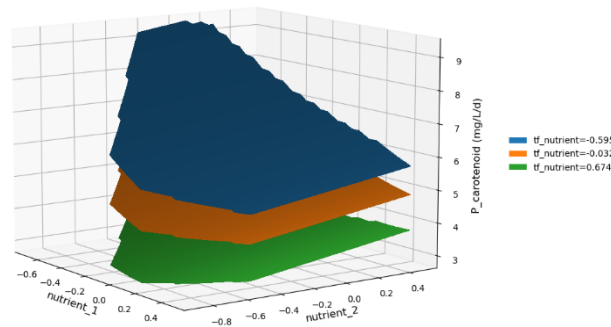

Figure 51 surface plot of carotenoid productivity (2)

The highest value in this plot is around 9 mg/L/d.

Regarding the nutrient the highest response is achieved when *nutrient_2* has a high negative value around 0.8 while *nutrient _1* is close to 0.

3.4.6 Optimization

The model developed is used for the optimization of carotenoid productivity.

 All DoDE constraints are considered during the optimization to satisfy the limitations imposed by the experimental campaign (constraints on the factors' values, derivatives of light and nutrient profiles, and total amount of nutrient fed).

Starting the optimization from an experimental point with high carotenoid productivity leads to the predicted optimal carotenoid productivity of 10.47 mg/L/day using the factor values **[1,1,0,0.9999, −0.6896, −0.7154, −0.1249]**.

The optimal light and nutrient profiles associated with these factors are reported, while the experiment pCO₂ selected for the optimal experiment is at the higher bound 10%. According to these results, the light should start at a high value around $300 \frac{\mu mol}{m^2 \cdot s}$ and increase linearly to the maximum intensity of $800 \frac{\mu mol}{m^2 \cdot s}$s while staying to the peak values the smallest amount of time.

A low initial nutrient amount should be fed at the beginning, while that amount should decrease rapidly after 1.5 day.

The total amount of nitrogen fed is equal to 6 mg.

In figure 52 are presented the optimal profile to increase the carotenoid productivity.
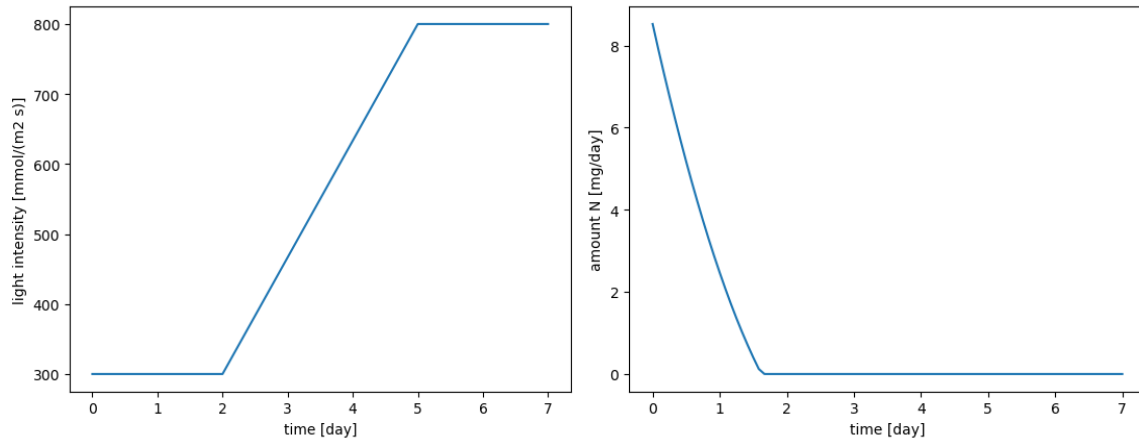
Figure 52 Light and nitrogen optimal profile for maximize carotenoids productivity

3.4.7 DISCUSSION

The model returned an optimal value of 20.1 mg/gDW for the carotenoid content and 10.47 mg/L/d for the carotenoid productivity. The results obtained from the model are theoretical and must be validated by applying the conditions suggested for optimization.

The values obtained from the DoDE are significantly higher compared to experimental studies on *Coccomyxa onubensis*.

In literature, the highest reported content of carotenoids in *C. onubensis* was 12 mg/gDW, achieved after 7 days of batch cultivation under a light intensity of 140 $\frac{\mu mol}{m^2 \cdot s}$ and 5% CO_2 (Ruiz-Domínguez et al., 2015). Another study by Vaquero et al. (2012) examined the biochemical composition of C. *onubensis* at different copper concentrations up to 4 mM with the aim of maximising the carotenoid content.

The experiments were carried out in a batch system at 28°C and a light intensity of 160 $\frac{\mu mol}{m^2 \cdot s}$. The results showed that the maximum concentration of carotenoids was 9.5 mg/gDW achieved at a concentration of 0.2 mM.

From the model optimization, it was also possible to generate a profile of operational variables applicable for high cell density cultivations. Therefore, from the optimal light profile for the carotenoid content, it can be observed that the light intensity starts at high levels, 300 $\frac{\mu mol}{m^2 \cdot s}$ represents the maximum value of the starting light interval.

The evolution of the profile is a ramp that lasts for two and a half days until it reaches the maximum light intensity values of 475 $\frac{\mu mol}{m^2 \cdot s}$.

The optimal light profile is quite narrow, with an increase of only 175 $\frac{\mu mol}{m^2 \cdot s}$ during the experimental run.

A different light profiles to maximize the carotenoid productivity was predicted by the model. Here, the profile starts from the maximum initial value of 300 $\frac{\mu mol}{m^2 \cdot s}$ and then increases linearly up to 800 $\frac{\mu mol}{m^2 \cdot s}$.

If we observe optimal value of CO_2 of content and productivity, we can see some similarities on the 2 light profiles.

In the case of carotenoid content *C. onubensis* grow with a pCO_2 of 0.04% which limits the growth.

Due to its low concentration, it was not necessary to increase the light intensity to a high value to keep the algae under a light stress condition.

Differently, regarding the productivity of carotenoid, *C.onubensis* grow under high CO_2 concentrations which increased considerably the concentration of the culture, an high light intensity was required to sustain the high growth rate and to maintain the light stress condition in order to increase carotenoid synthesis.

The influence of light used as a stress factor to enhance the carotenoid production has been studied in several research studies.

Gwak et al. (2014) examined the effect of shifting light intensity from low to high on *Haematococcus pluvialis* to evaluate its impact on carotenoid production. In this study, the authors increased the light intensity from $20 \frac{\mu mol}{m^2 \cdot s}$ (control culture) to $400 \frac{\mu mol}{m^2 \cdot s}$.

The results showed that in the culture grown under high light, the concentration of total carotenoids was 4 times higher than in the control culture (6.7 g/L and 1.5 g/L, respectively).

Another study conducted by Lamers et al. (2010) assessed the effect of a sharp increase in light intensity on *Dunaliella salina*, from $200 \frac{\mu mol}{m^2 \cdot s}$ to a very intense light irradiance set at $1400 \frac{\mu mol}{m^2 \cdot s}$.

An increase in light irradiance induced increased production of intracellular β-carotene. After 2 days of stress conditions, the content of β-carotene was 3-fold higher compared to the situation without the increment of light (from 5 to 17 g/L).

All these studies reported that to increase carotenoid production, it is necessary to work under a high light regime.

Regarding the nitrogen content, it seems to have only a marginal role in maximizing carotenoid content. In the experiments performed at pCO_2 equal to 0.04% (v/v), and as confirmed by the measurement of the concentration of nitrogen in the culturing medium, the algal culture was never in a nitrogen-limited condition. Among all conditions cultivated in air, the lowest value of nitrogen concentration present in the supernatant in the last day of cultivation was equal to 42 mg/L. No considerations can be made about the possible increase in carotenoids due to a nitrogen-free condition.

A different situation occurs looking at the optimal nitrogen profile for carotenoid productivity. Nitrogen is fed at a low amount (60 mg/L), and the feeding is stopped at the second day of cultivation. In this condition, the culture is nitrogen-limited due to the sustained growth rate and the low nitrogen available in the medium.

Several studies investigate the effect of nitrogen starvation and limitation on microalgae as a strategy to enhance the production of carotenoids. Lamers et al. (2010) studied the accumulation of β-carotene in *Dunaliella salina* cultivated in a nitrogen-free medium. The study reported that the productivity in the nitrogen depletion condition was equal to 14.4 mg/L/d, while β-carotene productivity using the standard medium was 2.2 mg/L/d.

Another research from Mulders et al. (2014) investigated the carotenoid accumulation in *Chlorella zofingiensis* in a batch system, at different nitrogen concentration in the medium.

The highest amount of nitrogen was found in the nitrogen-deplete condition, with a content of total carotenoids equal to 4.5 mg/g, while in the nitrogen-replete condition, the amount of total carotenoid was only 0.05 mg/g.

In conclusion, the results of the present work are in accordance with the study found in literature, high light intensity and a reduced nitrogen concentration are 2 strategies to increase the production the carotenoid content.

3.5 Lutein

In this section the preliminary results of lutein content and productivity of 18 experiment out of 39 are reported. The batch analysed were B_03, B_04,B_08,B_09B_10,B_11, the others were not yet available by the time of this thesis was written. When the data set will be complete, the DODE approach will be applied also on lutein. In the figure 53 and 54, the results of the lutein content and productivity are presented in detail. In figure the results are divided in three colours that are representative of the pCO_2. The elaborated description of conditions for each experiment is reported in table 1.
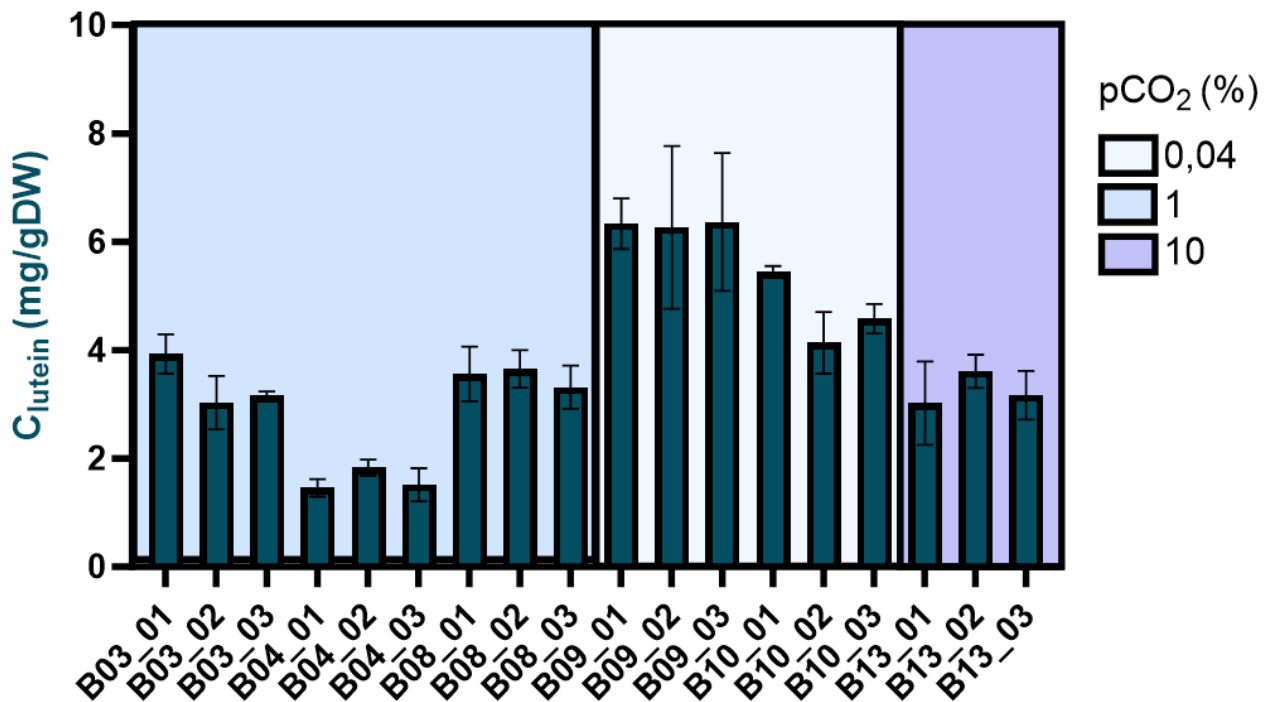
Figure 53 Lutein content in the experimental batches

From figure 53, it is evident that the batches cultivated in air reaches the maximum amount of lutein, B_10 had a mean value of lutein of 4.72 mg/gDW while in B_09 the content of lutein reaches 6.32 mg/gDW.

The batch grown with CO_2 enriched air shows lower concentrations of lutein between 2 and 4 mg/gDW.

Focusing on the 2 batches that had the best results, the following considerations can be made.

Regarding the light intensity in batch 09 the light starts from an initial value of $250 \frac{\mu mol}{m^2 \cdot s}$ and reaches a medium peak of $410 \frac{\mu mol}{m^2 \cdot s}$,, batch 10, on the other hand, had a slightly wider profile starting at $195 \frac{\mu mol}{m^2 \cdot s}$ and reaching a maximum value of $545 \frac{\mu mol}{m^2 \cdot s}$.

The nutrient profile in batch 09 had large differences, the amount of nitrogen in the 3 conditions was (11.7 mg, 31.0 mg, 14.3 mg), however, the differences between the 3 batches were negligible, suggesting that the nitrogen quantity present in the cultivars did not have a strong influence on the lutein content, this may be explained due to the fact that in air, growth is limited by carbon and the amount of nitrogen required is reduced.

In figure 54 is presented the productivity of lutein of the same batches analysed before.
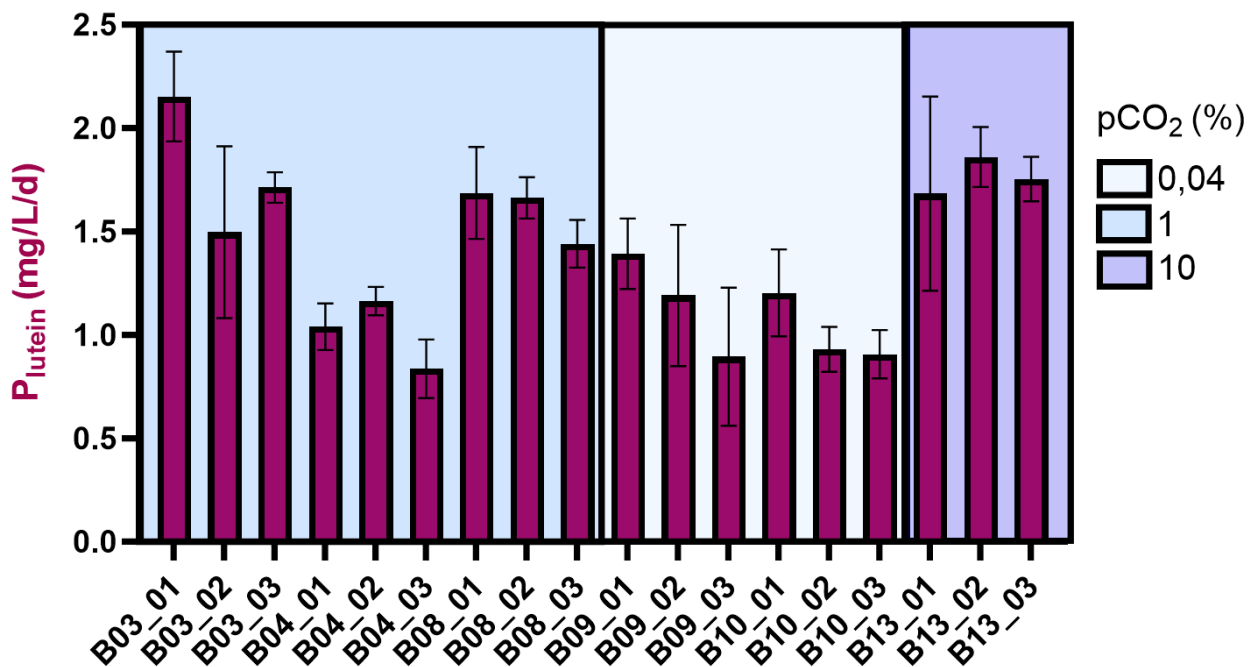
Figure 54 Lutein productivity in the experimental batches

In this case, the situation is opposite to the previous situation.

The batches that reach higher values of lutein productivity were B_03, B_08 and B_13, the first two were cultivated in 1% of CO_2 atmosphere while the second was under a 10% CO_2(v/v).

The productivity of these batches was between 1.79, 1.76 and 1.60 mg/L/d with a maximum value for batch 3 in condition 1 that reached a lutein productivity of 2.15 mg/L/d.

They were under a high light regime, B_03 and B_13 reached a maximum light peak of 800 $\frac{\mu mol}{m^2 \cdot s}$ while for B_08 the maximum peak was $600 \frac{\mu mol}{m^2 \cdot s}$.

Also, in this case the different concentrations of nitrogen inside the cultivators do not seem to impact the results, given the three different conditions of the same batch have the same quantity of lutein produced.

For example, in B_03 the nitrogen amount for the 3 cultivators was: 22.5, 51.7 and 13.3 mg each, but the difference in the lutein productivity was not significant and looking at the trends there seems to be no correlation between nitrogen quantities and lutein productivity.

Comparing the results of the present work with studies presents in literature on the lutein content on *Coccomyxa onubensis* some similarities can be found.

Bermejo et al. (2018) cultivate the *Coccomyxa* in a bubble column with a constant air with 5% of CO_2(v/v) in photoautotrophic modes, at 27 °C and with a constant light of 140 $\frac{\mu mol}{m^2 \cdot s}$.

In addition, the algal culture was stressed adding different concentrations of sodium chloride between 0 and 500mM. The outcome of this results was a maximum lutein content of 7.8 mg/gDW in the 500 mM NaCl situation, with a difference of 2 mg/gDW compared to preliminary result of this study (6.0 mg/g/DW). Therefore, it has been demonstrated that stressors known to affect the productivity of carotenoids, such as salinity, exert a significant influence on *C. onubensis*. However, employing osmotic stress presents a viable strategy, albeit with the drawback of necessitating high concentrations of NaCl, potentially hindering industrial-scale application due to the economic reason.

Vaquero et al. (2014) studied the correlation between the content of lutein in *C. onubensis* and different biomass concentrations (0.5 and 1.5 g/L), the results after 8 days of batch cultivation was the same for both conditions and the content of lutein was equal to 6 mg/gDW, in accordance with it has been found in this research. Nonetheless, the potential of *C. onubensis* as lutein producers has been fully exploited in the study of Fuentes et al. (2020) that reported a lutein content of 9.7 mg /gDW, that represent the highest ever reported for this strain. Furthermore, it was achieved in a semi-industrial system composed by a 400 litres plastic bags operated at 25°C at 150 $\frac{\mu mol}{m^2 \cdot s}$, the carbon was provided by an air stream with 2.5% of CO_2 (v/v).

Regarding the productivity, Vaquero et al. (2014) investigated also the effect of lutein productivity at different pH conditions, obtaining a maximum lutein productivity of 2.35 mg/L/d , comparable to the results of this work (2.15 mg/g/L).

If we enlarge the comparison with other microalgae more used at industrial level, we can see that the productivity of lutein in *C. onubensis* is lower, an example is *Chlorella minutissima* which was cultivated in a photoautotrophic batch process at 28 ∘C, with continuous illumination

with 150 $\frac{\mu mol}{m^2 \cdot s}$ and 2.5 % (v/v) of CO_2 reaches a lutein productivity of 3.45 mg/L/d (Dineshkumar et al., 2015). Schüler et al. (2020) cultivated in air *Tetraselmis* sp. CTP4 in batch autotrophic process, with nitrogen replete conditions, 35 ∘C and a light intensity of 170 $\frac{\mu mol}{m^2 \cdot s}$ reaching lutein productivity of 3.17 mg/gDW. Other studies were conducted under mixotrophic conditions and reached even higher productivities. *Chlorella sp. GY-H4* cultivated with an initial glucose concentration of 20 g/L shows a remarkable productivity of 10.5 mg/L/d (Wang et al., 2020).

Chen et al. (2019) studied *Chlorella sorokiniana* in mixotrophy with a 6 g/L of sodium acetate, at 150 $\frac{\mu mol}{m^2 \cdot s}$; the study revealed a lutein productivity of 6.24 mg/L/d, 3 times higher than our results. In general, all these studies focused on *Chlorella sp.* and mixotrophic condition that led higher lutein productivities than those presented in this work.

However, it must be underlined that these are only partial data, and it is fundamental to have all the information from all 13 batches to find the optimal operative variables that maximize the lutein productivity of *C. onubensis*.

It is important to emphasize that *C. onubensis* remains a viable lutein producer for industrial-scale applications. Despite exhibiting average lutein productivity compared to other microalgae, its ability to thrive at very low pH levels significantly mitigates the risk of contamination. Moreover, its resilience to low pH conditions proves beneficial at the industrial level by reducing operational and sterilization costs.

Conclusion

The aim of this thesis was to investigate the production of high value compounds exploiting the acidophilic microalgae *Coccomyxa onubensis*, given its abundant production in carotenoids, with a particular emphasis on lutein. In addition, this alga was selected due to its ability to grow under very low pH values (2.5) which make it a suitable candidate for industrial-scale production due to the low risk of contamination by other microorganisms in such extreme conditions.

The experiments were carried out using a high cell density cultivation system (CellDEG), a system that enable a rapid growth of the culture due an optimized light distribution and a controlled and adjustable supply of carbon dioxide.

The experimental campaign was performed according to a design of dynamic experiments, an innovative approach that allow to investigate the dynamic behaviour of variables and their interactions within a controlled environment. In particular, the time varying variables tested were the light intensity, the nitrogen feeding while the partial pressure of carbon dioxide was fixed on 3 levels.

Subsequently the results were analysed, and a data driven model was built to find the optimal growth conditions that maximize the production of the different outcomes.

From the optimization the suggested profiles and results were:

- For the carotenoid content, the light intensity started from 300 and reached a peak value of 475 $\frac{\mu mol}{m^2 \cdot s}$, the nitrogen feeding was 13.67 mg, supplied in 1 day and the CO_2 partial pressure was equal to 0.04%.

  The content of carotenoid with this configuration was 20.1 mg/gDW.

- For the carotenoid productivity, the light intensity started from 300 and reached a peak value of 800 $\frac{\mu mol}{m^2 \cdot s}$, the nitrogen feeding was 6 mg, supplied in 1 day and the CO_2 partial pressure was equal to 10%.

  The productivity of carotenoid with this configuration was 10.74 mg/L/d.

- For the biomass productivity, the light intensity started from 100 and reached a peak value of 800 $\frac{\mu mol}{m^2 \cdot s}$, the nitrogen feeding was 49.99 mg and supplied in 5 days and the CO_2 partial pressure was equal to 6.54%.

The biomass productivity with this configuration was 1.42 g/L/d.

Regarding the preliminary lutein productivity, the highest value of 2.15 mg/L/d was achieved when the microalga was cultivated under high light intensity (from 100 to 800 $\frac{\mu mol}{m^2 \cdot s}$) and 10% CO2.

In conclusion, the application of DoDE represents a valid and innovative approach to simplify the study of complex variables in order to define cultivation strategies for microalgae. The combination with the peculiar design of CellDEG PBR allowed rapid comparison of different conditions and achieved incomparable biomass productivity in photoautotrophy.

The profiles resulting from the optimization were in accordance with scientific literature: concerning carotenoids, high light and nutrient deficiency enhanced carotenoid production; a wide and incremental light profile associated with high nitrogen feeding and high partial pressure of CO_2 maximized biomass productivity.

The results predicted by the model were higher compared to the data found in literature and require experimental validation for complete assessment.

Regarding lutein productivity, preliminary results (2.15 mg/L/d) were comparable with other studies on *C. onubensis* present in literature.

Therefore, this strain can be considered a valid candidate for the production of carotenoids, particularly lutein. Moreover, its ability to thrive in acid environments hinders bacterial contamination, making *Coccomyxa onubensis* a promising strain for mass cultivation at an industrial scale.

Bibliography

Abiusi, F., Trompetter, E., Pollio, A., Wijffels, R.H., Janssen, M., 2022. Acid Tolerant and Acidophilic Microalgae: An Underexplored World of Biotechnological Opportunities. Front. Microbiol. 13. https://doi.org/10.3389/fmicb.2022.820907

Ahmad, I., Abdullah, N., Koji, I., Yuzir, A., Muhammad, S.E., 2021. Evolution of Photobioreactors: A Review based on Microalgal Perspective. IOP Conf. Ser.: Mater. Sci. Eng. 1142, 012004. https://doi.org/10.1088/1757-899X/1142/1/012004

Béchet, Q., Shilton, A., Guieysse, B., 2013. Modeling the effects of light and temperature on algae growth: state of the art and critical assessment for productivity prediction during outdoor cultivation. Biotechnol Adv 31, 1648–1663. https://doi.org/10.1016/j.biotechadv.2013.08.014

Becker, E.W., 1994. Microalgae: Biotechnology and Microbiology. Cambridge University Press.

Bermejo, E., Ruiz-Domínguez, M.C., Cuaresma, M., Vaquero, I., Ramos-Merchante, A., Vega, J.M., Vílchez, C., Garbayo, I., 2018. Production of lutein, and polyunsaturated fatty acids by the acidophilic eukaryotic microalga *Coccomyxa onubensis* under abiotic stress by salt or ultraviolet light. Journal of Bioscience and Bioengineering 125, 669–675. https://doi.org/10.1016/j.jbiosc.2017.12.025

Bernard, O., Mairet, F., Chachuat, B., 2016. Modelling of Microalgae Culture Systems with Applications to Control and Optimization. Adv Biochem Eng Biotechnol 153, 59–87. https://doi.org/10.1007/10_2014_287

Borowitzka, M.A., 1999. Commercial production of microalgae: ponds, tanks, tubes and fermenters. Journal of Biotechnology, Biotechnological Aspects of Marine Sponges 70, 313–321. https://doi.org/10.1016/S0168-1656(99)00083-8

Breithaupt, D.E., Wirt, U., Bamedi, A., 2002. Differentiation between lutein monoester regioisomers and detection of lutein diesters from marigold flowers (Tagetes erecta L.) and Several fruits by liquid chromatography-mass spectrometry. Journal of Agricultural and Food Chemistry 50, 66–70. https://doi.org/10.1021/jf010970l

Chanquia, S.N., Vernet, G., Kara, S., 2022. Photobioreactors for cultivation and synthesis: Specifications, challenges, and perspectives. Engineering in Life Sciences 22, 712–724. https://doi.org/10.1002/elsc.202100070

Chen, J.-H., Chen, C.-Y., Hasunuma, T., Kondo, A., Chang, C.-H., Ng, I.-S., Chang, J.-S., 2019. Enhancing lutein production with mixotrophic cultivation of *Chlorella sorokiniana* MB-1-M12 using different bioprocess operation strategies. Bioresource Technology 278, 17–25. https://doi.org/10.1016/j.biortech.2019.01.041

Converti, A., Casazza, A.A., Ortiz, E.Y., Perego, P., Del Borghi, M., 2009. Effect of temperature and nitrogen concentration on the growth and lipid content of *Nannochloropsis oculata* and *Chlorella vulgaris* for biodiesel production. Chemical Engineering and Processing: Process Intensification 48, 1146–1151. https://doi.org/10.1016/j.cep.2009.03.006

Cuaresma, M., Janssen, M., van den End, E.J., Vílchez, C., Wijffels, R.H., 2011. Luminostat operation: A tool to maximize microalgae photosynthetic efficiency in photobioreactors during the daily light cycle? Bioresource Technology 102, 7871–7878. https://doi.org/10.1016/j.biortech.2011.05.076

Daneshvar, E., Sik Ok, Y., Tavakoli, S., Sarkar, B., Shaheen, S.M., Hong, H., Luo, Y., Rinklebe, J., Song, H., Bhatnagar, A., 2021. Insights into upstream processing of microalgae: A review. Bioresource Technology 329, 124870. https://doi.org/10.1016/j.biortech.2021.124870

Dao, G.-H., Wu, G.-X., Wang, X.-X., Zhang, T.-Y., Zhan, X.-M., Hu, H.-Y., 2018. Enhanced microalgae growth through stimulated secretion of indole acetic acid by symbiotic bacteria. Algal Research 33, 345–351. https://doi.org/10.1016/j.algal.2018.06.006

Davies, J.P., Grossman, A.R., 1998. Responses to Deficiencies in Macronutrients, in: Rochaix, J.-D., Goldschmidt-Clermont, M., Merchant, S. (Eds.), The Molecular Biology of Chloroplasts and Mitochondria in Chlamydomonas. Springer Netherlands, Dordrecht, pp. 613–635. https://doi.org/10.1007/0-306-48204-5_32

Dineshkumar, R., Dhanarajan, G., Dash, S.K., Sen, R., 2015. An advanced hybrid medium optimization strategy for the enhanced productivity of lutein in *Chlorella minutissima*. Algal Research 7, 24–32. https://doi.org/10.1016/j.algal.2014.11.010

Fernandes, B.D., Mota, A., Teixeira, J.A., Vicente, A.A., 2015. Continuous cultivation of photosynthetic microorganisms: Approaches, applications and future trends. Biotechnol Adv 33, 1228–1245. https://doi.org/10.1016/j.biotechadv.2015.03.004

Fernández-Sevilla, J.M., Acién Fernández, F.G., Molina Grima, E., 2010. Biotechnological production of lutein and its applications. Appl Microbiol Biotechnol 86, 27–40. https://doi.org/10.1007/s00253-009-2420-y

Fiordalis, A., Georgakis, C., 2013. Data-driven, using design of dynamic experiments, versus model-driven optimization of batch crystallization processes. Journal of Process Control, IFAC World Congress Special Issue 23, 179–188. https://doi.org/10.1016/j.jprocont.2012.08.011

Freudenberg, R.A., Baier, T., Einhaus, A., Wobbe, L., Kruse, O., 2021. High cell density cultivation enables efficient and sustainable recombinant polyamine production in the microalga *Chlamydomonas reinhardtii*. Bioresource Technology 323, 124542. https://doi.org/10.1016/j.biortech.2020.124542

Fuentes, J.-L., Montero, Z., Cuaresma, M., Ruiz-Domínguez, M.-C., Mogedas, B., Nores, I.G., González del Valle, M., Vílchez, C., 2020. Outdoor Large-Scale Cultivation of the Acidophilic Microalga Coccomyxa onubensis in a Vertical Close Photobioreactor for Lutein Production. Processes 8, 324. https://doi.org/10.3390/pr8030324

Gao, K., 2021. Approaches and involved principles to control pH/pCO2 stability in algal cultures. J Appl Phycol 33, 3497–3505. https://doi.org/10.1007/s10811-021-02585-y

Garbayo, I., Torronteras, R., Forján, E., Cuaresma, M., Casal, C., Mogedas, B., Ruiz-Domínguez, M.C., Márquez, C., Vaquero, I., Fuentes-Cordero, J.L., Fuentes, R., González-del-Valle, M., Vílchez, C., 2012. Identification and Physiological Aspects of a Novel Carotenoid-Enriched, Metal-Resistant Microalga Isolated from an Acidic River in Huelva (spain)1. Journal of Phycology 48, 607–614. https://doi.org/10.1111/j.1529-8817.2012.01160.x

Georgakis, C., 2013. Design of Dynamic Experiments: A Data-Driven Methodology for the Optimization of Time-Varying Processes. Ind. Eng. Chem. Res. 52, 12369–12382. https://doi.org/10.1021/ie3035114

Gwak, Y., Hwang, Y., Wang, B., Kim, M., Jeong, J., Lee, C.-G., Hu, Q., Han, D., Jin, E., 2014. Comparative analyses of lipidomes and transcriptomes reveal a concerted action of multiple defensive systems against photooxidative stress in Haematococcus pluvialis. Journal of Experimental Botany 65, 4317–4334. https://doi.org/10.1093/jxb/eru206

Han, F., Huang, J., Li, Y., Wang, W., Wan, M., Shen, G., Wang, J., 2013. Enhanced lipid productivity of *Chlorella pyrenoidosa* through the culture strategy of semi-continuous cultivation with nitrogen limitation and pH control by CO2. Bioresource Technology 136, 418–424. https://doi.org/10.1016/j.biortech.2013.03.017

https://www.polarismarketresearch.com, P.M.R., n.d. Microalgae Market Size, Share Global Analysis Report, 2023-2032 [WWW Document]. Polaris. URL https://www.polarismarketresearch.com/industry-analysis/microalgae-market (accessed 2.29.24).

Khan, M.I., Shin, J.H., Kim, J.D., 2018. The promising future of microalgae: current status, challenges, and optimization of a sustainable and renewable industry for biofuels, feed, and other products. Microbial Cell Factories 17, 36. https://doi.org/10.1186/s12934-018-0879-x

Klebanov, N., Georgakis, C., 2016. Dynamic Response Surface Models: A Data-Driven Approach for the Analysis of Time-Varying Process Outputs. Ind. Eng. Chem. Res. 55, 4022–4034. https://doi.org/10.1021/acs.iecr.5b03572

Lamers, P.P., van de Laak, C.C.W., Kaasenbrood, P.S., Lorier, J., Janssen, M., De Vos, R.C.H., Bino, R.J., Wijffels, R.H., 2010. Carotenoid and fatty acid metabolism in light-stressed

Dunaliella salina. Biotechnology and Bioengineering 106, 638–648. https://doi.org/10.1002/bit.22725

Lippi, L., Bähr, L., Wüstenberg, A., Wilde, A., Steuer, R., 2018. Exploring the potential of high-density cultivation of cyanobacteria for the production of cyanophycin. Algal Research 31, 363–366. https://doi.org/10.1016/j.algal.2018.02.028

Luo, Y., Stanton, D.A., Sharp, R.C., Parrillo, A.J., Morgan, K.T., Ritz, D.B., Talwar, S., 2023. Efficient optimization of time-varying inputs in a fed-batch cell culture process using design of dynamic experiments. Biotechnology Progress 39, e3380. https://doi.org/10.1002/btpr.3380

Lutein Market Size & Share, Growth Analysis Report 2024-2032 [WWW Document], n.d. . Global Market Insights Inc. URL https://www.gminsights.com/industry-analysis/lutein-market (accessed 2.27.24).

Maghzian, A., Aslani, A., Zahedi, R., 2024. A comprehensive review on effective parameters on microalgae productivity and carbon capture rate. Journal of Environmental Management 355, 120539. https://doi.org/10.1016/j.jenvman.2024.120539

Makrydaki, F., Georgakis, C., Saranteas, K., 2010. Dynamic Optimization of a Batch Pharmaceutical Reaction using the Design of Dynamic Experiments (DoDE): the Case of an Asymmetric Catalytic Hydrogenation Reaction. IFAC Proceedings Volumes, 9th IFAC Symposium on Dynamics and Control of Process Systems 43, 260–265. https://doi.org/10.3182/20100705-3-BE-2011.00043

Markou, G., Vandamme, D., Muylaert, K., 2014. Microalgal and cyanobacterial cultivation: The supply of nutrients. Water Research 65, 186–202. https://doi.org/10.1016/j.watres.2014.07.025

McGee, D., Archer, L., Fleming, G.T.A., Gillespie, E., Touzet, N., 2020. Influence of spectral intensity and quality of LED lighting on photoacclimation, carbon allocation and high-value pigments in microalgae. Photosynth Res 143, 67–80. https://doi.org/10.1007/s11120-019-00686-x

Mulders, K.J.M., Janssen, J.H., Martens, D.E., Wijffels, R.H., Lamers, P.P., 2014. Effect of biomass concentration on secondary carotenoids and triacylglycerol (TAG) accumulation in nitrogen-depleted *Chlorella zofingiensis*. Algal Research 6, 8–16. https://doi.org/10.1016/j.algal.2014.08.006

Neves, F. de F., Hoinaski, L., Rörig, L.R., Derner, R.B., de Melo Lisboa, H., 2019. Carbon biofixation and lipid composition of an acidophilic microalga cultivated on treated wastewater supplied with different CO_2 levels. Environmental Technology 40, 3308–3317. https://doi.org/10.1080/09593330.2018.1471103

Piiparinen, J., Barth, D., Eriksen, N.T., Teir, S., Spilling, K., Wiebe, M.G., 2018. Microalgal CO_2 capture at extreme pH values. Algal Research 32, 321–328. https://doi.org/10.1016/j.algal.2018.04.021

Prasad, R., Gupta, S.K., Shabnam, N., Oliveira, C.Y.B., Nema, A.K., Ansari, F.A., Bux, F., 2021. Role of Microalgae in Global CO_2 Sequestration: Physiological Mechanism, Recent Development, Challenges, and Future Prospective. Sustainability 13, 13061. https://doi.org/10.3390/su132313061

Procházková, G., Brányiková, I., Zachleder, V., Brányik, T., 2014. Effect of nutrient supply status on biomass composition of eukaryotic green microalgae. J Appl Phycol 26, 1359–1377. https://doi.org/10.1007/s10811-013-0154-9

Rath, B., 2012. BIOACTIVE COMPOUNDS FROM MICROALGAE AND CYANOBACTERIA: UTILITY AND APPLICATIONS. international journal of pharmacutical science and research Vol. 3, 4123–4130.

Richmond, A. (Ed.), 2007. Handbook of microalgal culture: biotechnology and applied phycology, Nachdr. ed. Blackwell Science, Oxford.

Richmond, A. (Ed.), 2004. Handbook of microalgal culture: biotechnology and applied phycology. Blackwell Science, Oxford, OX, UK ; Ames, Iowa, USA.

Robles, M., Torronteras, R., Ostojic, C., Oria, C., Cuaresma, M., Garbayo, I., Navarro, F., Vílchez, C., 2023. Fe (III)-Mediated Antioxidant Response of the Acidotolerant Microalga Coccomyxa onubensis. Antioxidants (Basel) 12, 610. https://doi.org/10.3390/antiox12030610

Rosso, L., Lobry, J.R., Flandrois, J.P., 1993. An unexpected correlation between cardinal temperatures of microbial growth highlighted by a new model. J Theor Biol 162, 447–463. https://doi.org/10.1006/jtbi.1993.1099

Ruiz-Domínguez, M.C., Vaquero, I., Obregón, V., de la Morena, B., Vílchez, C., Vega, J.M., 2015. Lipid accumulation and antioxidant activity in the eukaryotic acidophilic microalga Coccomyxa sp. (strain onubensis) under nutrient starvation. J Appl Phycol 27, 1099–1108. https://doi.org/10.1007/s10811-014-0403-6

Schüler, L.M., Santos, T., Pereira, H., Duarte, P., Katkam, N.G., Florindo, C., Schulze, P.S.C., Barreira, L., Varela, J.C.S., 2020. Improved production of lutein and *β*-carotene by thermal and light intensity upshifts in the marine microalga *Tetraselmis* sp. CTP4. Algal Research 45, 101732. https://doi.org/10.1016/j.algal.2019.101732

Takenaka, H., Yamaguchi, Y., 2014. Commercial-scale culturing of cyanobacteria: an industrial experience, in: Cyanobacteria. John Wiley & Sons, Ltd, pp. 293–301. https://doi.org/10.1002/9781118402238.ch18

Tang, H., Chen, M., Simon Ng, K. y., Salley, S.O., 2012. Continuous microalgae cultivation in a photobioreactor. Biotechnology and Bioengineering 109, 2468–2474. https://doi.org/10.1002/bit.24516

Trentin, G., Bertucco, A., Georgakis, C., Sforza, E., Barbera, E., 2023. Using the design of dynamic experiments to optimize photosynthetic cyanophycin production by *Synechocystis* sp. Journal of Industrial and Engineering Chemistry 117, 386–393. https://doi.org/10.1016/j.jiec.2022.10.026

Van Vooren, G., Le Grand, F., Legrand, J., Cuiné, S., Peltier, G., Pruvost, J., 2012. Investigation of fatty acids accumulation in *Nannochloropsis oculata* for biodiesel application. Bioresource Technology 124, 421–432. https://doi.org/10.1016/j.biortech.2012.08.009

Vaquero, I., Ruiz-Domínguez, M.C., Márquez, M., Vílchez, C., 2012. Cu-mediated biomass productivity enhancement and lutein enrichment of the novel microalga *Coccomyxa onubensis*. Process Biochemistry 47, 694–700. https://doi.org/10.1016/j.procbio.2012.01.016

Vaquero, I., Vázquez, M., Ruiz-Domínguez, M.C., Vílchez, C., 2014. Enhanced production of a lutein-rich acidic environment microalga. Journal of Applied Microbiology 116, 839–850. https://doi.org/10.1111/jam.12428

Varshney, P., Mikulic, P., Vonshak, A., Beardall, J., Wangikar, P.P., 2015. Extremophilic micro-algae and their potential contribution in biotechnology. Bioresour Technol 184, 363–372. https://doi.org/10.1016/j.biortech.2014.11.040

Venkata Subhash, G., Rajvanshi, M., Navish Kumar, B., Govindachary, S., Prasad, V., Dasgupta, S., 2017. Carbon streaming in microalgae: extraction and analysis methods for high value compounds. Bioresource Technology, SI:Algal Biorefinery 244, 1304–1316. https://doi.org/10.1016/j.biortech.2017.07.024

Wang, B., Lan, C.Q., Horsman, M., 2012. Closed photobioreactors for production of microalgal biomasses. Biotechnology Advances, Biorefining: Thermochemical and Enzymatic Biomass Conversion 30, 904–912. https://doi.org/10.1016/j.biotechadv.2012.01.019

Wang, X., Zhang, M.-M., Sun, Z., Liu, S.-F., Qin, Z.-H., Mou, J.-H., Zhou, Z.-G., Lin, C.S.K., 2020. Sustainable lipid and lutein production from *Chlorella* mixotrophic fermentation by food waste hydrolysate. Journal of Hazardous Materials 400, 123258. https://doi.org/10.1016/j.jhazmat.2020.123258

Wellburn, A.R., 1994. The Spectral Determination of Chlorophylls *a* and *b*, as well as Total Carotenoids, Using Various Solvents with Spectrophotometers of Different Resolution. Journal of Plant Physiology 144, 307–313. https://doi.org/10.1016/S0176-1617(11)81192-2

Yaakob, M.A., Mohamed, R.M.S.R., Al-Gheethi, A., Aswathnarayana Gokare, R., Ambati, R.R., 2021. Influence of Nitrogen and Phosphorus on Microalgal Growth, Biomass, Lipid, and Fatty Acid Production: An Overview. Cells 10, 393. https://doi.org/10.3390/cells10020393

Yao, C., Ai, J., Cao, X., Xue, S., Zhang, W., 2012. Enhancing starch production of a marine green microalga *Tetraselmis subcordiformis* through nutrient limitation. Bioresource Technology 118, 438–444. https://doi.org/10.1016/j.biortech.2012.05.030

Zhao, B., Su, Y., 2014. Process effect of microalgal-carbon dioxide fixation and biomass production: A review. Renewable and Sustainable Energy Reviews 31, 121–132. https://doi.org/10.1016/j.rser.2013.11.054

Zheng, H., Wang, Y., Li, S., Nagarajan, D., Varjani, S., Lee, D.-J., Chang, J.-S., 2022. Recent advances in lutein production from microalgae. Renewable and Sustainable Energy Reviews 153, 111795. https://doi.org/10.1016/j.rser.2021.111795